Design, Synthesis and Characterization of Porous Materials made from Nucleobases and Metals

by

Jihyun An

B.S., Seoul National University, 2004

Submitted to the Graduate Faculty of

Arts and Sciences in partial fulfillment

of the requirements for the degree of

Master of Science

University of Pittsburgh

2008

UNIVERSITY OF PITTSBURGH

SCHOOL OF ARTS AND SCIENCES

This thesis was presented

by

Jihyun An

It was defended on

April 22, 2008

and approved by

Dr. Toby Chapman, Associate Professor, Chemistry

Dr. Stéphan Petoud, Assistant Professor, Chemistry

Thesis Director: Dr. Nathaniel Rosi, Assistant Professor, Chemistry

Design, Synthesis and Characterization of Porous Materials made from Nucleobases and Metals

Jihyun An, M.S.

University of Pittsburgh, 2008

This research is aimed at designing and synthesizing porous biomolecule-based materials for biological applications, such as a drug delivery. As a first step in this direction, developing a rational synthetic method to control the coordination chemistry between nucleobases and metal ions with the aim of organizing nucleobases into structurally well-defined porous materials has been studied. As a result, several interesting frameworks have been synthesized and characterized so far. They exhibit not only interesting structures but also unique physical properties.

Interestingly, many of the adenine binding motifs are somewhat analogous to various carboxylate motifs which have been extensively used in MOF chemistry, suggesting that adenine could be a very versatile molecule for the construction and design of new MOFs. Furthermore, the successful synthesis of a porous material with adenine is very significant because it proves that porous material with bio-molecules can be rationally designed and synthesized for target applications.

TABLE OF CONTENTS

LIST OF TABLES

LIST OF FIGURES

LIST OF SCHEMES

1.0 INTRODUCTION

Many important biological structures result from the self-assembly of complex biological molecules. Examples include membrane protein assemblies and viral capsids[1]. Membrane protein assemblies control analyte diffusion across cell membranes, and viral capsids are highly symmetric assemblies of protein molecular building blocks that not only protect the viral genetic material but also deliver it to a suitable host cell. Virus capsids like bacteriophage HK97 and bacteriophage P22 have icosahedral structures. Synthesizing structurally well-defined materials via molecular self-assembly has attracted and challenged chemists and materials scientists.

For example, there has been an effort to synthesize porous materials with metals and organic molecules by using a molecular building block approach. Such materials are called metal organic frameworks (MOFs), metal organic polyhedra, or coordination polymers. They are composed of metal ions/clusters that serve as vertices and organic ligands that serve as linkers that connect the vertices into periodic structures (Scheme 1). This approach is attractive for a number of reasons: the functionality of the framework can be tuned by carefully choosing the metal and organic components and the metrics of the framework can be carefully tuned by modulating the length of the organic linker molecule.

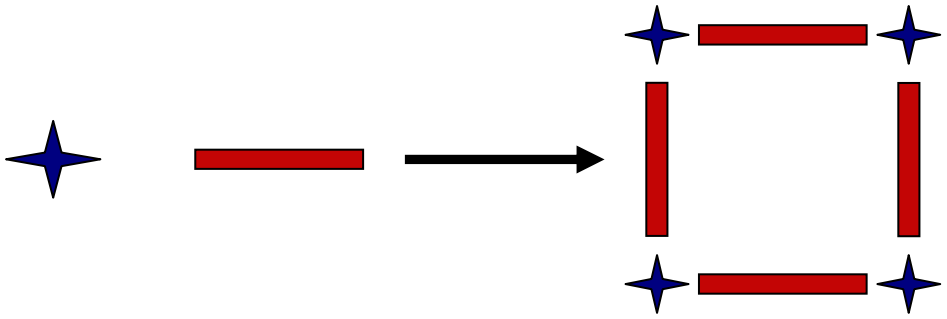

Scheme 1. General MOFs assembly scheme (Blue star: metal ion or cluster; Red rod: organic linker

These materials have been designed and studied for various applications including guest recognition[2], gas storage[3], separations[4], catalysis[5], and ion-exchange[6]. Typically, simple multitopic ligands such as organic carboxylic acids are used for MOFs; in rare cases, however, researchers have begun to investigate the use of biological molecules as linkers. Fujita[7] and coworkers made a mimic of an enzyme capsule or pocket by using metal ions and organic ligands which are functionalized with biological molecules such as amino acids or peptides. Very few examples exist where biomolecules are used as the linkers (ligands) in MOFs.[8, 9] Porous materials constructed with biological molecules may have potential bio-medical impact. For instance, such materials could be used to store and deliver drug molecules. Very recently, there have been some efforts to utilize MOFs as drug delivery vessels[10]; however, the MOFs investigated contain chromium ions and thus are not very bio-compatible. If MOFs were constructed from biological molecules and biologically benign metal cations, they could be a powerful potential drug delivery material. Depending upon how the ligands are functionalized, delivering the drug molecules to specific host cells might be possible. Moreover, the pore size and functionality of MOFs can be tuned to carefully modulate the release profile of the drug molecule. My research goal is to develop rational synthetic methods for organizing biological

molecules into structurally well-defined porous materials that can be used for biomedical applications such as drug delivery.

1.1 Adenine

Many biological molecules could potentially be used as linking ligands for MOF construction, as the only prerequisite is that they have multiple sites for coordinating metal ions or clusters. Nucleobases have been chosen for this study. Nucleobases are one of the simplest biological molecules and interaction studies between nucleobases and metal ions might be also interesting due to it's an important role in biological processes[11]. My studies have concentrated on using adenine. I have begun by investigating and studying the coordination chemistry of adenine in the context of constructing discrete and extended coordination assemblies.

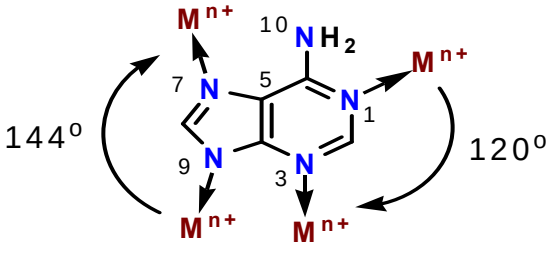

Figure 1. Adenine

Adenine contains 5 Lewis base donors sites (N1, N3, N7, N9, and N10) which allow versatile bonding patterns by coordination with metal ions. The possible bonding angle between adenine and metal ions is also an important reason for using adenine in this study. The bonding angle between metal ions and nitrogens (N7, N9) on the imidazole ring of adenine is 144°, and the bonding angle between metal ions and nitrogens (N1, N3) on the hexameric ring of adenine is 120°. These potential binding motifs rationalize targeting known structure types that require such angles. For example, zeolitic structures are composed of SiO_4 tetrahedra which are bridged together at approximately 144° angles, and polyhedra such as the truncated cuboctahedron or truncated icosadodecahedran are composed of square planar building units connected by either 120° or 144° angles, respectively.

1.2 Potential Target

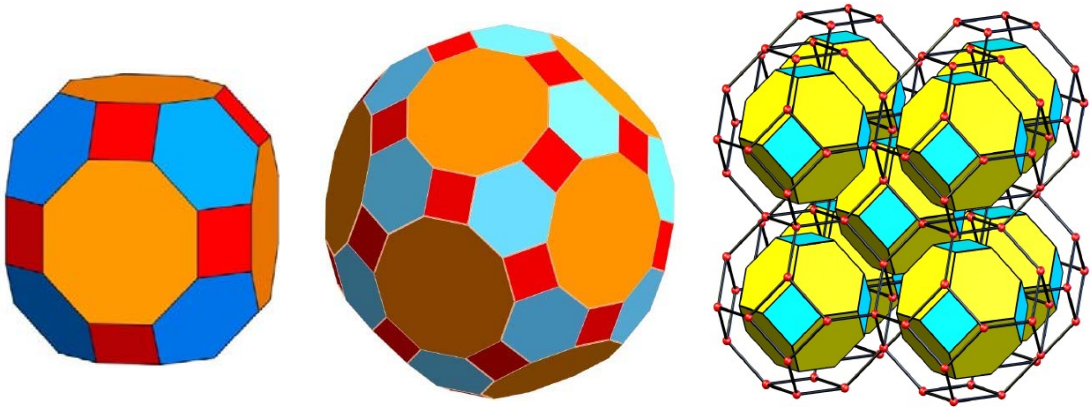

Truncated Cuboctahedron | Truncated Icosidodecahedron | Zeolitic Topologies, such as Sodalite

Figure 2. Potential target structures

As mentioned above, truncated cuboctahedra, and truncated icosidodecahedra, and structures with zeolitic topologies (Figure 2) are potential targets due to the bonding angle of adenine and metals ions. When metals that prefer to coordinating in square planar geometries bind to the adenine, the angle between adenine and square planar building unit can be either 144° or 120°. For example, as shown in Figure 3, the square planar coordination of metals like nickel, palladium or platinum can be considered as the red square block in truncated icosidodecahedron structure.

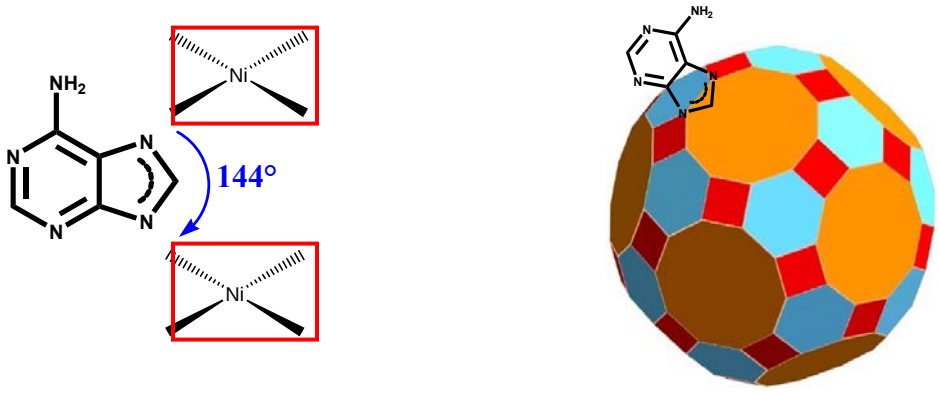

Figure 3. Adenine and metal ions coordination for target structures

Since red squares in the truncated icosidodecahedron structure are connected together by 144° angles, extending to a polyhedron structure, adenine can serve to link the squares by coordinating with nickel metals by 144° angles. In addition, Si-O-Si angle in zeolites is approximately 145° which is close to that of adenine. If tetrahedral metal ions are bridged together by adenine at 144°, zeolite-like structures can be potentially synthesized. For instance,

zeolitic structures made from imidazole and zinc/cobalt tetrahedra have been reported by Hayashi et al.[12] and Banerjee et al.[13].

1.3 General Reaction Strategy

In order to design and synthesize the potential target structures, a variety of synthetic conditions have been investigated. The general reaction strategy is shown in Scheme 2.

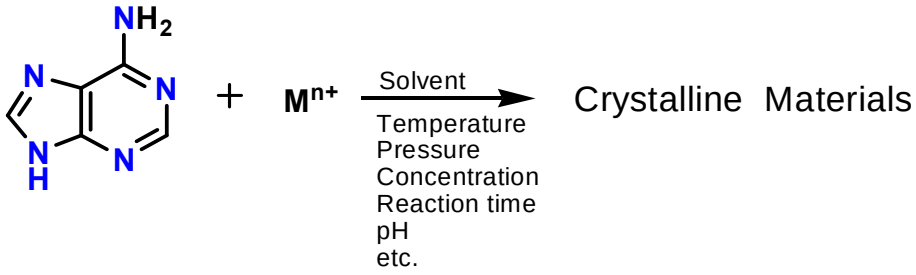

Scheme 2. General reaction conditions

Adenine and metal salts are reacted under solvothermal conditions using different reactant concentrations, solvents, pH, pressures, temperatures and reaction times in general. Nickel and palladium have been used to synthesize target polyhedral structures. At the same time, other metal salts which bind in a tetrahedral fashion in the presence of nitrogen-donor ligands, such as divalent zinc, cobalt, have been studied to synthesize zeolite-like structures. Thus far, I have developed a new category of materials made from adenine and metal ions. Some of these structures have interesting features which could potentially be useful for gas storage and gas separations. In addition, one of the structures is exceptionally stable in aqueous solutions and biological buffers, indicating that it may be a candidate material for drug-delivery applications.

However, the targeted structures exploiting the full advantages of adenine as a linker have not been made yet.

1.4 Previous Research of Adenine/ Metal Frameworks

Though not many adenine-metal frameworks are reported, some previous work has been published recently. The first adenine-metal framework has published in 2004. Garcia-Teran et al. [8a] synthesized a three-dimensional coordination polymer made from adenine and copper that has antiferromagnetic properties. Purohit et al. reacted 9-allyladenine with silver(I) generate a helical one-dimensional polymer structure having interesting luminescent properties. In 2007, the first two-dimensional trinuclear cadmium complex with adenine was reported by Yang et al.[8c] Finally, adenine and lithium metal coordination studies were published in 2008 by Kruger et al.[8d] The lithiated adenine self-assembled into a one dimensional polymeric chain and its structure has been characterized and reactivity has been studied in the context of alkali metal - nucleobase interaction research. However, none of these reports have targeted biological applications.

2.0 ZINC - ADENINE MACROCYCLES AND POLYMERS

In studying the coordination chemistry between adenine and metal ions, several interesting coordination patterns have been discovered. This section focuses on studies aimed at controlling the coordination so that it occurs exclusively between the metal cation and the imidazole ring of adenine (Figure 4). By restricting the metal coordination to the imidazole ring while leaving the pyramidal nitrogens uncoordinated, one can potentially target structures with zeolitic topologies as long as a metal ion such as Zn(II), which forms tetrahedra in the presence of nitrogen donors, is used. Thus far, two compounds have been discovered that exhibit this coordination mode: a zinc-adeninate coordination polymer and a zinc-adeninate hexameric macrocycle. The structures and physical properties of these new materials have been examined. Together, these materials represent the first steps toward isolating compounds with zeolitic topologies.

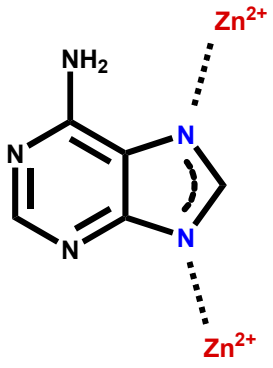

Figure 4. Zinc coordination to the imidazole ring of the adenine

2.1 Zn(Ad)(Py)(CH_3CO_2) · (1.5DMF)

2.1.1 Structure

The macrocycle is composed of six adeninates and six zinc(II) cations. Each Zn(II) is bound to either the N7 or N9 position two different adeninates. The imidazole rings of the adeninates bridge the Zn(II) centers. In addition, each Zn(II) is coordinated to a single acetate and a single pyridine, which complete the tetrahedral coordination sphere (Figure 5). Since only the imidazole nitrogens are coordinated to the metal centers, the pyramidal nitrogens and the amino groups remain free to participate in hydrogen bonding interactions. In the crystal structure, the macrocycles form layers and stack in an A-B-C fashion (Figure 6 (a)). Each macrocycle forms a total of 12 hydrogen bonds to neighboring macrocycles in adjacent layers through the amino group hydrogens and N1 the adeninates (Figure 6 (b)).

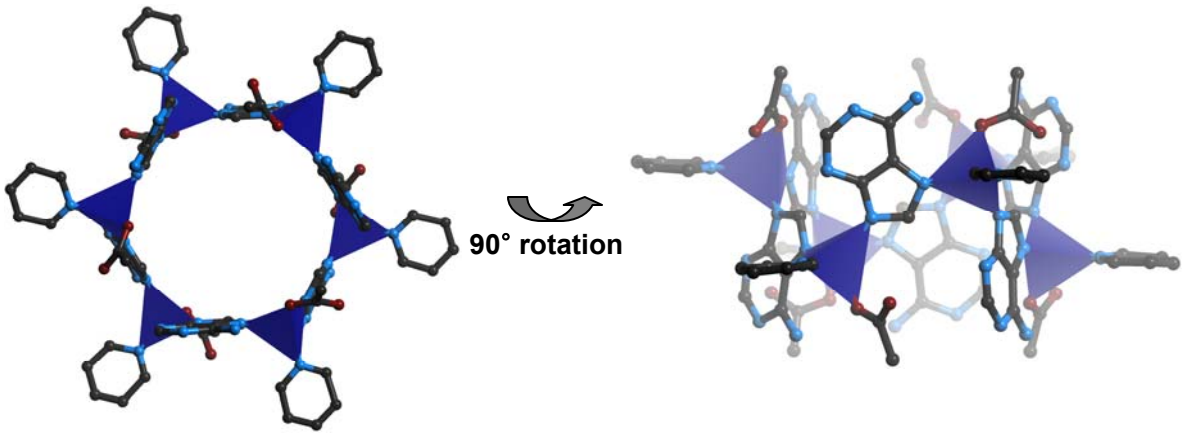

Figure 5. Zn(Ad)(Py)(CH_3CO_2) · (1.5DMF) (a) top view, (b) side view

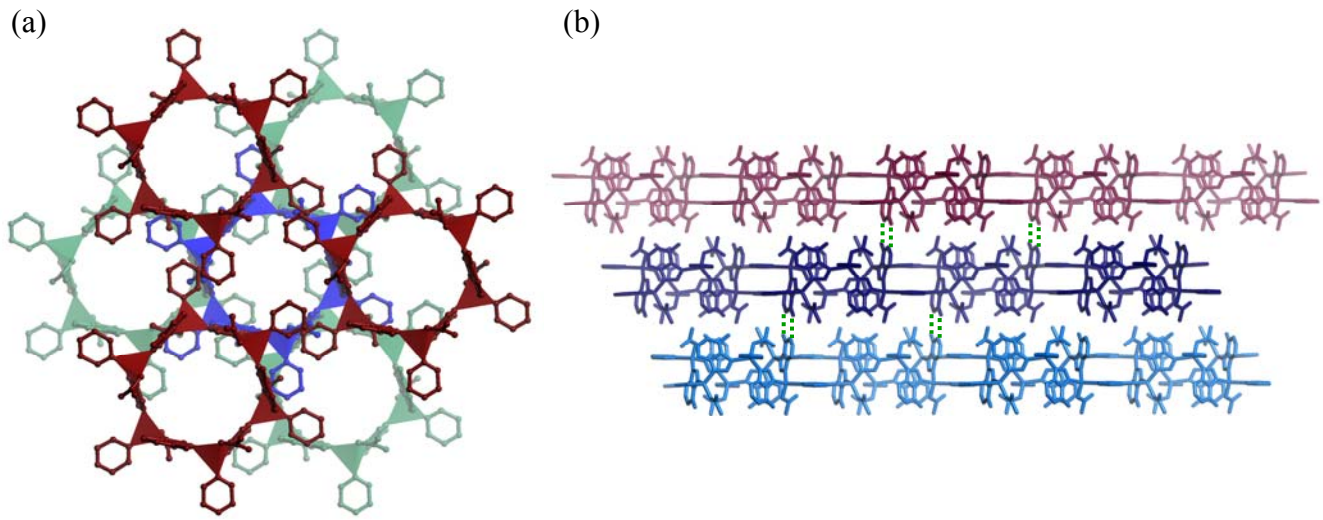

Figure 6. (a) Packing of the macrocycles in A-B-C fashion (b) packing via hydrogen bonding

The packing of macrocycles through hydrogen-bonding results in the formation of one-dimensional tubular cavities within the structure as shown in Figure 7. Each channel is made from one hexameric macrocycle in the middle, and parts from the other six macrocycles on the top and the bottom. (Figure 8)

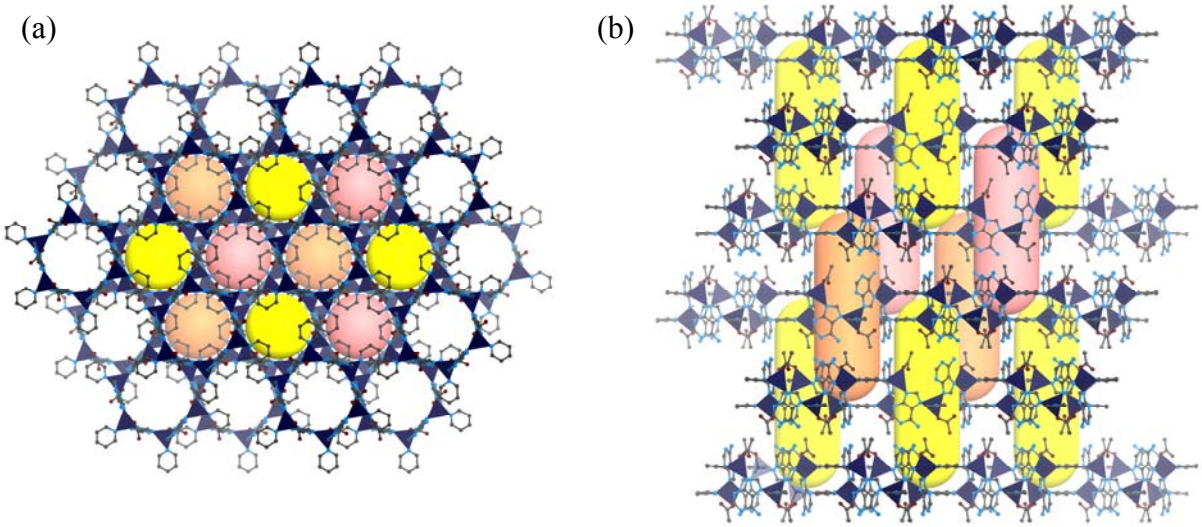

Figure 7. (a) Packed macrocycles viewing along *C*-crystallographical axis (b) side view of packing (the yellow and orange cylinders represents the space in the channel)

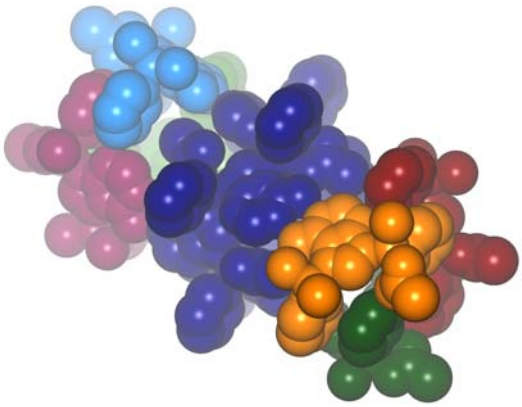

Figure 8. 1-D Channel composition (purple; a hexameric ring, yellow, red, green, violet, blue, light green; parts of different hexameric macrocycles)

2.1.2 Characterization - EA, XPRD, and TGA

The crystalline material has been characterized using elemental analysis (EA), thermogravimetric analysis (TGA), X-ray powder diffraction (XRPD), IR, and gas sorption. The experimental section explains the details of these experiments. These characterization methods are used to study the physical properties of the material such as integrity, purity, stability, and porosity. Comparison of the experimental powder X-ray diffraction pattern (Figure 9) to the pattern simulated from single crystal X-ray data verifies the phase purity of the product.

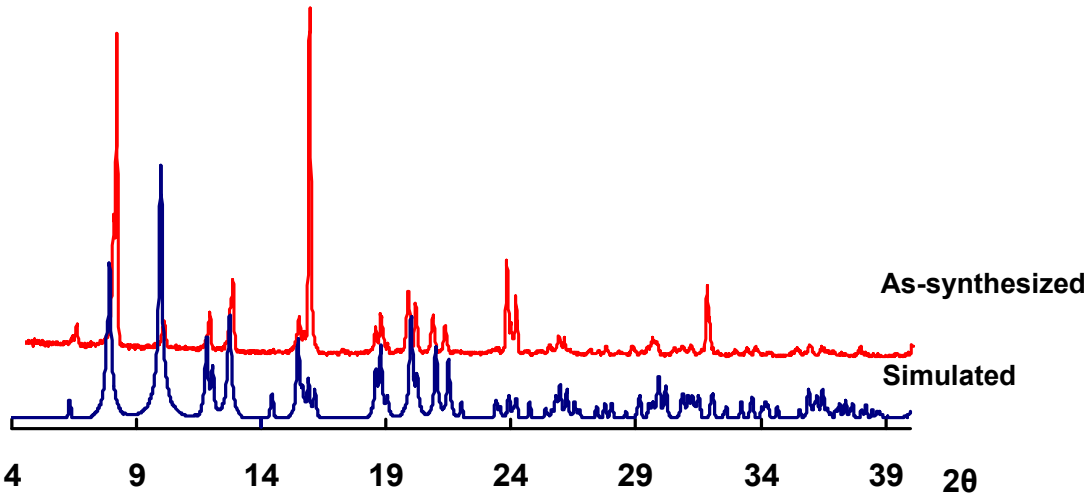

Figure 9. XRPD of Zn(Ad)(Py)(CH_3CO_2) · (1.5DMF)

Elemental Analysis (EA) data of the as-synthesized material reveals that there are potentially nine N, N'-dimethylformamide (DMF) molecules per each hexameric macrocycle unit. The presence of DMF molecules inside the pore has been questioned because the radius of the hexamer ring is approximately 1.2 Å, which is the Van der Waals radius of a hydrogen atom. As shown in Figure 10, the size of the entrance of the pore is limited because the pyridine molecules coming from adjacent hexamer rings are blocking the entrance; therefore, it might be difficult for DMF to penetrate into the pore. On the other hand, it can be argued that the framework of macrocycles forms around the DMF molecules, trapping them inside the cavity. Single crystal X-ray data also shows that there is residual electron density within the cavities of the crystal structure. However, this electron density could not be refined or assigned to a specific molecule. Furthermore, the size of void is too small to fit the DMF molecules. Therefore, 9 DMF molecules must exist outside of the framework binding to the crystalline material strongly. Further TGA study can help to understand the presence of 9 DMF molecules as well.

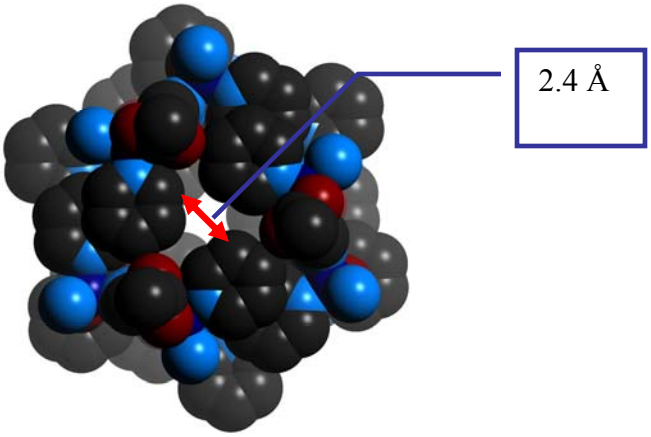

Figure 10. Top view of the channel; the diameter of the macrocycle is 2.4 Å

TGA data (Figure 11) is used to study the thermal stability of the materials, and it is an effective way to determine the amount of solvent residing within a material. The as-synthesized sample was prepared in the same way as for EA, and it was heated from room temperature to 800 °C at the rate of 1 °C/min.

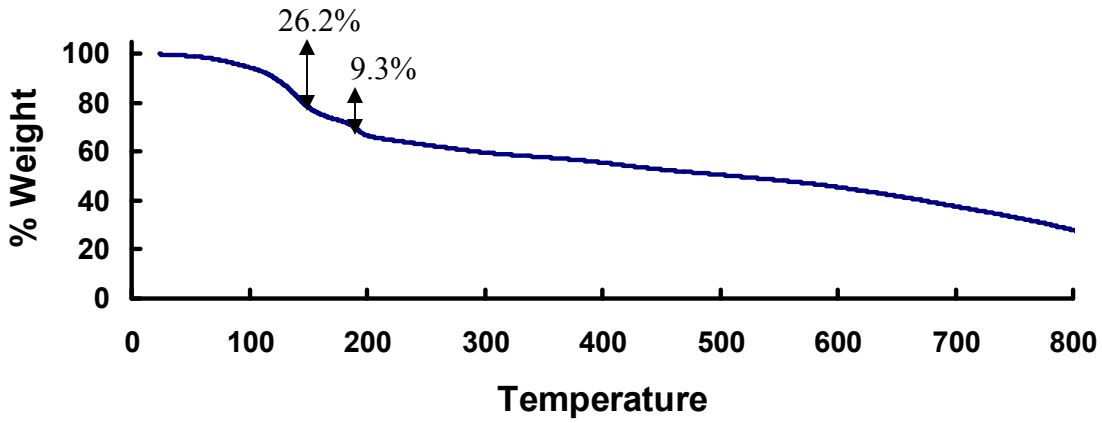

Figure 11. TGA data of the as synthesized crystals

As depicted in Figure 11, there are two major weight reductions in the TGA graph. The first weight loss is 26.2% at 170 °C, and the second one is 9.3% at 225 °C. After the two major weight losses were observed from TGA, powder X-ray pattern were collected with the sample heated at 170 and 225 °C.

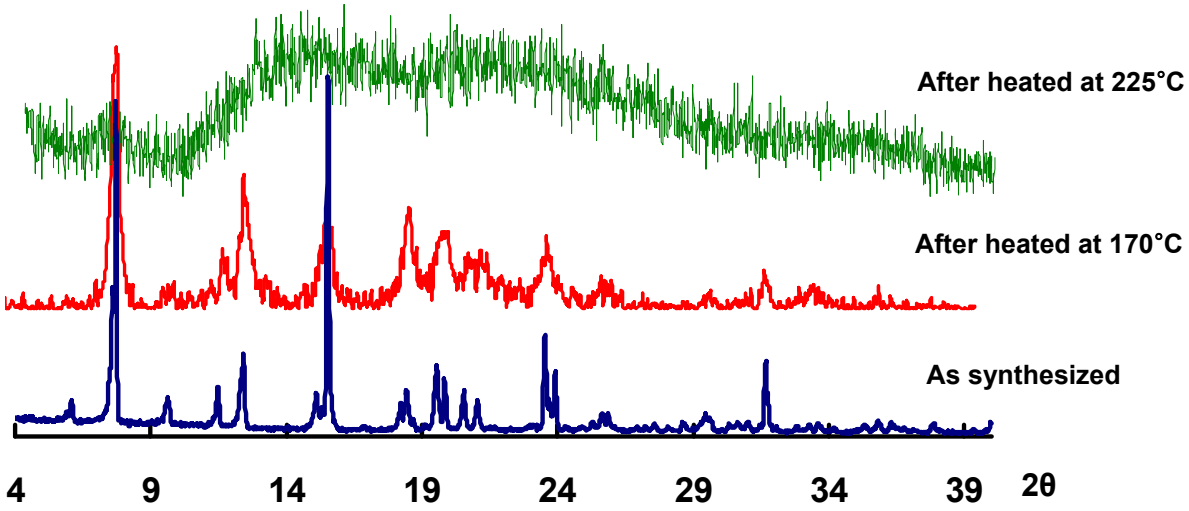

Figure 12. XPRD data of heated crystal at 170°C, 225°C

As shown in XPRD (Figure 12), the crystallinity of the framework is still intact after the first major weight loss. However, after the second weight loss, the crystalline integrity of the sample was destroyed. This implies that when the second weight loss happens, a component of the material that is necessary for structural integrity might combust. The first weight loss of 26.2% corresponds approximately to the loss of the 9 DMF molecules, which is a calculated 24.5% reduction. The second weight loss matches the loss of the coordinated pyridine. To confirm this, further systematic EA and XPRD experiments of the crystals heated at different temperatures have been performed.

Temp.	Calculated Formula from EA	Weight loss (TGA% / Cal. %)
100°C	(Zn)(Ad)(OAc)$(Py)_{0.9}$·1.0(DMF),0.5(H_2O)	7.0 / 9.9
125°C	(Zn)(Ad)(OAc)$(Py)_{0.9}$·0.5(DMF), 0.5(H_2O)	17.0 / 18.1
150°C	(Zn)(Ad)(OAc)$(Py)_{0.6}$·0.1(DMF), 0.4(H_2O)	25.8 / 29.9
175°C	(Zn)(Ad)(OAc)$(Py)_{0.6,}$ 0.4(H_2O)	28.6 / 31.6
200°C	(Zn)(Ad)(OAc)$(Py)_{0.3,}$ 0.2(H_2O)	33.0 / 36.9

Table 1. EA data of macrocycle crystal after heated at 100, 125, 150, 175, 200°C

EA data and TGA data of the crystal heated at 100, 125, 150, 175, 200 °C have been analyzed in order to track the type of molecules being removed upon increasing the temperatures. The best molecular formula fit for the EA data has been determined as shown in Table 1. It shows that the number of DMF molecules and pyridine changes upon heating to different temperatures. Most of the DMF is removed by 150 °C. The coordinated pyridine molecules are slowly removed along with DMF molecules at lower temperatures; this loss accelerates at temperatures higher than 150 °C. The EA data explain the powder x-ray pattern. The removal of DMF does not affect the integrity of the crystal. However when most of pyridine molecules are removed, especially at 200 °C, the crystal loses its integrity as shown in Figure 12. The weight loss from TGA also corresponds with the calculated weight loss based on the formula from EA data. The closely-matching values confirm the loss of DMF molecules on the surface of crystals first, then the coordinated pyridine, and lastly the decomposition of the material as temperature increases. The calculated formula from EA shows the presence of extra water molecules. It is difficult to determine the source of water because the as-synthesized crystal contains no water. Further careful study is needed for the better understanding of the composition of this framework. It is not clear where the 9 DMF molecules reside. To determine

whether the DMF molecules were merely on the surface of the crystals, a sample of the material was placed under high vacuum for 36 hours and thereafter the material was analyzed using TGA. As shown in Figure 13, two major weight losses are observed: 15.4% at 107°C and 9% at 186°C. In comparison with the as synthesized sample, there is approximately an 11% weight difference for the first weight loss, which corresponds to the DMF molecule loss. DMF molecules removed under high vacuum could be the one from the surface of the compound or from the loosely binding DMF molecules to the outside of the framework.

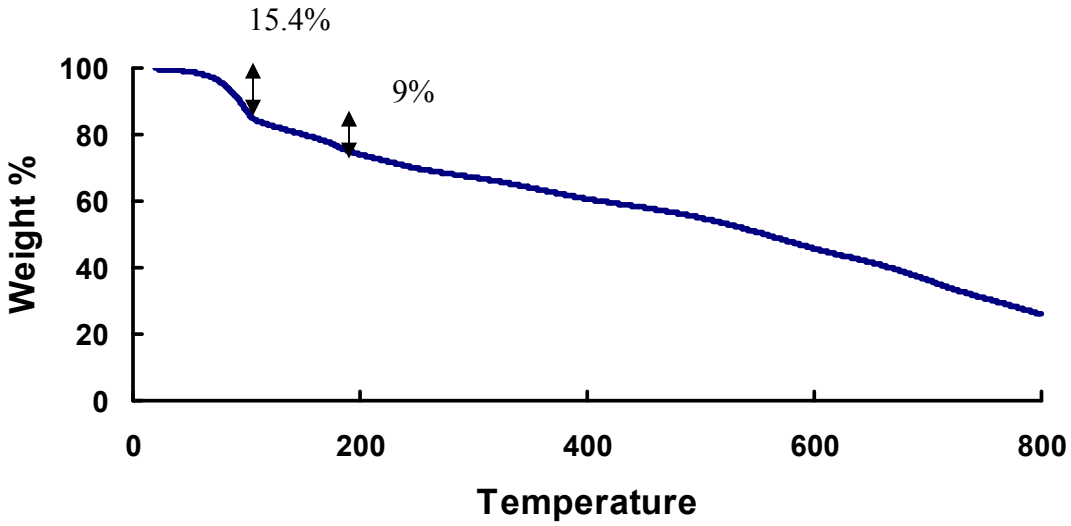

Figure 13. TGA of the as-synthesized, after 36 hours under high vacuum

2.1.3 Stability, Solubility, NMR, and Mass spectrometry

The solubility and stability of the crystals in various solvents were also tested. The crystals were soaked in various solvents such as $CHCl_3$, MeCN, DMSO, H_2O, EtOH and pyridine for 24 hours and then powder X-ray diffraction patterns were collected. The powder X-ray pattern showed that crystals are not stable in any solvents but pyridine, which is interesting. If the crystal loses its integrity by losing a coordinated pyridine in the presence of other solvents or upon heating, then the converse, increased crystalline stability in pyridine, should be and has been proven true. Pyridine also plays an important role in forming crystals because the crystals grow faster and bigger when more pyridine is added. While testing the stability of crystals, it was found that the crystals were soluble in DMSO, which allows investigations into the solution chemistry of the macrocycles. First, though, the compound's integrity in DMSO needed to be proven. NMR and mass spectrometry studies were performed to determine whether the hexameric macrocycles remained intact in DMSO. In the ^{1}H NMR of the compound, peaks of DMF, pyridine, acetate and coordinated adenine were seen. (Figure 14) The signal for H9 at 12.8 ppm in the ^{1}H NMR of pure adenine disappears in the ^{1}H NMR of crystal, implying that the H9 is removed through coordination of N9 with the zinc metal ion. Plus, H8 has been shifted downfield due to coordination between the nitrogen and zinc atom. However, these observations do not conclusively prove that the macrocycle is intact since the signals could result from fragments of the macrocycle. Mass spectroscopy data were also inconclusive.

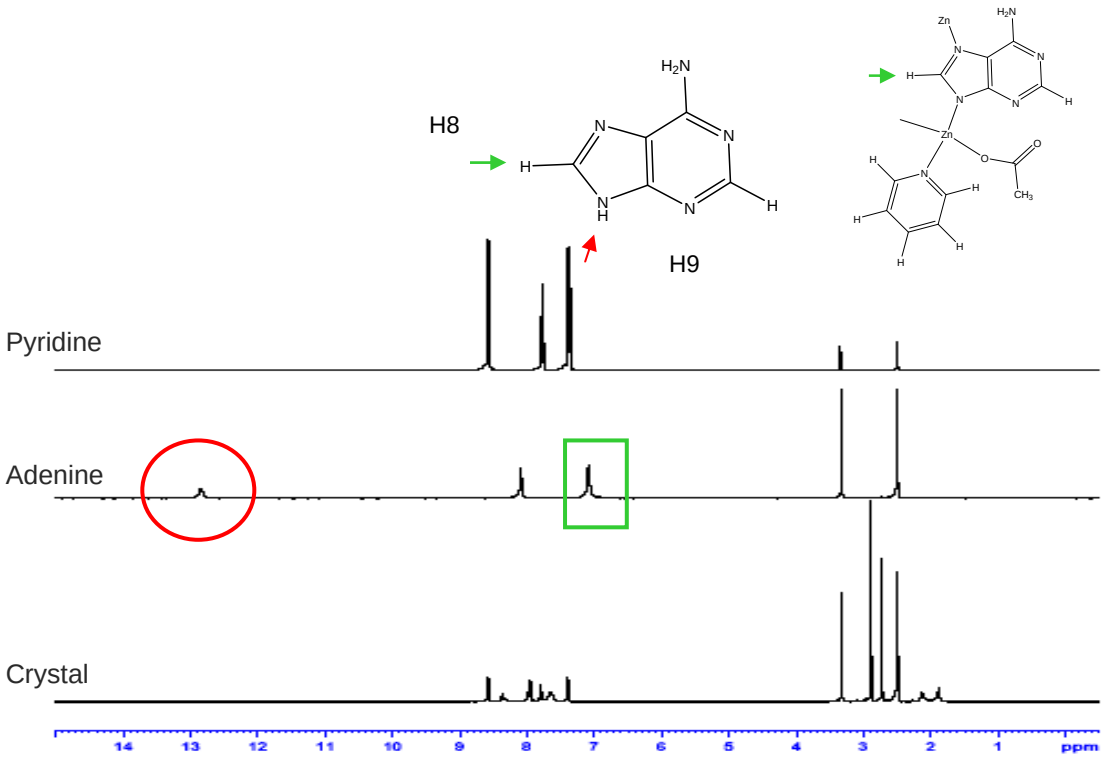

Figure 14. ^{1}H NMR spectrum; pyridine, adenine, hexameric macrocycle crystals

2.1.4 Gas Sorption Study

Since there are one-dimensional channels in the 3-D structure of the crystal, the porosity of the structure was examined using gas sorption measurements. Nitrogen and hydrogen sorption experiments were performed. An isotherm of both gas sorptions showed a type III pattern[14] which represents a non-porous material. Since the pore size of this material is approximately the size of a hydrogen atom, these results are reasonable. Although the pore size is approximately the size of a hydrogen atom, hydrogen gas sorption might be difficult because hydrogen gas molecule is diatomic. Currently we are investigating methods aimed at making the pores of this

material more accessible to gas molecules. As mentioned earlier, the coordinated pyridine molecules block the entrance to the internal cavities within the crystal structure. We are trying to replace these pyridine molecules with smaller species to gain accessibility to the pores.

2.1.5 Linking the macrocycles into extended structures

Since the zinc tetrahedra in the macrocycle are coordinated to an acetate and a pyridine, we reasoned that we might be able to link the macrocycles together into a 3-D framework if we used a bipyridine instead of pyridine or a dicarboxylate instead of acetate. In this fashion, we envisioned using the macrocycle as a "building block" for the construction of frameworks with 3-D connectivity. The first trial was to remove the coordinated pyridine or acetate group from the zinc metal, so that a non-coordinated site could be available for the further connection of the macrocycles. In order to prevent pyridine coordination, pyridine was substituted with analogues: 2, 6-lutidine, 1-picolin, 3-picolin, etc. The nitrogen on these molecules may not easily coordinate to the zinc metal due to steric hindrance from the alkyl groups adjacent to the nitrogen. We also reasoned that we might be able to link the macrocycles together if we used zinc salts with non-coordinating anions such as Zinc tetrafluoroborate. These efforts were unsuccessful. In addition, secondary linkers that could replace the pyridine and acetate groups have also been investigated. Various bipyridines or dicarboxylic acids were used to link the macrocycles by replacing the pyridine or the acetate groups. To date, these strategies have not been successful.

2.2 Zn(Ad)(Py)(NO_3) · (xDMF)

If zinc acetate is replaced with zinc nitrate in the synthesis for the hexameric macrocycle, yellow block-shaped crystals are produced. The reaction conditions were similar to those of the zinc acetate hexameric macrocycles except for the reaction temperature. The crystal structure of the material reveals that Zn(II) tetrahedra are bridged together by the imidazolate rings of the adeninate, forming a one-dimensional helical coordination polymer. A nitrate group and a pyridine complete the tetrahedral coordination around the Zn(II). The overall crystal structure is composed of both right-handed and left-handed helices. Neighboring helices hydrogen bond to each other through the amino hydrogens and the N1 nitrogens of adjacent adeninates. It is interesting to note that the zinc in the hexameric macrocycle also coordinate with adenine in the same manner (nitrogens of the imidazole ring) but it forms a macrocyclic ring. (Figure 15) Complete characterization of this 1-D coordination polymer (XPRD, EA and TGA) has been performed.

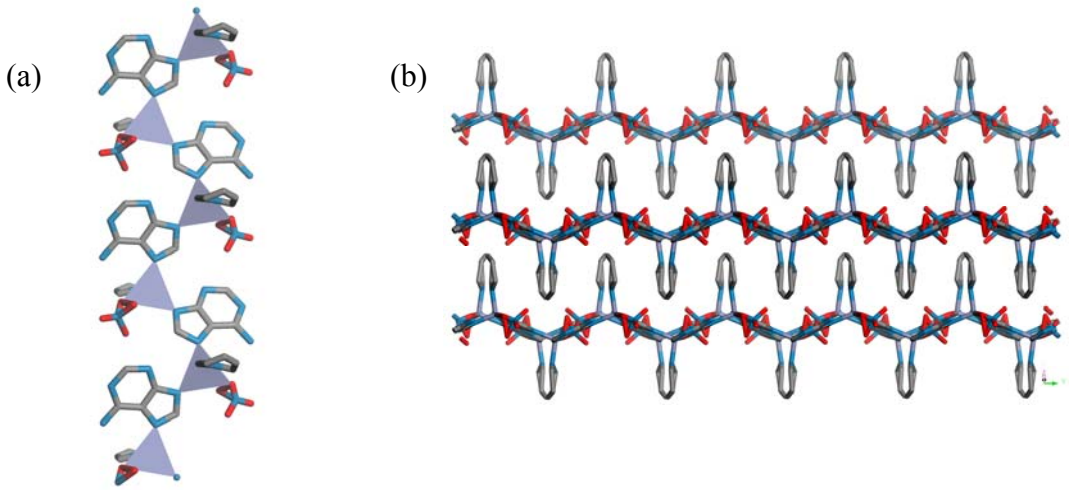

Figure 15. Zn(Ad)(Py)(NO_3) · (xDMF), 1-D polymeric chain (a)1-D helix (b) packing of the chains

After approximately 1 year, an XPRD pattern of an aged polymer crystal was collected. Surprisingly, the XPRD pattern was the same as that of the macrocycle, not the polymer. A question was raised: “Could the polymer rearrange to form the macrocycle?” This formation of the macrocycle crystal from the polymer crystal after a certain time led to a study about relationship between the polymer and macrocycle crystals. The polymer might be the kinetically stable product, while the macrocycle is the thermodynamically stable product. This idea was supported by the fact that the macrocycle crystal could be synthesized using the same reaction conditions but at higher temperature than those of the polymer, as described in the following section.

2.3 $Zn(Ad)(Py)(O_2CN(CH_3)_2) \cdot (1.75DMF)$

2.3.1 Structure

The basic coordination pattern is similar to that of Zn(Ad)(Py)(OAc) · (1.5DMF**).** Six of the adenines and zinc ions are connected to each other, forming hexameric macrocycles. The zinc cations adopt a tetrahedral geometry. Interestingly, pyridine and N, N-dimethyl carbamate are connected to the zinc instead of the acetate group (Figure 16). These macrocycles are also packed together by hydrogen bonding in the extended crystal structure. Further explanation about generation of the carbamate group will be in the next section.

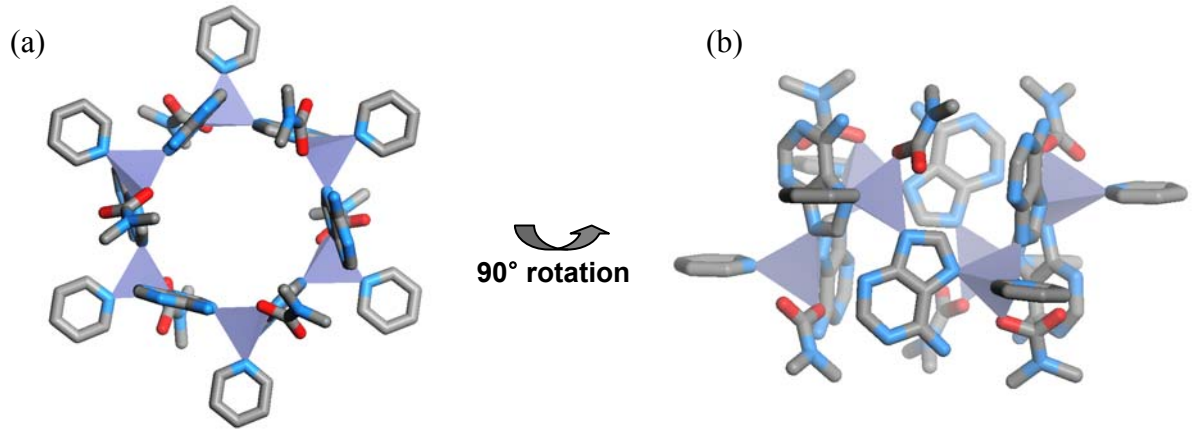

Figure 16. Zn(Ad)(Py)($O_2CN(CH_3)_2$) · (1.75DMF) (a) top view, (b) side view

2.3.2 Reaction Condition Optimization

Temperature is the key for synthesizing the zinc-adeninate macrocycle rather than the polymeric chain. Macrocycle was synthesized when the reaction was heated at 130 °C for 24 hours. This condition however was problematic because the crystals formed with a low success rate after one week. However, when the reaction was heated at 130 °C for 36 hours, the crystals grew after 3-4 days, and half of the reactions were successful. It is apparently difficult to synthesize the macrocycle compared to the polymer, but extending the heating time produced faster-growing macrocycle crystals with a better yield. However, there was a purity problem when the reaction was performed in sealed glass tubes. Often the crystals were synthesized with some powder, and separation of the pure crystals proved difficult. Further reaction condition optimization was carried out: the reaction was performed in a Teflon-lined autoclave at 140 °C for 24 hours. These conditions resulted in good crystal growth after 1-2 days with excellent

yield and purity. The reason for the difficult synthesis of the macrocycle can be explained in two ways. First, there is an entropic penalty in folding the free chain into a limited shape like the hexameric ring. Second, the macrocycle crystal is attached to a N, N-dimethyl carbamate group instead of nitrate group. According to Dell'Amico et al, N, N-dialkyl carbamate can be synthesized successfully in the presence of Zn/CO2/$NH(Et)_2$ at 150 °C and a higher pressure (180 atm).[15] When the reaction was performed in Teflon-lined autoclave at conditions at 140 °C, N, N-dimethyl carbamato can be synthesized through the decomposition of H_2O and DMF.

2.3.3 Properties

Since the two hexameric macrocycle crystals (one with acetate and another with carbamate) are structurally similar, they share similar properties but behave differently. $Zn(Ad)(Py)(O_2CN(CH_3)_2)\cdot$ (1.75DMF) has an N, N-dimethyl carbamate group coordinated in the framework rather than an acetate group. The radius of the pore is approximately 1.2 Å but slightly bigger than the zinc acetate hexameric macrocycle. It is probably due to the carbamate group. One of the big differences lies within TGA data. As shown in Figure 17, there is a single significant weight change around 100 °C of 43%. From the EA data, 1.75 DMF molecules were removed and either carbamate group or pyridine must be combusted.

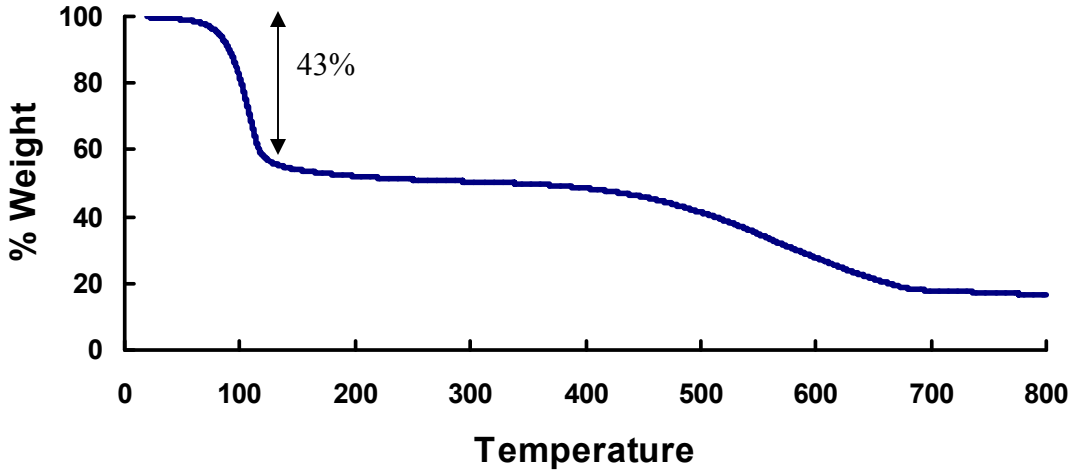

Figure 17. TGA of Zn(Ad)(Py)($O_2CN(CH_3)_2$) · (1.75DMF), as synthesized

2.3.4 Kinetic vs. Thermodynamic Control Study

The formation of polymer and hexameric macrocycle crystals can be explained through kinetic and thermodynamic control (Figure 18). At low temperatures, product A (1-D polymeric chain) is favored because the barriers for the formation of the product determine the product ratio. At higher temperatures, product B (hexameric macrocycle) is favored because all barriers on the energy surface are surmountable, allowing all the molecules to find the most stable point on the surface. Therefore, the polymer crystal can be easily formed after heating to 100 °C due to a lower energy barrier, whereas the macrocycle crystal can be formed at a higher pressure and temperature to overcome the higher barrier.

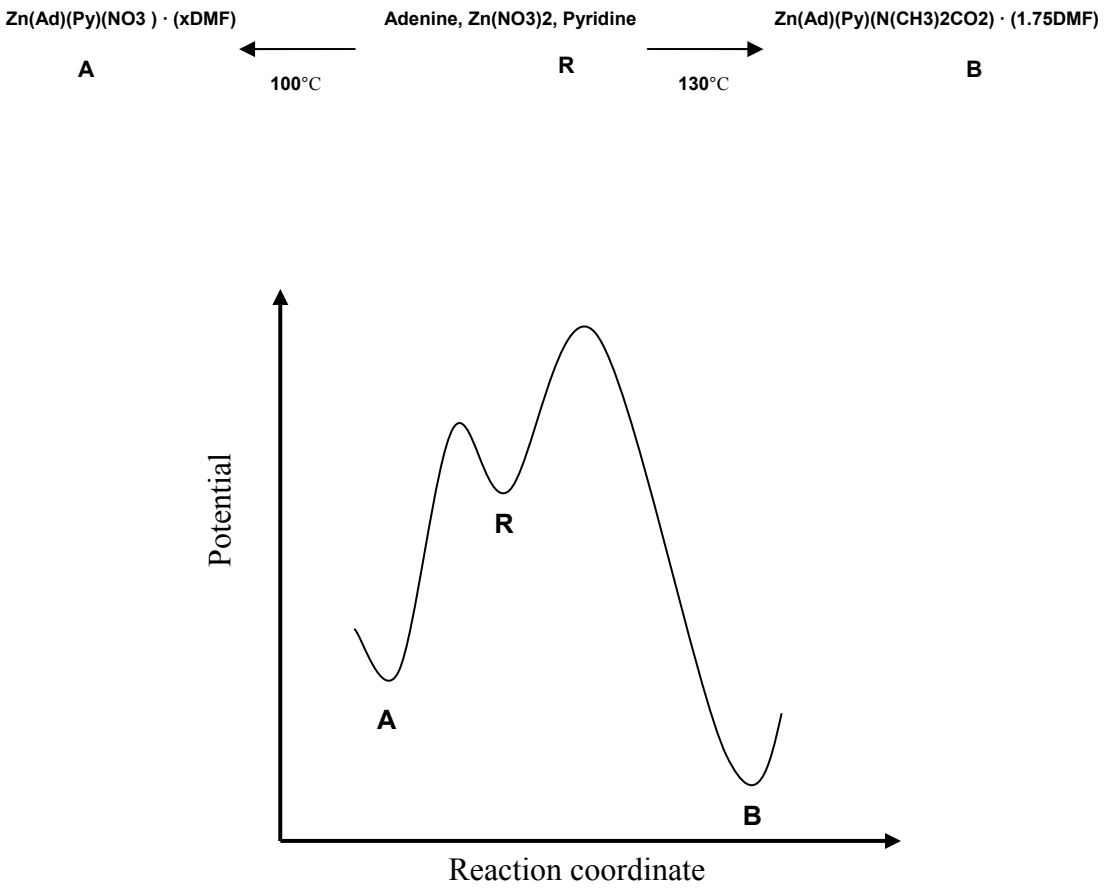

Figure 18. Kinetic product A and the thermodynamic product B

3.0 ZINC – ADENINE/BPDC FRAMEWORK

3.1 $Zn_2(Ad)(BPDC)_{1.5}O_{0.25} \cdot 0.5(NH_2(CH3)_2)^+$, 2.75($H_2O$), 2(DMF)

This framework was made while attempting to link the hexamer rings into a three-dimensional structure using a dicarboxylate. It has a unique structure and properties to be a candidate for various potential applications. It is a three-dimensional porous framework in which zinc-adenine clusters are linked by 4, 4'-biphenyldicarboxylic acids. Thus far, several interesting properties have been discovered and investigated: the crystals are very stable in various solvents and under the atmosphere, and it is an anionic framework containing cations inside. This compound has been fully characterized and currently it is being investigated as a potential material for gas storage and drug delivery.

3.1.1 Structure

This framework has a unique and interesting structure. First of all, there are adenine-zinc motifs which have an octahedron shape as shown in Figure 19. N1 and N2 of the adenine bridge the Zn^{2+} metal ions and N7 and N9 also connects other Zn^{2+} metal ions together. The zinc cations adopt a tetrahedral geometry by coordinating to two adenines and two oxygen atoms from the dicarboxylate linker. Four adenines are connecting eight zinc metal ions together in this fashion. As seen Figure 20, the zinc cations located in the middle of the octahedra are coordinated by two

dicarboxylic acids, expanding the structure by connecting zinc-adenine octahedra together. Two zinc cations on the top and bottom of the octahedra are bridged by sharing an oxo anion. This oxo anion is also shared by another two zinc cations from another zinc/adenine octahedra, thus fusing the two octahedra together. The zinc-adeninate octahedra are connected in this manner and form a one-dimensional chain of fused zinc-adeninate octahedra.

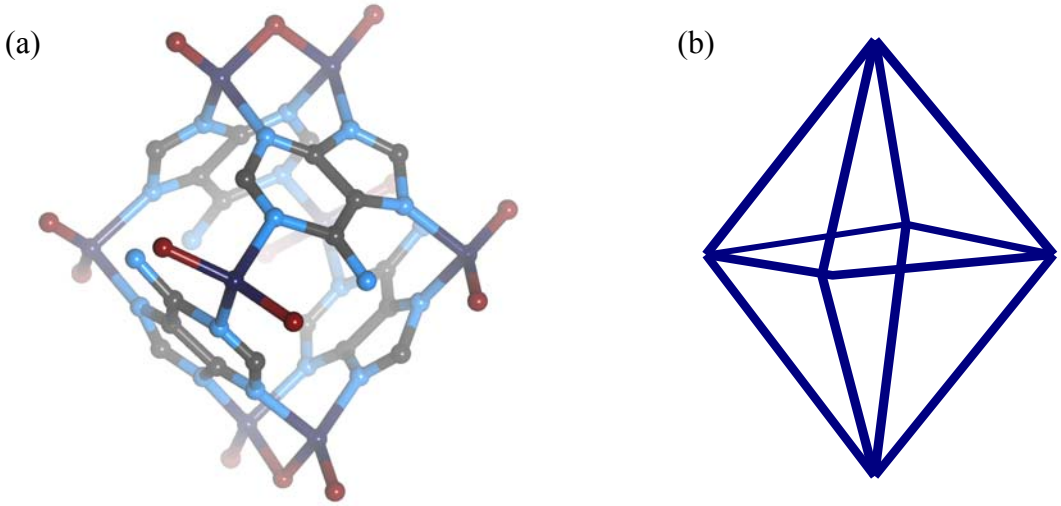

Figure 19. (a) Zinc-adenine cluster, (b) octahedron shape of the cluster

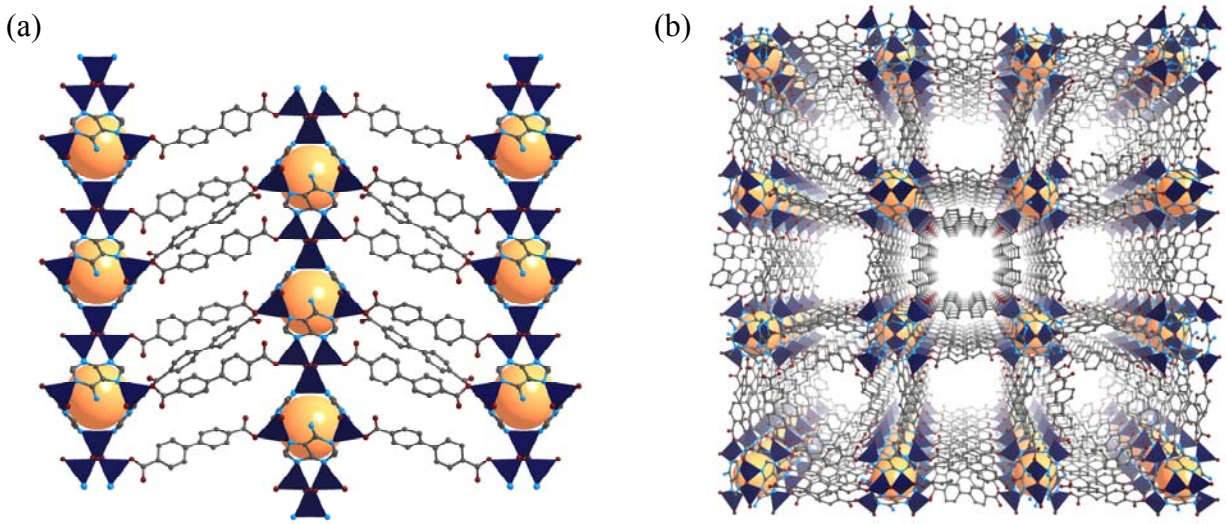

Figure 20. (a) Zinc-adenine cluster lined by BPDC, (b) perspective view along *C*- crystallographic axis. (O red, N blue, C gray, Zn polyhedra purple, space in the Zn/ad cluster orange ball)

4, 4-Biphenyldicarboxylates connect the chains of zinc-adeninate octahedra, resulting in the formation of one-dimensional channels as seen Figure 21. The resulting channels have two different sizes and they are approximately 7.6 Å and 9.4 Å.

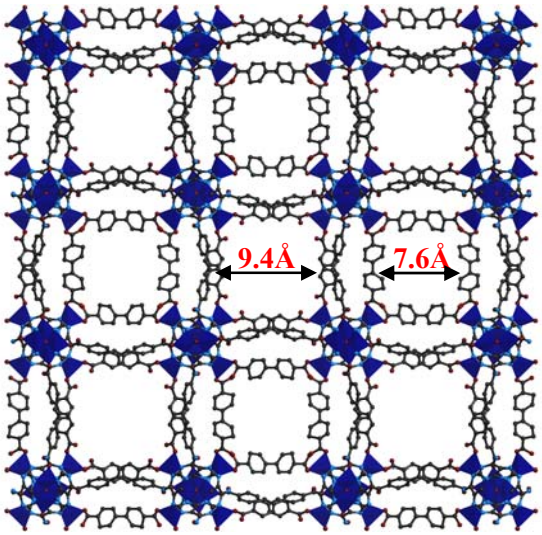

Figure 21. Two different sizes of the pores

One thing to take note of in this framework is the size of the zinc/adeninate octahedra. Each octahedron has a small space inside as represented by the yellow ball in Figure 20(a). However, the NH_2 group of the adenine effectively obstructs the entrance to these small cavities, rendering the space inaccessible.

3.1.2 As-synthesized and solvent-exchanged framework

Because the structure is composed of large zinc-adeninate chains connected by biphenyl linkers, I decided to study its structural stability in the presence of various solvents. The composition of the solvent-exchanged frameworks was assessed by EA and TGA while power X-ray patterns were collected to assess the stability of the framework.

3.1.2.1 EA

From the EA data, the number of molecules inside of pores in the framework has been estimated. It also verified the cationic molecules in frameworks as well. The as synthesized crystals are estimated to contain 2.75 water molecules, 2 DMF molecules and 0.5 dimethyl ammonium cations within the channels per formula unit. Since the framework has a net anionic charge (-0.5 per formula unit), the overall framework can be neutralized with 0.5 dimethyl ammonium cations which have the charge or +0.5. Crystals have also been exchanged with different solvents in order to check the stability of the framework. $CHCl_3$ exchange is useful because chloroform is easily removed from the pores due to its low boiling point (61°C) compared to that of DMF (153°C), which is used as a mother liquor. Due to the necessity to empty the framework before the gas sorption experiment is performed, the $CHCl_3$ exchange is better because it can be easily removed.

3.1.2.2 XRPD

Powder X-ray of the as synthesized crystal and the solvent exchanged crystals has been studied. As shown Figure 22, the crystals are stable in water, acetonitrile, chloroform, and ethanol. More interestingly, this framework is very stable in water, whereas many MOFs are unstable in water. Since the adeninate framework can be used as a target for biological applications, its stability in aqueous solution is very important and beneficial.

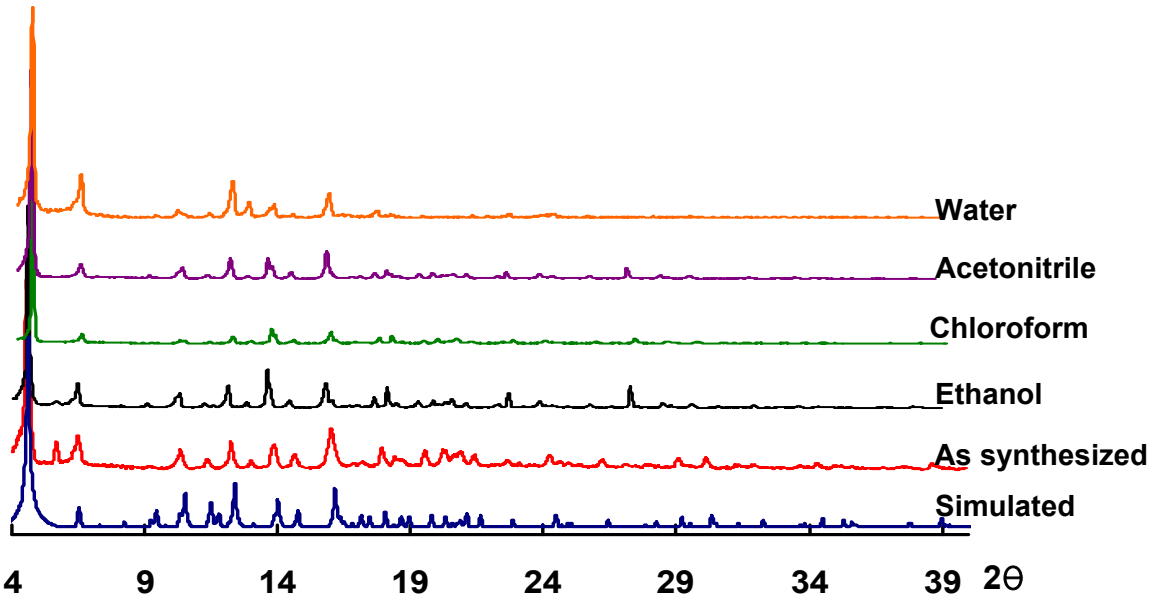

Figure 22. Powder X-ray Pattern of solvent exchanged crystal

This framework is also stable in biological buffers and different pHs. (Figure 23) The framework maintains its crystalline integrity at pH7.4 and pH6.5. When it was treated at pH5.5, the powder x-ray pattern shows that there are some peaks indicating that it still has the original crystallinity, but there are also new peaks, indicating that the structure of the framework changes slightly at pH5.5.

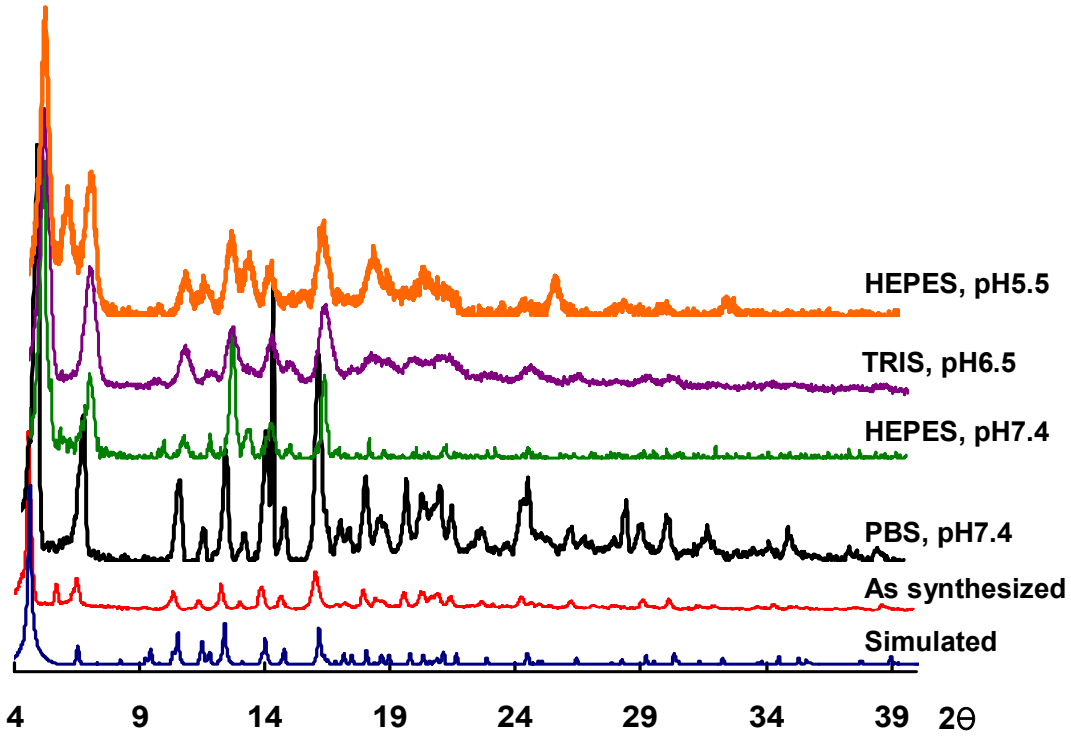

Figure 23. XPRD in different buffers

The stability of the framework in biological buffers, especially from pH7.4 to pH6.5 shows that the framework has a potential for biological application.

3.1.2.3 TGA

TGA data verify the amount of solvent molecules and thermal stability of the crystals. There are two major weight reductions in TGA graph. (Figure 24) The first one corresponds to the loss of water and DMF molecules, which are 25.3% and the second weight loss is 2.6% which corresponds to the dimethyl ammonium cation molecules. After removal of solvent

molecules, the framework is stable up to 330°C. When the temperature was increased above 330°C, the framework started to decompose.

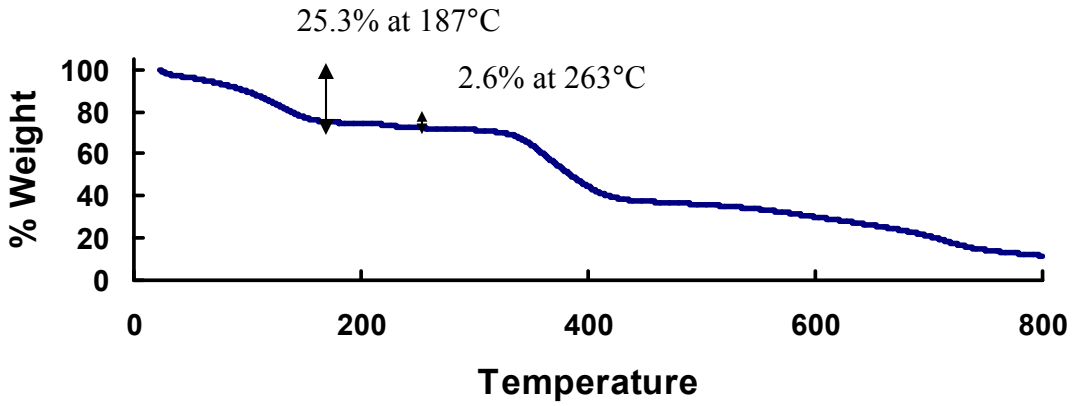

Figure 24. TGA of $Zn_2(Ad)(BPDC)_{1.5}O_{0.25}\cdot 0.5(NH_2(CH_3)_2)^+$, $2.75H_2O$, 2DMF

3.1.3 Cation Exchange Experiments

As mentioned before, the framework is anionic, and contains 0.5 dimethyl ammonium cations. These cation molecules are not part of the framework structure and they exist outside of the framework. Thus dimethylammonium cations can be easily exchanged with other cationic molecules.

3.1.3.1 Potential Application

The cation exchange of anionic framework has been studied beforehand.[16] Cationic exchange frameworks can be useful for various applications by exploiting the unique properties

of the exchanged cationic molecules. For example, gas sorption capacities can be tuned depending on the interaction between cations and gas molecules. Thus the impact of the cations in the framework for gas sorption can be studied. For example, when big organic cations are exchanged into the pores, the overall pore volume will decrease, and the framework could then be used to selectively adsorb molecules of certain sizes. In addition to studying the impact of the exchanged cations on the gas sorption properties, we also want to study the mobility of the cations within the pores by measuring the cationic conductivity.[17] Given that these materials have ordered, one dimensional pores, they may be suitable as a conduit for small metal cations such as Li^+ or Na^+ or even H^+. Finally, one of the important aspects of the adeninate framework is biological application. Cationic drug molecules can be loaded in to the framework readily by a cation exchange process. We can then study the release profile of these drug molecules in biological buffers, as the sodium and potassium ions in the buffers will slowly replace the drug molecules within the framework. By measuring the amount of cation molecules exchanged, the controlled release of the drug molecules in biological system can be studied.

3.1.3.2 Experiment Results

The procedure of the cation exchange is similar to the solvent exchange experiments. The crystals are soaked in the concentrated solution of cationic molecules until it is fully exchanged. The results of the cation exchange experiments are shown in Table 2. Its completion is confirmed by EA. After a success of the lithium and sodium cation exchange experiments, further systematic cation exchange study has been decided. Thus, nickel and cobalt exchanges were tried besides lithium and sodium. Plus, big organic cationic molecules also have been used. Organic molecules are chosen depending on the size and functional group (Figure 25). EA data confirmed the completion of the exchanging experiments. For Ni^{2+}, Co^{2+} exchanged sample, the ratio of

both metals (Zn/Ni, Zn/Co) could be checked by EDX (Energy-dispersive X-ray Spectroscopy). EDX data supported the full exchanged of the metal ions nicely. However, Li^+, Na^+ were not able to be checked by EDX. EDX cannot detect Li^+ due to its light weight. For the sodium, because ZnL peak of the zinc and NaK peak of the sodium were overlapping each other, it was impossible to calculate the accurate ratio between zinc and sodium metals unless overlapped peaks were separated. However, ICP (Inductively coupled plasma) would be the alternate way to find out the ratio of the lithium and sodium.

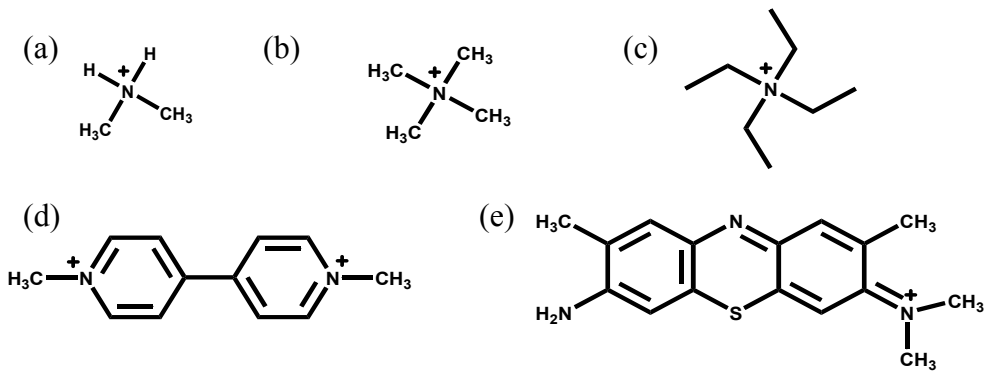

Figure 25. Cationic organic molecules (a) dimethyl ammonium (as synthesized), (b) tetraethyl ammonium, (c) tetraethyl ammonium , (d) methyl viologen, (e) toluidine blue O

Cationic Molecules	Formula
Li^{+}	$Zn_2(Ad)(BPDC)_{1.5}O_{0.25} \cdot 0.5(Li)^{+}$, $1.75H_2O$, $1.75CHCl_3$
Na^{+}	$Zn_2(Ad)(BPDC)_{1.5}O_{0.25} \cdot 0.5(Na)^{+}$, $2.0H_2O$, $0.75\ CHCl_3$
Co^{2+}	$Zn_2(Ad)(BPDC)_{1.5}O_{0.25} \cdot 0.3(Co)^{2+}$, $2.75H_2O$, $1.0\ CHCl_3$, $0.1(BF_4)^{-}$
Ni^{2+}	$Zn_2(Ad)(BPDC)_{1.5}O_{0.25} \cdot 0.78(Ni)^{2+}$, $2.25H_2O$, $0.75\ CHCl_3$, $1.06(Cl)^{-}$
$N(CH_3)_4^{+}$	$Zn_2(Ad)(BPDC)_{1.5}O_{0.25} \cdot 0.5(N(CH_3)_4)^{+}$, $0.75H_2O$, $2.25\ CHCl_3$
$N(CH_2CH_3)_4^{+}$	$Zn_2(Ad)(BPDC)_{1.5}O_{0.25} \cdot 0.5(N(CH_2CH_3)_4)^{+}$, $0.25H_2O$, $2.0\ CHCl_3$
Toluidine Blue O	$Zn_2(Ad)(BPDC)_{1.5}O_{0.25} \cdot 0.5(TBO)^{+}$, $0.75H_2O$, $2.25\ CHCl_3$
As synthesized (dimethyl ammonium)	$Zn_2(Ad)(BPDC)_{1.5}O_{0.25} \cdot 0.5(NH_2(CH_3)_2)^{+}$, $2.75H_2O$, $2\ CHCl_3$

Table 2. Calculated formula of the cation exchanged frameworks

The stability of the framework after cation exchange is also important and it is confirmed by XRPD data as shown as Figure 26.

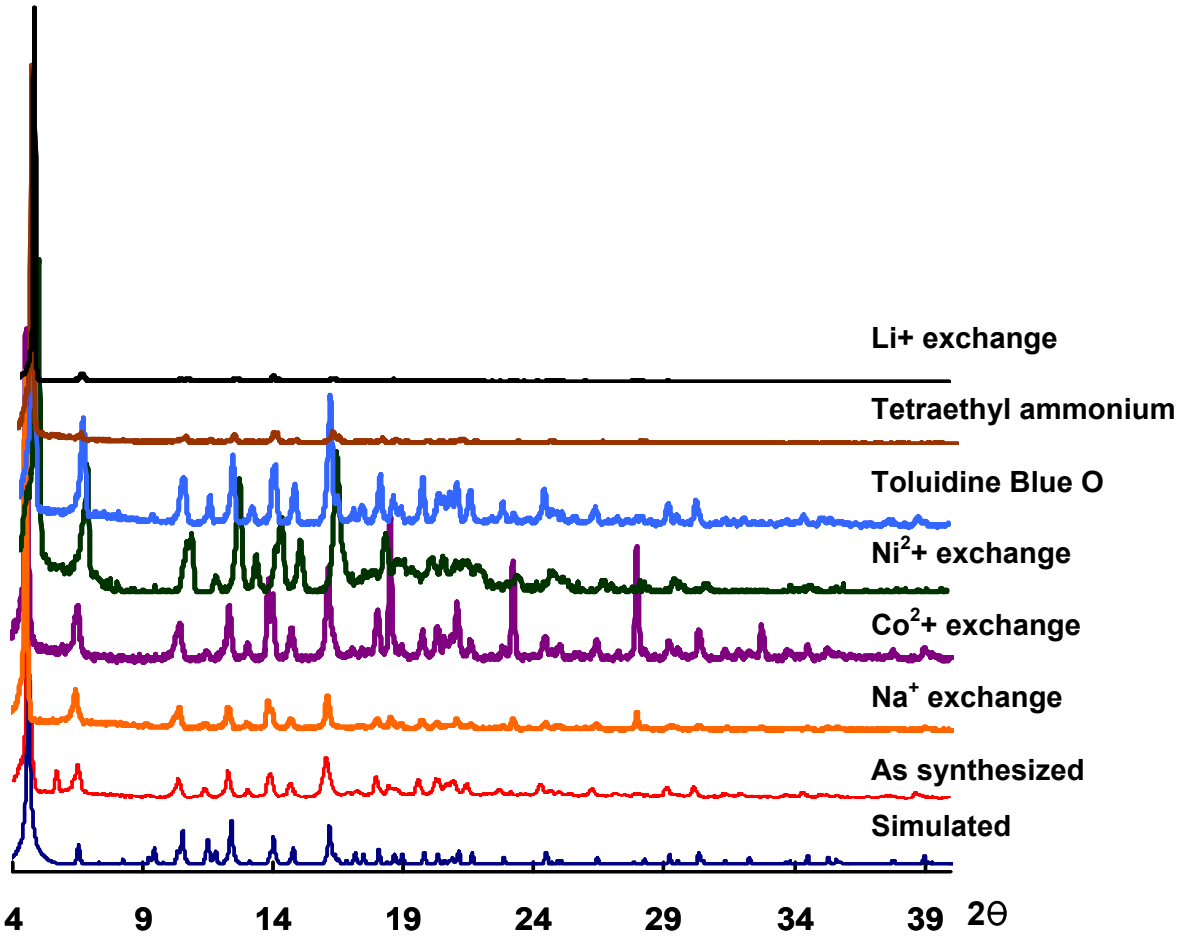

Figure 26. Powder pattern of cation exchanged crystals

3.1.4 Gas Sorption Studies

3.1.4.1 Activation Temperature

The preparation of a sample for a sorption experiment has a significant impact on the outcome of the experiment.[18] Activation of the framework is part of sample preparation. The framework can be activated by heating at different temperatures. The crystals were first chloroform exchanged, which enabled facile removal of the guest molecules, and then the crystal sample was treated at different temperatures, such as at rt, 100, 150, and 200°C. Crystals were heated at each temperature during the degassing process. Interestingly, the amount of gas uptake changed depending upon the activation temperature. BET surface area were shown as rt <150°C < 100°C. As a result, when the crystals were heated at 100°C, the gas sorption showed highest surface area. This trend was the same for both N_2 and H_2 sorption. When the material was activated at 200°C, the framework was not porous. Therefore, all further gas sorption experiments were performed with 100°C activated samples.

3.1.4.2 Cation Exchange

The sorption experiments of the cation exchanged crystals showed interesting results. So far, the N_2, H_2 gas sorption experiments of Li^+, Na^+, Co^{2+}, Ni^{2+} exchanged crystal have been done. The impact of the cations for gas sorption can be different depending on the degree of the interaction between cations and gas molecules. The space that cations occupied inside of the pore can also impact the results. The experimental results show that BET surface area for N_2 sorption is $Li^+ < Na^+ <$ As synthesized $< Ni^{2+} < Co^{2+}$. The maximum H_2 uptake percentage is $Li^+ < Na^+ <$ As synthesized $< Ni^{2+} < Co^{2+}$. It might be early to conclude anything without further studies, but it seems that when heavier atoms are inside, the more gas molecules are adsorbed. When smaller

cations are inside the pores, one might expect more adsorption of gas molecules due to bigger space availability. Ni^{2+} and Co^{2+} are bigger than Na^{+} and Li^{+} but they only exist in the framework as half occupancy due to the double charge. Therefore, the observed results could be due to stronger interaction between cations and gas molecules rather than space. Further study with heavier atoms such as cadmium and lead will provide a better understanding.

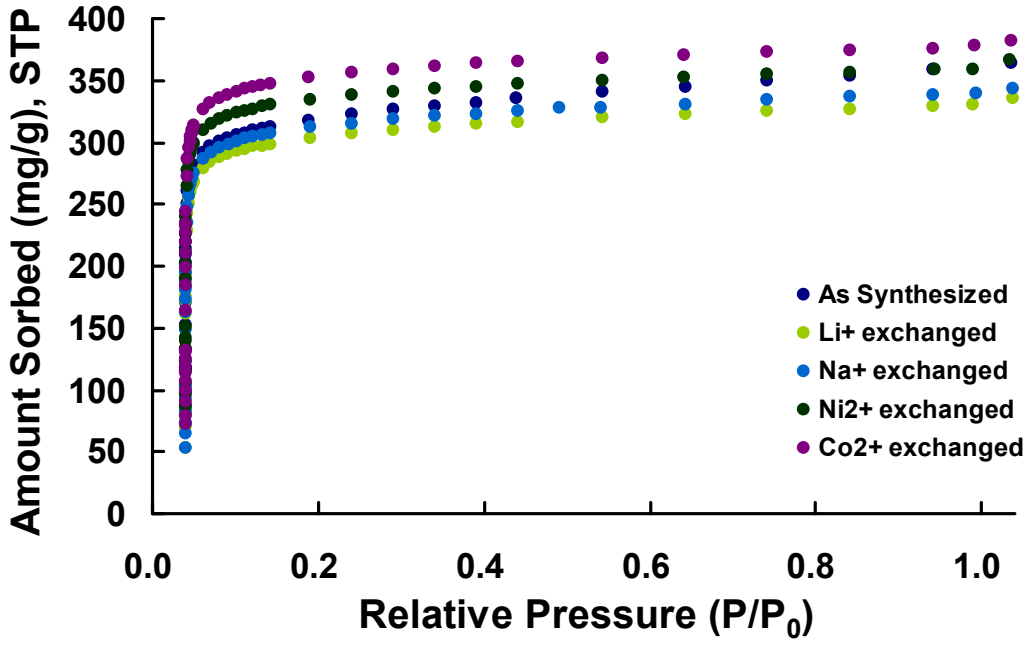

Figure 27. N_2 Isotherm for the as synthesized and cation exchanged

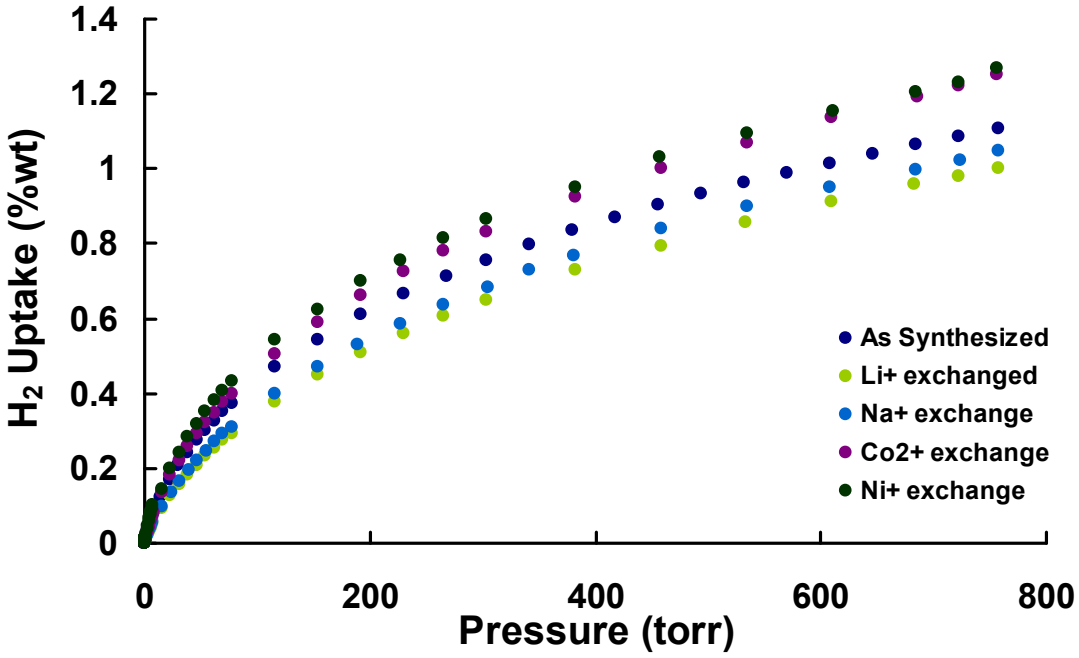

Figure 28. H_2 Isotherm for the as synthesized and the cation exchanged materials

3.1.5 Cation Controlled Release

In general, porous materials[19] are attractive for drug delivery applications. So far, most of drug deliveries depend upon using biocompatible dendrimers or polymer materials. Recently, metal organic frameworks[10(a)] have been investigated as materials for drug delivery. MOFs have many characteristics which make them attractive candidates for drug delivery: 1) MOFs have very rigid structures with high surface areas and pore volumes, 2) they can be rationally designed and synthesized by using different organic building blocks or biological molecules. By making MOFs with biological building block molecules, the biocompatibility of the framework can be improved and ultimately these molecules could be used to deliver drug molecules to a specific

target. One of the great aspects of adeninate framework is assembled from biological molecules. It can be more bio-compatible compare to the structure made by organic molecules. Therefore, drug delivery study with adeninate framework may give us a great chance to discover a future drug delivery vessel.

3.1.5.1 Experiment

The framework of $Zn_2(Ad)(BPDC)_{1.5}O_{0.25} \cdot 0.5(NH_2(CH_3)_2)^+$, $2.75(H_2O)$, $2(DMF)$ is anionic and easily exchanged with cation molecules. Cationic drug molecules can be readily loaded into the framework as well. After full loading of the drug molecules, the release profile of the drug can be measured in biological buffers such as PBS, as the sodium cations in the buffer will promote the release of the drug molecules via cation exchange. A proof-of-principle experiment was performed using Toluidine Blue O exchanged material. Toluidine Blue O is a blue dye molecule which is visible to the naked eye, and it has an absorption at 626 nm. Thus, its concentration can be easily calculated by UV-VIS.

3.1.5.2 Preliminary Results

The toluidine blue exchanged crystals and PBS buffer (0.1M, pH 7.4) were added to the UV-cell. The amount of the toluidine blue O molecules released over time was measured by UV-VIS.

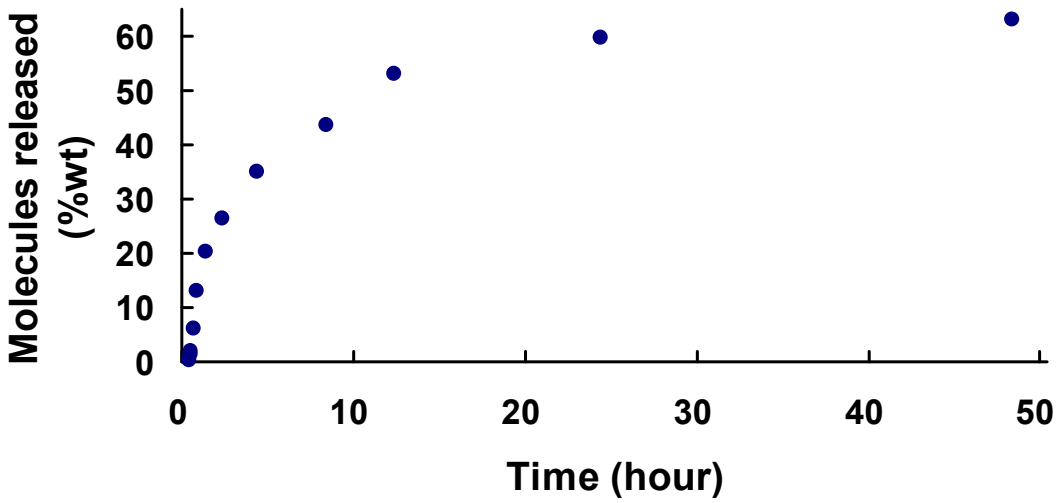

Figure 29. Toluidine blue O release measurement in PBS buffer (0.1M, pH7.4) at 37°C

As shown in Figure 29, the rate of the molecule released is faster at the beginning and it slows down over time. In the context of a drug delivery experiment, one could say that this material would give a large initial dose of the drug molecule followed by steady slow release over time. More experiments with an optimized condition need to be done for further study. Nevertheless, this preliminary result is meaningful in that it provides evidence that cation exchange processes can be used to control the release of molecules from the material.

3.1.6 Binding Motif

It is interesting that adenine binding motifs are somewhat analogous to various carboxylate motifs which have been extensively used in MOF chemistry. This can be observed from the zinc/adenine cluster in this framework. As seen Figure 30, the oxo-centered Zn_4O

cluster in this structure is similar to the one of the basic zinc acetate cluster that is commonly found for carboxylate MOFs.

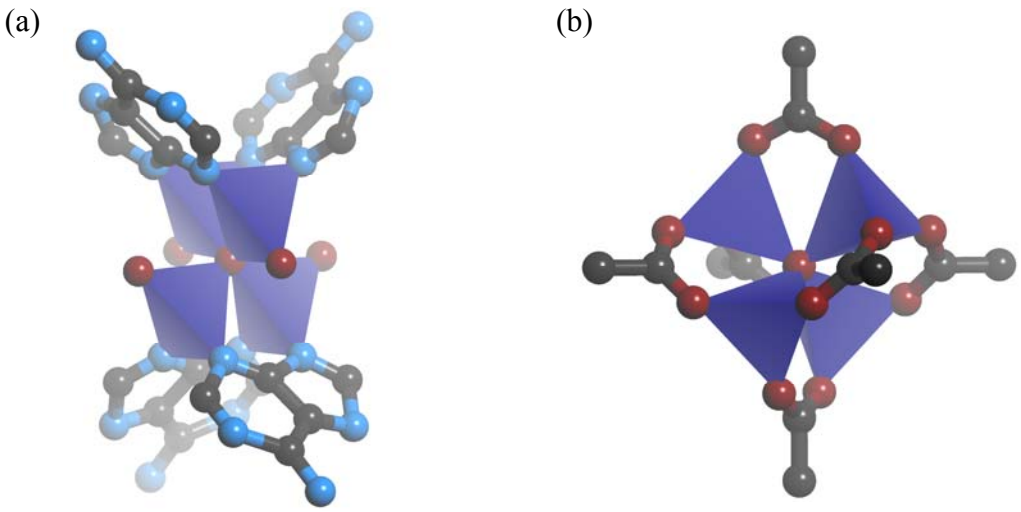

Figure 30. (a) Zn_4O cluster from Zn/Ad cluster, (b) Zn_4O cluster from carboxylate MOFs

Four zinc metals are coordinated to the center oxygen, forming a Zn_4O cluster. Adenine plays a role as a linker of the cluster, similar to the one of the carboxylic acids in carboxylate MOFs. Thus, this analogous binding motif of the adenine to the carboxylic acids shows a great potential of adenine as a ligand in future MOF chemistry. This observation points toward the eventual ability to use design strategies developed for carboxylate MOFs for adenine-based MOFs.

4.0 OTHER ADENINE CRYSTALS

4.1 $(Zn)_3(Ad)(BTC)_2 \cdot (NH_2(CH_3)_2)^+$, 5.75(DMF), 0.25($H_2O$)

When the framework of $Zn_2(Ad)(BPDC)_{1.5}O_{0.25} \cdot 0.5(NH_2(CH_3)_2)^+$, 2.75($H_2O$), 2(DMF) was made, different carboxylic acids such as 2,6-naphthalene dicarboxylic acid, benzene dicarboxylic acid, and benzene tricarboxylic acid were utilized to replace the BPDC using similar reaction conditions. We expected that we might be able to construct a similar framework, but with different organic linkers. This framework has been synthesized when benzene tricarboxylic acid (BTC) was used as a building block in the structure instead of BPDC.

4.1.1 Structure

There are two different types of Zn^{2+}: one that is a tetrahedron coordinated to three BTC's and one adenine, and two that are bridged together to form a dinuclear cluster. The two zincs in the cluster are bridged by the adenine and also by two carboxylates from two different BTC's. The final coordination site on each of the bridged tetrahedra is occupied by the oxygen from a non-bridging carboxylate of another BTC. The coordination of adenine and BTC expands the structure into different directions, resulting in a three dimensional structure. This framework also contains a pore and the size of the pore is 6.6 x 3.9 Å.

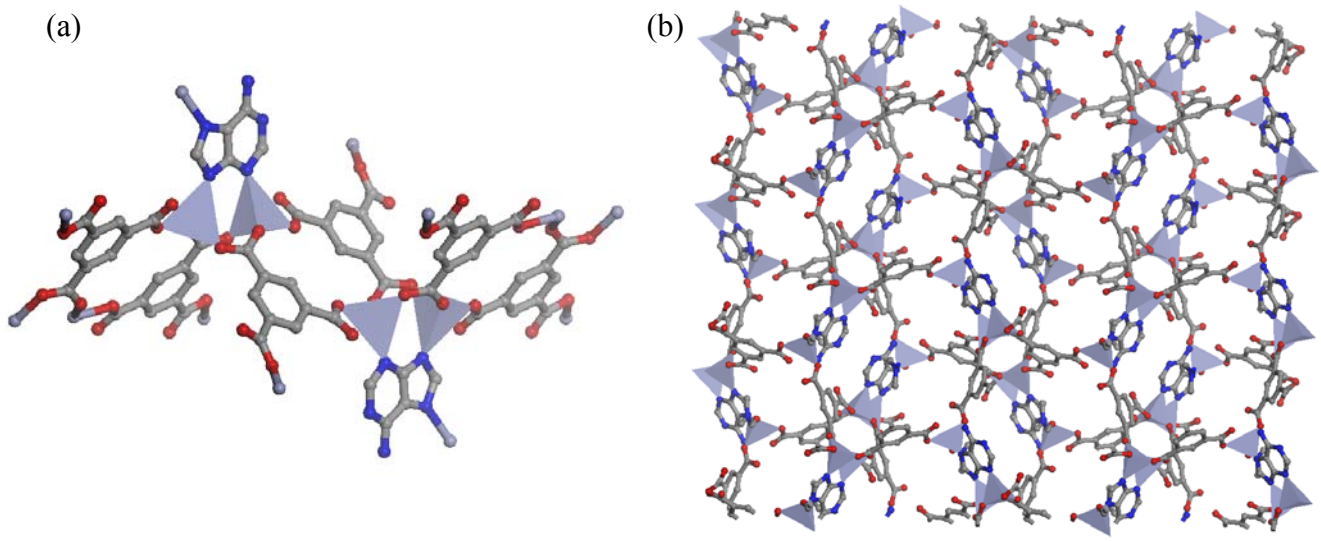

Figure 31. (a) View of the building unit (b) packing along *C*-crystallographic axis

4.1.2 XPRD, EA, and TGA

The powder X-ray pattern has been examined first. It confirmed the crystal structure and purity. The best data is shown in Figure 32. The data is complicated, because many of the diffraction peaks overlap, as seen in the simulated powder pattern. When the crystals were soaked in chloroform to remove the DMF molecules, they maintained their crystallinity, but they appeared to be less stable than the as-synthesized crystals.

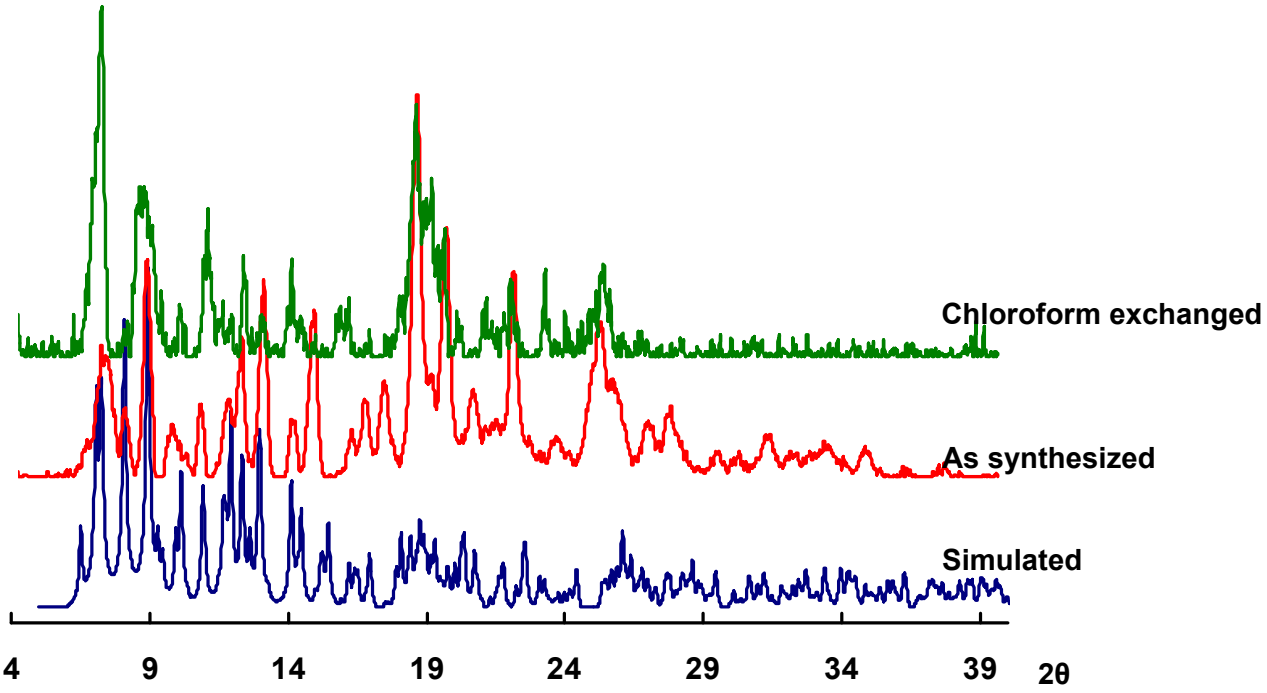

Figure 32. XPRD of the $(Zn)_3(Ad)(BTC)_2(NH_2(CH_3)_2)^+ \cdot 5.75DMF, 0.25H_2O$

This framework is anionic, and dimethyl ammonium cations are present as the corresponding cations, as confirmed by single crystal data and EA analysis. TGA data supports the EA data. The weight loss at 145°C was 38.2%, approximately the same as the calculated weight loss of the DMF and water from the structure, which is 35%. It seems that the weight loss after removal of the solvent molecules still happens even though the rate of the weight loss is subtle. Therefore, the TGA plot does not have a real plateau part which indicates the some parts of the material are still being combusted. The power pattern of the crystal heated at 165°C revealed that the crystal loses its integrity as it heated.

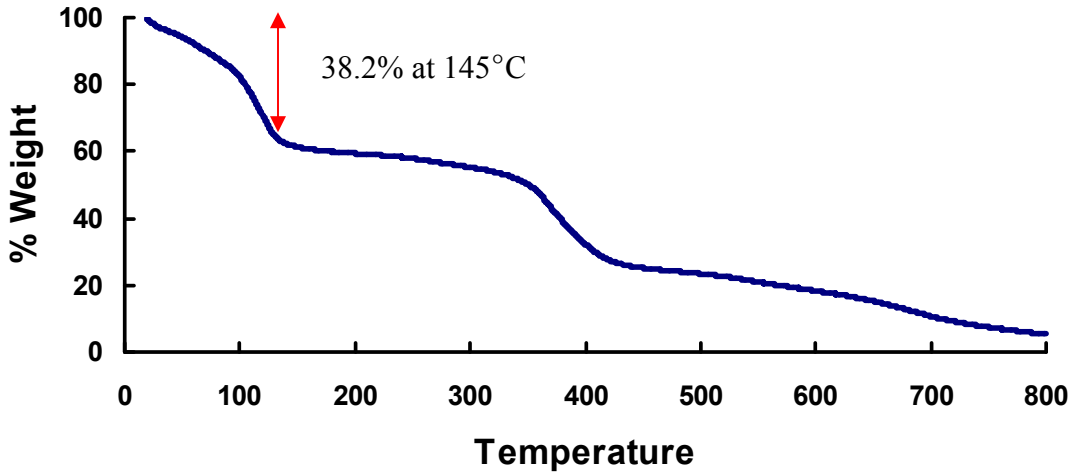

Figure 33. TGA of the as-synthesized crystal

4.1.3 Cation Exchange

Since the framework is anionic, cation exchange studies are currently being performed, but at this point they are inconclusive.

4.2 Co(Ad)(OCH_3) · 1.0(DMF), 0.25(H_2O)

4.2.1 Structure

The structure of this framework is interesting. Two cobalt metals are coordinated with four adenine and two acetate group. The coordination environment around the Co(II) is square pyramidal.

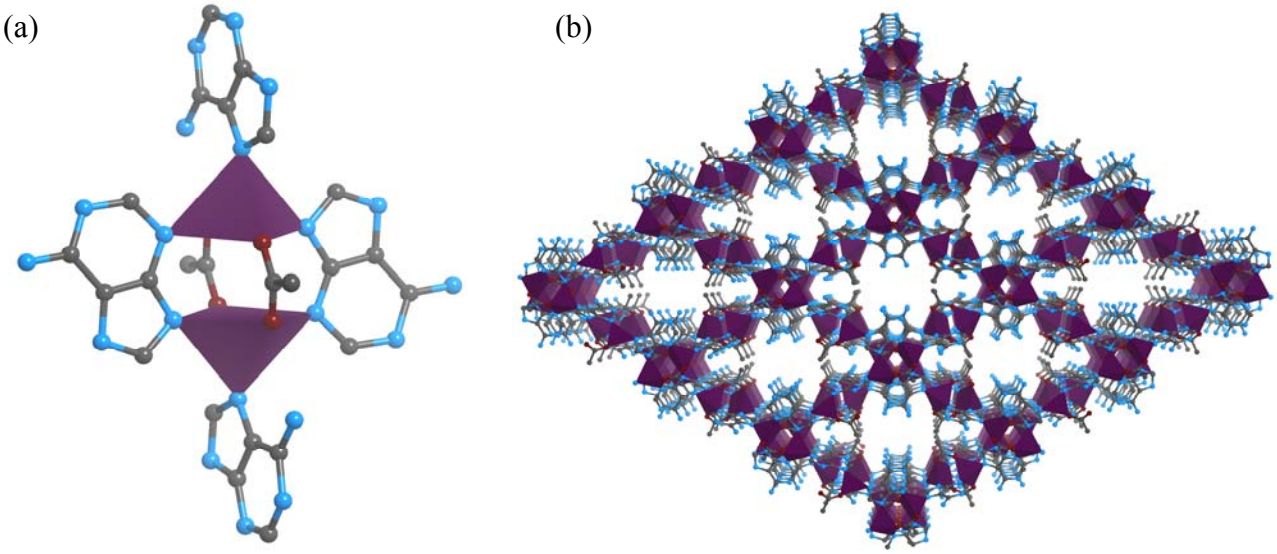

Figure 34. (a) Paddle wheel shape of the unit (b) perspective view along *C*-crystallographic axis

This unit repeats and builds a three-dimensional structure. The repeated coordination of N3, N9 of adenine and N7 of adenine to the cobalt metal builds the crystalline structure. The unit of cobalt and adenine forms a paddle wheel shape, which is ubiquitous in metal-carboxylate chemistry. This adeninate-based framework also has small pores that are approximately 4.4 x 1.8 Å. Since its pore size is small, it could potentially be used as a molecular sieve for gas

molecules. Many of the frameworks discussed thus far have metal-adeninate clusters that are analogous to the well-known metal-carboxylate clusters. When the carboxylate clusters are used to construct MOFs, they are typically linked together by linkers such as 1,4-BDC (Figure 35), so the distance between the clusters is large, resulting in larger pores. In the metal-adeninate frameworks, however, the clusters are linked together by the adenine ring. This results in smaller pores.

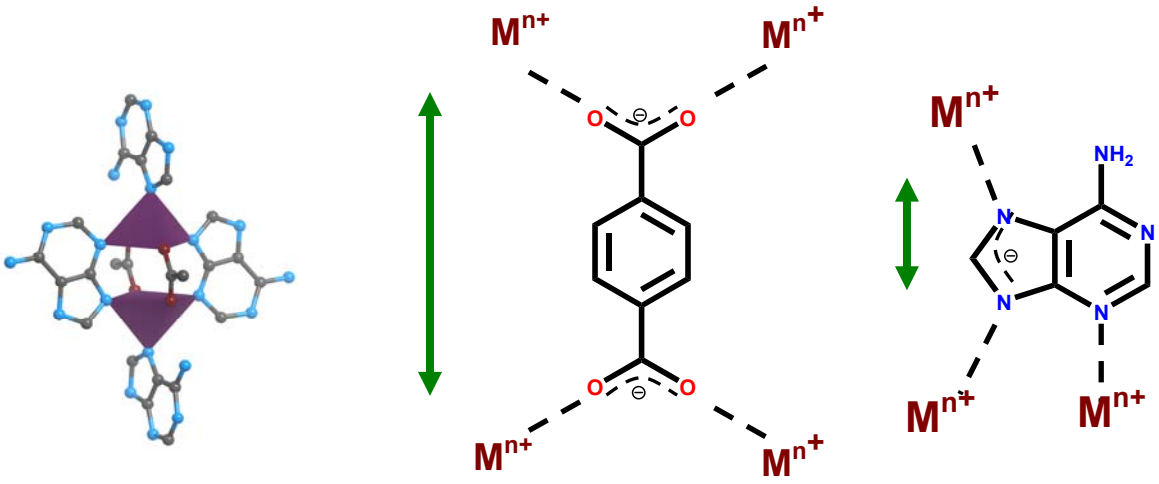

Figure 35. Comparison of the adenine and carboxylate as a ligand

4.2.2 XPRD, EA, and TGA

XPRD confirmed the phase purity of the material and its stability in chloroform (Figure 36).

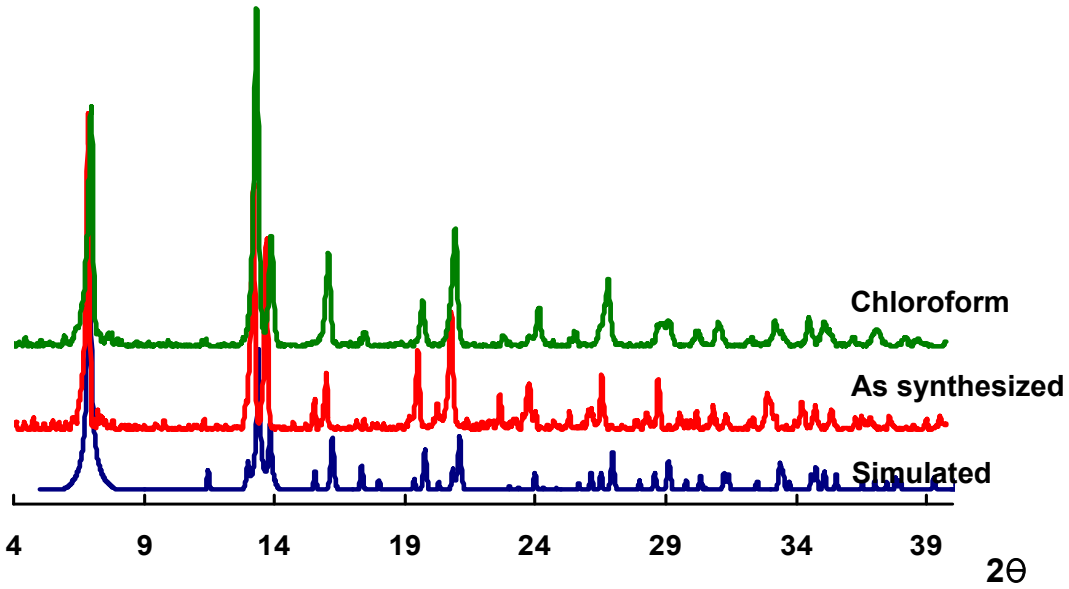

Figure 36. XPRD of the Co(Ad)(OCH_3) · (DMF), 0.25(H_2O)

EA data confirmed that there is 1.0 DMF molecule and 0.25 water molecules per unit cell. The TGA data is consistent with the EA data. The weight loss at 175°C is 21.7% which corresponds to the removal of the 1.0 DMF molecule and 0.25water molecules, which is 22.5%. The framework starts to decompose above 250°C

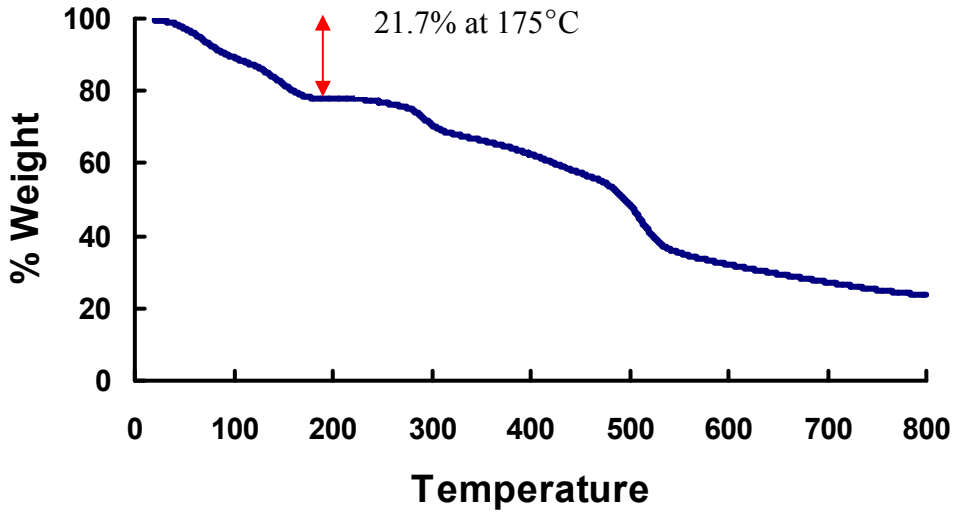

Figure 37. TGA of the as-synthesized crystal

4.3 $ZN_{1.5}(AD)(CH_3CO_2)_2 \cdot 0.75DMA, 0.5H_2O$

When zinc acetate and adenine were reacted together in the presence of 1.2'-Bis (4-pyridyl)-ethane in DMA, crystals of this material formed. Even though 1.2'-Bis (4-pyridyl)-ethane is added to the reaction, it is not a part of the framework structure, but it must play an important role to form the crystal.

4.3.1 Structure

The structure of this framework is interesting. It consists of trinuclear zinc clusters that are linked together by adeninates into two-dimensional sheets. The cluster is composed of a central octahedral Zn(II) that is bridged to two identical Zn(II) tetrahedra (related by a center of inversion at the center of the octahedral Zn(II)) via the N9 and N3 of adeninate, a di-monodentate acetate, and a monodentate acetate. The tetrahedral coordination sphere around the Zn(II) is completed by an adeninate bound through N7. (Figure 38) The layers within the crystal are held together via hydrogen bonding between the adeninates and interactions with disordered solvent molecules.

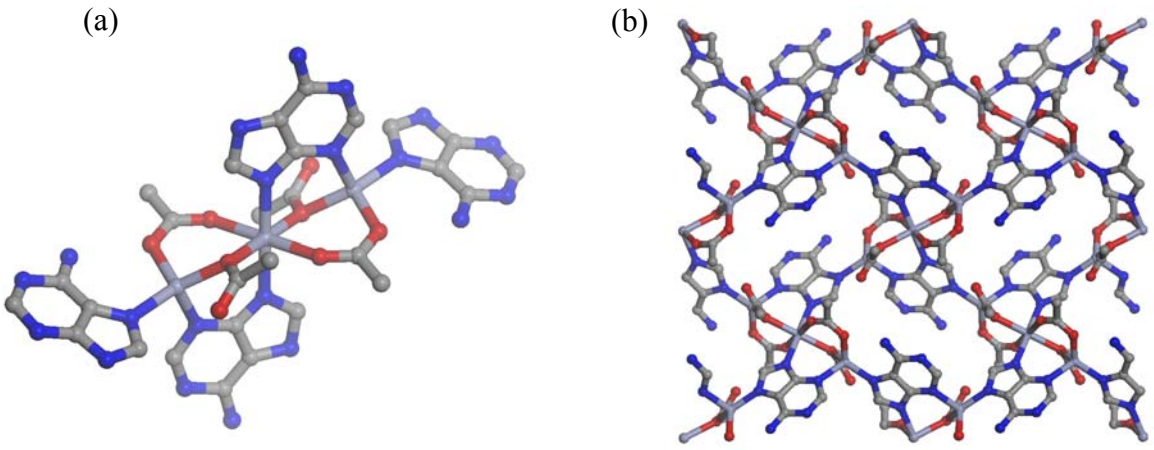

Figure 38. (a) Zn/Ad/OAc unit (b) packing view along to C-crystallographic axis

4.3.2 XPRD, EA, and TGA

XPRD has confirms the phase purity of the material (Figure 39). TGA of this framework shows that there is no porosity in the structure, which is reasonable since this structure is two-dimensional and fairly condensed. Single crystal X-ray data reveals the presence of disordered guest molecules, but they could not be completely resolved.

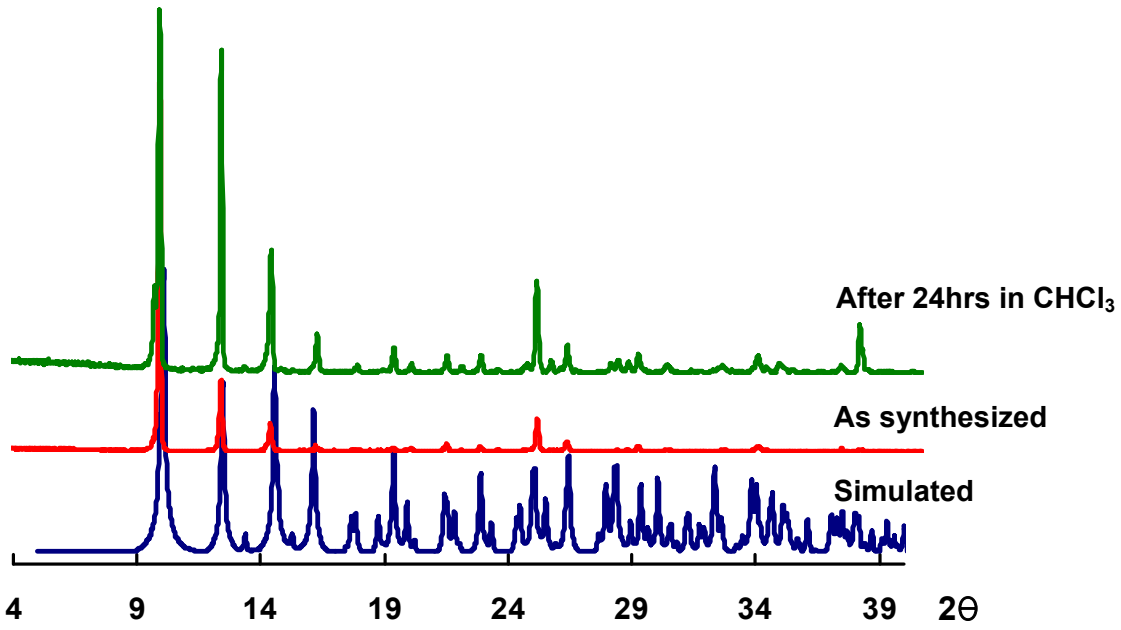

Figure 39. XPRD of the $Zn_{1.5}(Ad)(CH_3CO_2)_2 \cdot 0.75DMA, 0.5H_2O$

TGA shows that there is no weight changed in the structure until 260°C. There are guest molecules in the framework but they do not get removed because they interact with the structure, helping layers pack together.

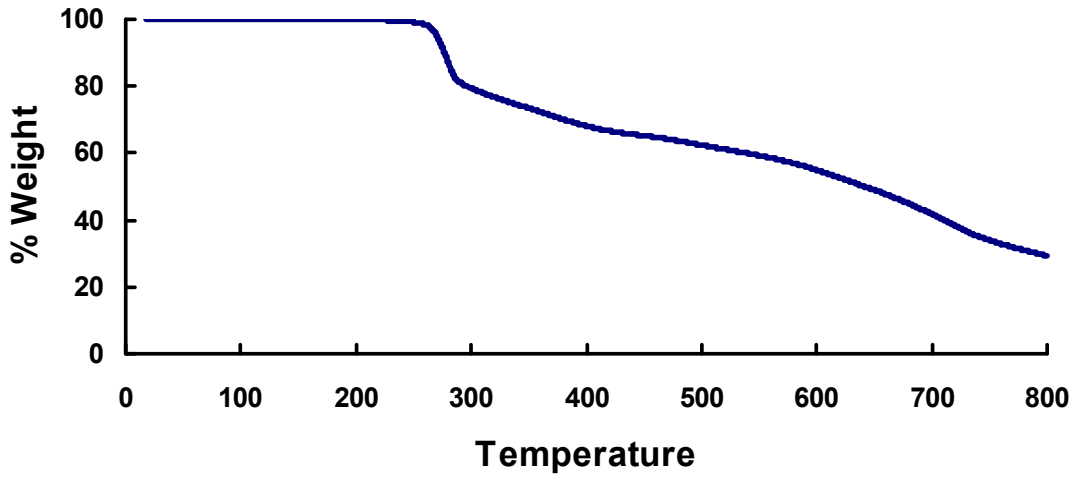

Figure 40. TGA of the as-synthesized crystal

5.0 CONCLUSION

This research is aimed at designing and synthesizing porous biomolecule-based materials for biological applications, such as drug delivery. As a first step in this direction, developing methods to control the coordination chemistry between nucleobases and metal ions with the aim of producing porous metallo-nucleobase frameworks and polyhedra has been studied. As a result, several interesting frameworks have been synthesized and characterized so far. Zn/Adenine hexamer/polymer showed interesting relationships between synthetic methods and structures. Its full characterization study led to the further design and synthesis of the frameworks. $Zn_2(Ad)(BPDC)_{1.5}O_{0.25} \cdot 0.5(NH_2(CH_3)_2)^+$, $2.75H_2O$, 2.0 DMF exhibits an interesting structure and physical properties. Gas sorption studies and cation - controlled molecular release studies have been performed. Other adeninate crystals also showed interesting structures, providing useful information about adenine-metal binding motifs. Though further properties have not been found yet, the structures themselves are meaningful in terms of developing and exploring the trends in adenine coordination chemistry.

Overall, by studying the metal-adeninate frameworks which had been synthesized so far, interesting metal-adenine binding motifs have been discovered. The binding motifs of adenine are analogous to carboxylate binding motifs, suggesting that adenine could be a very versatile molecule for the construction and design of MOFs. Moreover, the successful synthesis of a

porous material with adenine is very meaningful because it proves that porous material with bio-molecules can be rationally designed and synthesized for target applications.

6.0 FUTURE WORK

Since I am continuing to characterize $Zn_2(Ad)(BPDC)_{1.5}O_{0.25} \cdot 0.5(NH_2(CH_3)_2)^+$, $2.75(H_2O)$, 2.0 (DMF), the completion of this project would be the first work to be done. Gas sorption studies of the $Cd^{2+}$and Pb^{2+} exchanged material will be studied to better understand the relationship between the size of the metal cation and the adsorption properties. The cation conductivity study of the framework is also being pursued in collaboration with Yushan Yan's group at UC Riverside. In addition, controlled release studies will be performed with actual drug molecules. Depending on the promise of these studies, we will begin to assess the biocompatibility of these frameworks and assess their viability and applicability in cellular environments. The exceptional stability of this framework and its anionic nature opens the door to a number of additional possible studies: 1) chiral cations can be implanted within the pores and chiral separations could be attempted; 2) fluorescent cations could be implanted in the pore to examine sensing applications; 3) cationic metal catalysts could be implanted in the pore to study catalytic applications, etc.

Studying the structure of $Zn_2(Ad)(BPDC)_{1.5}O_{0.25} \cdot 0.5(NH_2(CH_3)_2)^+$, $2.75(H_2O)$, 2.0(DMF) has inspired us to ask the following question: can we systematically increase the size of the octahedral cage to make it accessible to guest molecules? This may provide a route toward designing frameworks with two distinctly different pore sizes in the framework: one small and one large. Such a material could be very interesting for molecular sieving of gas

molecules. In order to accomplish this goal, we have designed a ligand that should have similar coordination preferences as adeninate, but it is larger. As seen in Figure 41, the targeted ligand has an expanded length between metal binding sites.

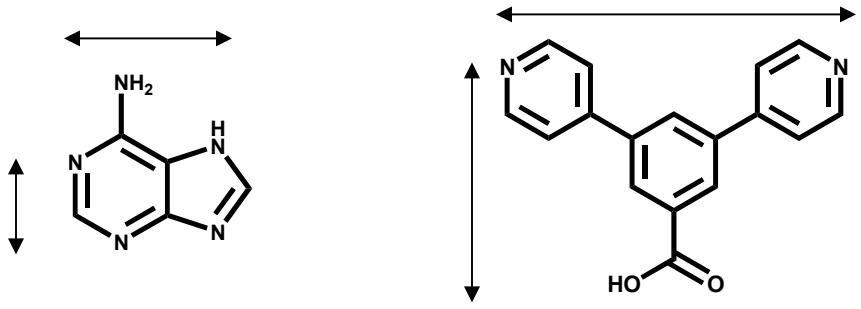

Figure 41. Adenine and the target molecule

The ultimate goal of the research is to synthesize the biologically functionalized porous structure for the bio-medical application. Thus, moving forward to more complicated biological molecules as building blocks is necessary.

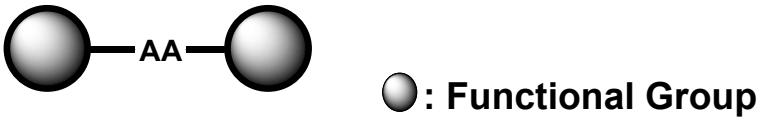

Figure 42. Poly-nucleobases with functional group

We are targeting molecules that contain multiple nucleobases with functionalized molecules attached at the end. Such ligands would allow for the construction of more complex bio-MOFs with possible larger pore sizes for the inclusion of drug molecules, enzymes, and other biologically relevant species.

APPENDIX: SUPPORTING INFORMATION

Experimental Section

Reagents and General Procedures. Chemicals were purchased from Aldrich Chemical Co. Pyridine and N, N'-dimethylformamide (DMF) were purchased from the Fisher Scientific International Inc. All starting materials were used without further purification. All experimental operations were performed in air. The elemental microanalysis was performed by Galbraith Laboratories. INC. using the Perkinelmer 240 Elemental Analyzer and by the University of Illinois, Department of Chemistry Microanalytical Laboratory using an Exeter Analytical CE440. Thermogravimetric analysis (TGA) was performed using TGA Q500 thermal analysis system. All TGA experiments were run under a N_2 atmosphere from 25-800 °C at a rate of 1 °C/min. Data were analyzed using TA Universal Analysis software package.

Solvent exchange of guest molecules in the frameworks was performed using solvents as follows: Rinse with DMF twice; 10 min soak in exchange solvent (ES) followed by solvent removal; 10 min soak in exchanged solvent – solvent removal; 24 hours soak in fresh ES. Fourier transform infrared (FT-IR) spectra were measured using a Nicolet Avatar 360 FTIR E.S.D. and KBr pellet samples. Absorptions are described as follows: very strong (vs), strong(s), medium (m), weak (w), shoulder (sh), and broad (br). Data were analyzed using Omnic Software package X-ray powder diffraction patterns were taken using a Philips X'pert diffractometer at 40

kV, 30 mA for Cu Kα (λ= 1.5406 Å) with scan speed of 0.50 sec/step and a step size of 0.02°. The data were analyzed for d-spacing measurements using X'pert Software program from the Philips Powder Analysis Software package. The simulated powder patterns were calculated using Mercury 2.0. The purity and homogeneity of the bulk products were determined by comparison of the simulated and experimental X-ray powder diffraction patterns.

Synthesis of Zn(Ad)(Py)(CH_3CO_2) · 1.5DMF (1): A stock solution of adenine (0.05 M) in N,N-dimethylformamide (DMF) was prepared. Ultra-sonification and heating was carried out in order to dissolve adenine completely in DMF. A stock solution of Zinc acetate dihydrate (0.05 M) in DMF was prepared. The adenine stock solution (2.5 mL, 0.125 mmol adenine in DMF) and the zinc acetate dihydrate stock solution (5.0 mL, 0.25 mmol Zinc acetate dehydrate in DMF) were added to a 20 mL vial. DMF (2.5 mL, 32.3 mmol) and pyridine (2.5 mL, 30.9 mmol) were added to the vial. The vial was capped and remained at room temperature. After 8 hours, the colorless crystal were produced, washed with DMF (3 mL x 3) and dried in air (15 min) (yield: 0.039 g, 70 % based on adenine) ***Elemental analysis*** $C_{16.5}H_{22.5}N_{7.5}O_{3.5}Zn$ = Zn(Ad)(Py)(CH_3CO_2)·(1.5DMF): Calcd. C, 44.31; H, 5.07; N, 23.49. Found C, 44.50; H, 4.98; N, 23.62. ***FT-IR*** **:** (KBr 4000-400 cm-1): 3324.99(br), 3184.27(br), 2926.97(w), 1662.44(s), 1600.80(s), 1470.30(m), 1395.40(s), 1326.02(m), 1219.67(s), 1149.59(m), 1046.02(w), 801.65(m), 744.20(w)

Zn(Ad)(Py)($O_2CN(CH_3)_2$) · 1.75DMF (2): A stock solution of adenine (0.05 M) in N,N-dimethylformamide(DMF) was prepared. Ultra-sonification and heating was carried out in order

to dissolve adenine completely in DMF. A stock solution of zinc nitrate tetrahydrate (0.05 M) in DMF was prepared. 3 mL of the adenine solution, 6mL of the zinc nitrate solution and 3 mL of pyridine were added to teflon-lined autoclave. The reaction was heated at 140 °C for 24 hours in Teflon-lined autoclave. After the teflon-lined autoclave was cooled down to rt, the reaction solution was transferred to the vial. And after 3 days, crystals start to grow at rt. Colorless crystals were produced, washed with DMF (3 mL x 3) and dried under Ar gas (15 min) (yield: 0.0171 mg, 23 % based on adenine) ***Elemental analysis*** $C_{18.25}H_{27.25}N_{8.75}O_{3.75}Zn$ = $Zn(Ad)(Py)(O_2CN(CH_3)_2) \cdot (1.75DMF)$: Calcd. C, 44.32; H, 5.55; N, 24.78. Found C, 44.39; H, 4.72; N, 24.88. ***FT-IR*** **:** (KBr 4000-400 cm^{-1}) : 3306.41(br), 3114.13(br), 2923.04(w), 1668.24(s), 1652.79(m), 1601.52(s), 1475.03(s), 1402.75(m), 1387.33(m), 1223.63(w)

$Zn(Ad)(Py)(NO_3)\cdot(xDMF)$ (3): To a 20 mL vial, 54 mg of adenine (0.4 mmol) and 238 mg of zinc nitrate hexahydrate (0.8 mmol) were added. 10 mL of N,N'-dimethylformamide (DMF) was added. Additional 2.5 mL of pyridine was followed. The vial was sealed with the cap, and heated at 100 °C for 24 hours. After cooling to room temperature, crystals start to grow (about after 3 hours). Crystals were pale yellow, rod shape. They were washed with DMF (3 mL X 3) and dried under Ar gas. (yield : 92.8mg) ***FT-IR*** **:** (KBr 4000-400 cm^{-1}) : 3338.39(br), 3193.21(br), 2930.69(w), 2859.81(w), 1659.17(s), 1603.03(s), 1469.36(m), 1409.55(m), 1384.32(s), 1296.92(m), 1153.96(m), 1098.43(w), 796.59(w), 743.57(w)

$Zn_2(Ad)(BPDC)_{1.5}O_{0.25} \cdot 0.5(NH_2(CH_3)_2)^+$, 2DMF, $2.75H_2O$ (4) : A stock solution of adenine (0.05 M) in N,N-dimethylformamide (DMF) was prepared. Ultra-sonification and heating was carried out in order to dissolve adenine completely in DMF. A stock solution of zinc

acetate dihydrate (0.05 M) in DMF was prepared. 0.1 M stock solution of 4, 4'-biphenyl dicarboxylic acid (BPDC) in DMF was prepared as well. Since BPDC does not completely dissolved in DMF, the solution was constantly stirred. The adenine stock solution (2.5 mL, 0.125 mmol) and the zinc acetate dihydrate stock solution (7.5 mL, 0.375 mmol) were added to a 20.0 mL vial. Addition of 2.5 mL of the BPDC stock solution (0.25 mmol) followed. 1 mL of 1 M nitric acid in DMF and 1mL of D.I. water were added to the vial. The vial was capped and heated at 130 °C for 3 hours. The rod shape of colorless crystals were produced, washed with DMF (3 mL x 3) and dried in air (30 min) (yield 0.106g, 100% based on adenine) ***Elemental analysis*** $C_{33}H_{39.5}N_{7.5}O_{11}Zn_2$ = $Zn_2(Ad)(BPDC)_{1.5}O_{0.25} \cdot 0.5(NH_2(CH_3)_2)^+$, $2.75H_2O$, 2DMF Calcd. C, 46.74; H, 4.70; N, 12.39. Found C, 46.58; H, 4.55; N, 12.49. ***FT-IR*** **:** (KBr 4000-400 cm^{-1}) : 3341.39(br), 3188.47(br), 2930.38(w), 1663.76(s), 1606.79(s), 1544.77(m), 1472.12(m), 1382.97(s), 1280.50(w), 1213.98(m), 1176.56(m), 1153.11(m), 1100.61(m), 845.33(m), 772.43(s), 702.00(m)

Cation Exchange Experiment: The solution of cation molecules (0.1 M) was prepared. Cation exchange of the frameworks was performed using the prepared solution as follows: Rinse with DMF twice; 10 min soak in exchange solution followed by solution removal; 10 min soak in exchanged solution – solution removal; 24 hours soak in fresh exchanged solution. The new solution was added every 24 hours until its completion.

Elemental analysis $C_{27.75}H_{21.25}N_5O_8Cl_{5.25}Li_{0.5}Zn_2$ = $Zn_2(Ad)(BPDC)_{1.5}O_{0.25} \cdot 0.5(Li)^+$, $1.75H_2O$, $1.75CHCl_3$ Calcd. C, 38.17; H, 2.45; N, 8.02. Found C, 38.21; H, 2.45; N, 7.97.

$C_{26.75}H_{20.75}N_5O_{8.25}Cl_{2.25}Na_{0.5}Zn_2$ = $Zn_2(Ad)(BPDC)_{1.5}O_{0.25} \cdot 0.5(Na)^+$, $2H_2O$, 0.75 $CHCl_3$ Calcd. C, 41.93; H, 2.73; N, 9.14. Found C, 41.95; H, 2.83; N, 9.14. $C_{27}H_{22.5}N_5O_9Cl_3Co_{0.3}Zn_2$ = $Zn_2(Ad)(BPDC)_{1.5}O_{0.25} \cdot 0.3(Co)^{2+}$, $2.75H_2O$, 1.0 $CHCl_3$, $0.1(BF_4)^-$ Calcd. C, 39.24; H, 2.74; N,

8.47. Found C, 39.35; H, 2.78; N, 8.54. $C_{26.75}H_{21.25}N_5O_{8.5}Cl_{2.25}Ni_{0.78}Zn_2$ = $Zn_2(Ad)(BPDC)_{1.5}O_{0.25} \cdot 0.78(Ni)^{2+}$, $2.25H_2O$, 0.75 $CHCl_3$, $1.06(Cl)^-$ Calcd. C, 38.13; H, 2.54; N, 8.31. Found C, 38.08; H, 2.51; N, 8.2. $C_{30.25}H_{25.75}N_{5.5}O_7Cl_{6.75}Zn_2$ = $Zn_2(Ad)(BPDC)_{1.5}O_{0.25} \cdot 0.5(N(CH_3)_4)^+$, $0.75H_2O$, $2.25CHCl_3$ Calcd. C, 38.31; H, 2.74; N, 8.12. Found C, 38.26; H, 2.64; N, 8.1. $C_{32}H_{28.5}N_{5.5}O_{6.5}Cl_6Zn_2$ = $Zn_2(Ad)(BPDC)_{1.5}O_{0.25} \cdot 0.5(N(CH_2CH_3)_4)^+$, $0.25H_2O$, $2CHCl_3$ Calcd. C, 40.99; H, 3.06; N, 8.22. Found C, 40.96; H, 2.92; N, 8.16. $C_{35.75}H_{27.75}N_{6.5}O_7Cl_{6.75}S_{0.5}Zn_2$ = $Zn_2(Ad)(BPDC)_{1.5}O_{0.25} \cdot 0.5$(toluidine blue o)$^+$, $0.75H_2O$, $2.25CHCl_3$ Calcd. C, 41.03; H, 2.67; N, 8.70. Found C, 41.07; H, 2.49; N, 8.78.

Toluidine Blue O Molecule Release Experiment: 2 mg of the toluidine blue o exchanged crystal ($Zn_2(Ad)(BPDC)_{1.5}O_{0.25}$·0.5(toluidine blue o)$^+$,$0.75H_2O$,$2.25CHCl_3$) was added to a UV-VIS cell (10 mm, 3.0 mL vol). 1 mL of PBS buffer (0.1 M, pH 7.4) was added to the cell. The cell was heated to at 37 °C and stirred at the rate of 100 rpm. The UV-VIS was measured at 30 s, 1 min, and 5 min at Abs 626 nm. From 10 min measurement, 0.1 mL of the solution was removed from the cell, and the solution was diluted to 100 times and an adsorption of UV-VIS was measured. Additional 0.1 mL of PBS buffer was added to the cell in order to keep the constant ratio of the crystal and solution (mg/mL). Further measurement was performed at 10 min, 20 min, 30 min, 1 hour, 2 hours, 4 hours, 8 hours, 12 hours, 24 hours, and 48 hours.

$Zn_3(Ad)(BTC)_2 \cdot (NH_2(CH_3)_2)^+$, 5.75DMF, $0.25H_2O$ (5) : A stock solution of adenine (0.05 M) in N,N-dimethylformamide (DMF) was prepared. Ultra-sonification and heating was carried out in order to dissolve adenine completely in DMF. A stock solution of Zinc acetate dehydrate (0.05 M) in DMF was prepared. 0.2 M stock solution of benzene tricarboxylic acid (BTC) in DMF was prepared as well. The adenine stock solution (5 mL, 0.25 mmol) and the zinc

acetate dihydrate stock solution (5 mL, 0.25 mmol) were added to a 20.0 mL vial. Addition of 2.5 mL of the BTC stock solution (0.5 mmol) followed. 1 mL of 1 M nitric acid in DMF was added. The vial was capped and heated at 130 °C for 24 hours. The rod shape of colorless crystals were produced, washed with DMF (3 mL x 3) and dried in air (30 min) (yield 0.107 g, 35 % based on adenine) ***Elemental analysis*** $C_{42.25}H_{58.75}N_{11.75}O_{18}Zn_3$ = $Zn_3(Ad)(BTC)_2 \cdot (NH_2(CH_3)_2)^+$, 5.75(DMF), 0.25($H_2O$) Calcd. C, 41.75; H, 4.87; N, 13.54. Found C, 41.78; H, 4.86; N, 13.54. ***FT-IR*** **:** (KBr 4000-400 cm^{-1}) : 3395.23(br), 3196.14(br), 2931.87(w), 2360.26(w), 1664.38(s), 1627.44(s), 1576.82(s), 1438.77(m), 1410.59(m), 1360.76(s), 1153.57(w), 1101.03(m), 767.24(s), 726.27(s)

Co(Ad)(CH_3CO_2) · DMF, 0.25H_2O (6): A stock solution of adenine (0.05 M) in N,N-dimethylformamide (DMF) was prepared. Ultra-sonification and heating was carried out in order to dissolve adenine completely in DMF. A stock solution of cobalt acetate tetrahydrate (0.05 M) in DMF was prepared. The adenine stock solution (0.75 mL, 0.0375 mmol adenine in DMF) and the cobalt acetate tetrahydrate stock solution (0.25 mL, 0.0125 mmol cobalt acetate tetrahydrate in DMF) were added to a tube (0.8 cm diameter). The tube was frozen in the liquid nitrogen and vacuumed to 200 millitorr. Then the tube was sealed and heated at 130 °C. After 24 hours, the reaction tube was cooled down as rate of 0.1 °C/min. The purple crystal were produced, washed with DMF (3 mL x 3) and dried in air (15 min) (yield: 0.0037 g, 30 % based on adenine) ***Elemental analysis*** $C_{10}H_{14.5}N_6O_{3.25}Co_1$ = Co(Ad)(OAc) · DMF, 0.25H_2O Calcd. C, 36.43; H, 4.43; N, 25.49. Found C, 36.19; H, 4.02; N, 25.44. ***FT-IR*** **:** (KBr 4000-400 cm^{-1}) : 3340.97(br), 3207.96(br), 1655.06(s), 1599.56(s), 1582.67(s), 1495.59(w), 1445.32(m), 1395.53(m), 1344.31(w), 1308.64(w), 1269.71(w), 1209.26(m), 1146.49(m)

$Zn_{1.5}(Ad)(CH_3CO_2)_2 \cdot 0.75DMA, 0.5H_2O$ (7): A stock solution of adenine (0.05 M) in N,N-dimethylacetamide (DMA) was prepared. Ultra-sonification was carried out in order to dissolve adenine completely in DMA. A stock solution of zinc acetate dihydrate (0.05 M) in DMA was prepared. 0.025 M stock solution of 1.2'-Bis(4-pyridyl)-ethane in DMA was prepared as well. The adenine stock solution (2.5 mL, 0.125 mmol) and the zinc acetate dihydrate stock solution (10 mL, 0.5 mmol) were added to a 20.0 mL vial. Addition of 2.5 mL of the 1.2'-Bis(4-pyridyl)-ethane stock solution (0.0625 mmol) followed. The vial was capped and heated at 130 °C for 3days. The colorless crystals were produced, washed with DMA (3 mL x 3) and dried under Ar gas (30min) (yield 0.0336 g, 63 % based on adenine) ***Elemental analysis*** $C_{12}H_{17.1675}N_{5.75}O_{5.25}Zn_{1.5}$ = $Zn_{1.5}(Ad)(CH_3CO_2)_2 \cdot 0.75DMA, 0.5H_2O$ Calcd. C, 33.94; H, 4.21; N, 18.97. Found C, 33.8; H, 3.67; N, 19.09. ***FT-IR*** **:** (KBr 4000-400 cm^{-1}) : 3260.349(br), 3082.47(br), 2930.14(w), 1686.38(m), 1592.65(s), 1308.06(w), 1274.28(m), 1220.86(m), 1157.29(m)

Gas sorption Measurements. Sorption isotherm studies for $Zn(Ad)(Py)(CH_3CO_2) \cdot 1.5DMF$ (1) , $Zn_2(Ad)(BPDC)_{1.5}O_{0.25} \cdot 0.5(NH_2(CH_3)_2)^+$, 2DMF, $2.75H_2O$ (4) and cation exchanged sample of (4) were performed by measuring the increase in volume at equilibrium as a function of relative pressure by using Autosorb 1 by Quantachrom. Measurements of the sample were performed using a AB54-S/FACT (Mettler Toledo) electrogravimetric balance (sensitivity 0.1 mg). A known weight (typically 50 mg) of the sample was placed in a 9mm large bulb cell (from Quantachrome) and then heated and vacuumed until rise pressures below 3.5 micron/min to remove the guest molecules. The N_2, H_2 adsorbate was of UHP grade. The

temperature of each sample was controlled by a refrigerated bath of liquid nitrogen (–195 °C) or liquid argon (-185 °C).

Single X-ray Diffraction Studies. Crystals were coated in an inert hydrocarbon–based oil and mounted on a Bruker SMART APEX CCD diffractometor equipped with a normal focus Mo–target X–ray tube (λ = 0.71073 Å) operated at 2000 W power (45 kV, 35 mA). Unless otherwise noted, the X–ray intensities were measured at 173 K; the detector was placed at a distance of 5.002 cm from the crystal. Frames were collected with a scan width of 0.3° in and phi with an exposure time of 30 s/frame. The frames were integrated with the SAINT software package with a narrow frame algorithm. The structure was solved by direct methods and the subsequent difference Fourier syntheses and refined with the SHELXTL (version 6.14) software package.

Zn(Ad)(Py)(CH_3CO_2) · 1.5DMF (1). An X-ray crystal structure was determined for a colorless crystal (0.18 x 0.22 x 0.26 mm^3). Unit-cell parameters and systematic absences indicated (**1)** crystallized in one of five rhombohedral space groups having equivalent systematic absences. Centrosymmetric R-3 was chosen based on *E*-values and the successful solution and refinement of the structure. Unit-cell dimensions were derived from the least-squares fit of the angular settings of 451 reflections obtained from 3 orthogonal sets of 20 frames. Data were corrected for absorption using the Bruker program Sadabs. The structure was solved via direct methods which located the positions of all non-hydrogen atoms, which were refined anisotropically. Idealized atom positions were calculated for all hydrogen atoms (*d*-(C-H) = 0.96A, $U = 1.2U_{iso}$ of attached carbon). The structure consists of Zn-adenine units arranged in a cyclic hexamer, with Zn atoms coordinated to two adenines at the N1 and N2 positions. Each

zinc is also *O*-bound to an acetate anion and *N*-bound to pyridine. The geometry about the Zn atoms may be described as a distorted tetrahedron. After refinement some large residual peaks remained centered on or about a (0, 0, 0) 3-bar site. Additionally, Platon found large void areas in the packing which could accommodate solvent molecules. Elemental analysis indicated approximately 1.5 dimethylformamides per Zn hexamer. Attempts at modeling the disordered solvent were unsuccessful. The Fobs component attributable to the disordered solvent was removed with the platon/Squeeze program. All computer programs used in the data collection and refinements are contained in the Bruker program packages SMART (vers. 5.625), SAINT (vers. 6.22), and SHELXTL (vers. 6.10) and Platon (Spek, A.L. (1990) **Acta Cryst. A46**, C34).

Zn(Ad)(Py)($O_2CN(CH_3)_2$) · 1.75DMF (2). An X-ray crystal structure was determined for $[C_{13}H_{15}N_7O_2Zn]_6$ (**2**), using a single crystal on a Bruker Smart Apex CCD diffractometer with graphite-monochromated MoKα (λ= 0.71073 A) radiation. The parameters used during the collection of diffraction data are summarized in Table 1. The crystal was adhered to a fine glass fiber with epoxy and placed in a cold N_2 stream (150 K) for data collection. Unit-cell parameters and systematic absences indicated **2** crystallized in one of five rhombohedral space groups having equivalent systematic absences. Centrosymmetric R-3 was chosen based on *E*-values and the successful solution and refinement of the structure. Unit-cell dimensions were derived from the least-squares fit of the angular settings of 999 reflections obtained from 3 orthogonal sets of 30 frames. The structure was found to be isomorphous with compound (jar130). Data were corrected for absorption using the Bruker program Sadabs. The structure was solved via isomorphous replacement using Zn atoms from compound (jar130). Remaining non-hydrogen atoms were located from subsequent difference Fourier syntheses. All non-hydrogen atoms were

refined anisotropically. Idealized atom positions were calculated for all hydrogen atoms (*d*-(C-H) = 0.96A, $U = 1.2U_{iso}$ of attached carbon). The structure consists of Zn-adenine units arranged in a cyclic hexamer, with Zn atoms coordinated to two adenines at the N1 and N2 positions. Each zinc is also *O*-bound to carbamato anion and *N*-bound to pyridine. The geometry about the Zn atoms may be described as a distorted tetrahedron. Three large residual peaks were refined as oxygen atoms believed to be part of unresolvable disordered solvate molecules. Additionally, Platon found large void areas in the packing which could accommodate solvent molecules. Elemental analysis indicated approximately 1.5 dimethyl formamides per Zn hexamer. Attempts at modeling the disordered solvent were unsuccessful. All computer programs used in the data collection and refinements are contained in the Bruker program packages SMART (vers. 5.625), SAINT (vers. 6.22), and SHELXTL (vers. 6.14) and Platon (Spek, A.L. (1990) **Acta Cryst. A46**, C34).

$Zn_3(Ad)(BTC)_2 \cdot (NH_2(CH_3)_2)^+$, 5.75DMF, 0.25$H_2O$ (5). An X-ray crystal structure was determined for C28 H23 N7 O13 Zn3 (**5**), using a single crystal on a Bruker Smart Apex CCD diffractometer with graphite-monochromated MoKα (λ= 0.71073 A) radiation. The parameters used during the collection of diffraction data are summarized in Table 1. The crystal was adhered to a fine glass fiber with epoxy and placed in a cold N_2 stream (173 K) for data collection. Unit-cell parameters and systematic absences indicated **(5)** crystallized in monoclinic space group P 2_1/n. Unit-cell dimensions were derived from the least-squares fit of the angular settings of 999 reflections obtained from 3 orthogonal sets of 30 frames. Data were corrected for absorption using the Bruker program Sadabs. The structure was solved via direct methods which located all non-hydrogen atoms. All non-hydrogen atoms were refined anisotropically.

Idealized atom positions were calculated for all hydrogen atoms (d-(C-H) = 0.96A, $U = 1.2U_{iso}$ of attached carbon). Final difference Fourier map showed maximum and minimum peaks of 1.73 and -0.68 e^- A^3, respectively, which were not near any refined atom positions, which we attributed to disordered solvent. Analysis of the final structure with Platon's Squeeze program showed two voids of 1380 A^3 each with 377 electrons per void. All computer programs used in the data collection and refinements are contained in the Bruker program packages SMART (vers. 5.625), SAINT (vers. 6.22), and SHELXTL (vers. 6.14) and Platon (Spek, A.L. (1990) **Acta Cryst. A46**, C34).

Co(Ad)(CH_3CO_2) · DMF, 0.25H_2O (6). An X-ray crystal structure was determined for C7 H7 Co N5 O2 (**6**), using a single crystal on a Bruker Smart Apex CCD diffractometer with graphite-monochromated MoKα (λ= 0.71073 A) radiation. The parameters used during the collection of diffraction data are summarized in Table 1. The crystal was adhered to a fine glass fiber with epoxy and placed in a cold N_2 stream (173 K) for data collection. Unit-cell parameters and systematic absences indicated **(6)** crystallized in tetragonal space group I $4_1/a$. Unit-cell dimensions were derived from the least-squares fit of the angular settings of 999 reflections obtained from 3 orthogonal sets of 30 frames. Data were corrected for absorption using the Bruker program Sadabs. The structure was solved via direct methods which located all non-hydrogen atoms. All non-hydrogen atoms were refined anisotropically. Idealized atom positions were calculated for all hydrogen atoms (d-(C-H) = 0.96A, $U = 1.2U_{iso}$ of attached carbon). Final difference Fourier map showed maximum and minimum peaks of 1.76 and -0.58 e- A3, respectively, which were not near any refined atom positions.

All computer programs used in the data collection and refinements are contained in the Bruker program packages SMART (vers. 5.625), SAINT (vers. 6.22), and SHELXTL (vers. 6.14) and Platon (Spek, A.L. (1990) **Acta Cryst. A46**, C34).

$Zn_{1.5}(Ad)(CH_3CO_2)_2 \cdot 0.75DMA, 0.5H_2O$ (7). An X-ray crystal structure was determined for C9 H10 N5 O4 Zn1.50 (**7**), using a single crystal on a Bruker Smart Apex CCD diffractometer with graphite-monochromated MoKα (λ= 0.71073 A) radiation. The parameters used during the collection of diffraction data are summarized in Table 1. The crystal was adhered to a fine glass fiber with epoxy and placed in a cold N_2 stream (173 K) for data collection. Unit-cell parameters and systematic absences indicated **(7)** crystallized in monoclinic $P2_1/c$. Unit-cell dimensions were derived from the least-squares fit of the angular settings of 999 reflections obtained from 3 orthogonal sets of 30 frames. Data were corrected for absorption using the Bruker program Sadabs.

The structure was solved via direct methods which located all non-hydrogen atoms. All non-hydrogen atoms were refined anisotropically. Idealized atom positions were calculated for all hydrogen atoms (d-(C-H) = 0.96A, $U = 1.2U_{iso}$ of attached carbon). Five large residual peaks were refined as carbon atoms, which were determined to be disordered solvent located on an inversion site and which could not be modeled. Final difference Fourier map showed maximum and minimum peaks of 1.393 and -1.258 $e^{-}Å^{-3}$, respectively, which were within the disordered solvent molecule. All computer programs used in the data collection and refinements are contained in the Bruker program packages SMART (vers. 5.625), SAINT (vers. 6.22), and SHELXTL (vers. 6.14) and Platon (Spek, A.L. (1990) **Acta Cryst. A46**, C34).

Zn(Ad)(Py)(CH_3CO_2) · 1.5DMF (1), As-synthesized

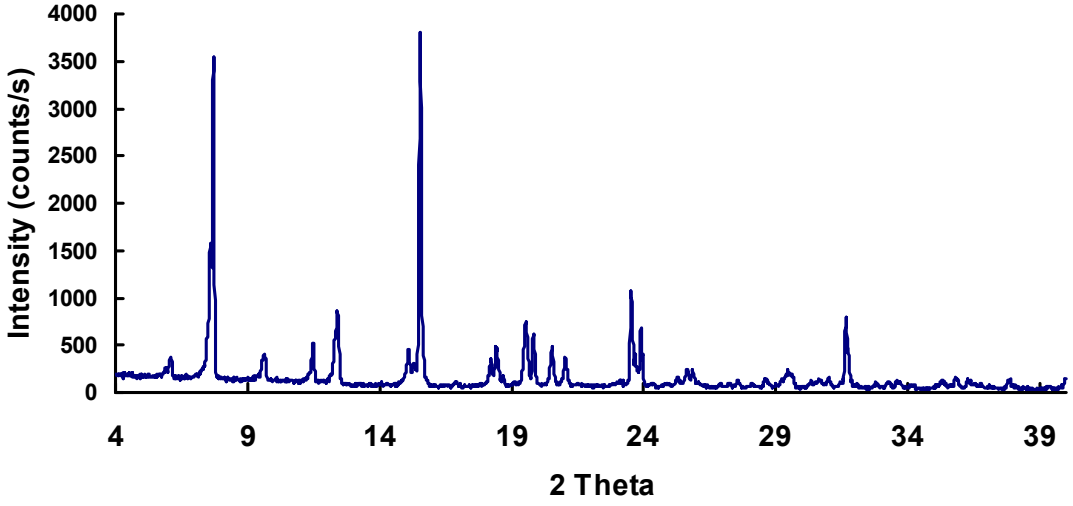

Angle (2θ°)	d-spacing (A°)	Intensity (%)	h,k,l
6.09068	14.49907	5.75	1.0.1
7.59855	11.62489	38.24	1,0,-2
7.71072	11.45602	89.08	0,0,3
9.64748	9.16010	7.05	2,-1,0
11.47484	7.70514	11.11	2,0,-1
12.41642	7.12287	20.49	2,-1,-3
15.10518	5.86049	9.89	3,-1,1
15.53762	5.69834	100	0,0,6
18.22043	4.86490	7.68	3,-2,4
18.43245	4.80942	9.83	2,-1,-6
18.68348	4.74536	3.08	3,0,-3
19.54265	4.53863	17.98	4,-2,0
19.83995	4.47129	14.38	3,-1,-5
20.54462	4.31949	11.06	4,-3,1
21.03680	4.21953	8.26	4,-1,2
23.53276	3.77733	26.64	0,0,9
23.91148	3.71790	16	2,0,8
31.66649	2.82321	19.62	0,0,12

Zn(Ad)(Py)(CH_3CO_2) · 1.5DMF (1), Simulated

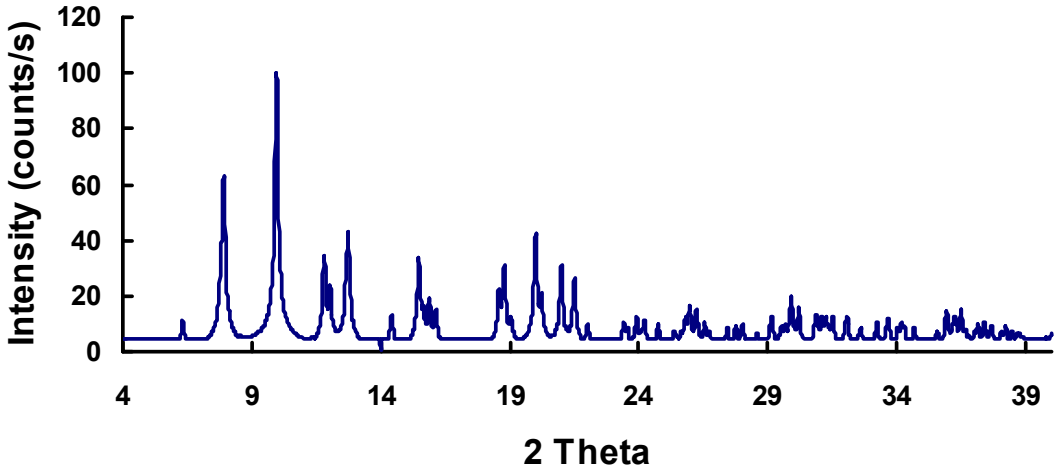

Angle (2θ°)	h,k,l
6.323	1.0.1
7.827	1,0,-2
7.913	0,0,3
9.964	2,-1,0
11.792	2,0,-1
12.051	1,0,4
12.724	2,-1,-3
14.426	1,0,-5
15.484	3,-1,1
15.883	0,0,6
16.142	3,-2,2
18.581	3,-2,4
18.781	2,-1,-6
19.055	3,0,-3
19.985	4,-2,0
20.240	3,-1,-5
21.006	4,-3,1
21.498	4,-1,2
23.923	0,0,9
24.219	2,0,8
32.090	0,0,12

$Zn(Ad)(Py)(O_2CN(CH_{3)2}) \cdot 1.75DMF$ (2), As-synthesized

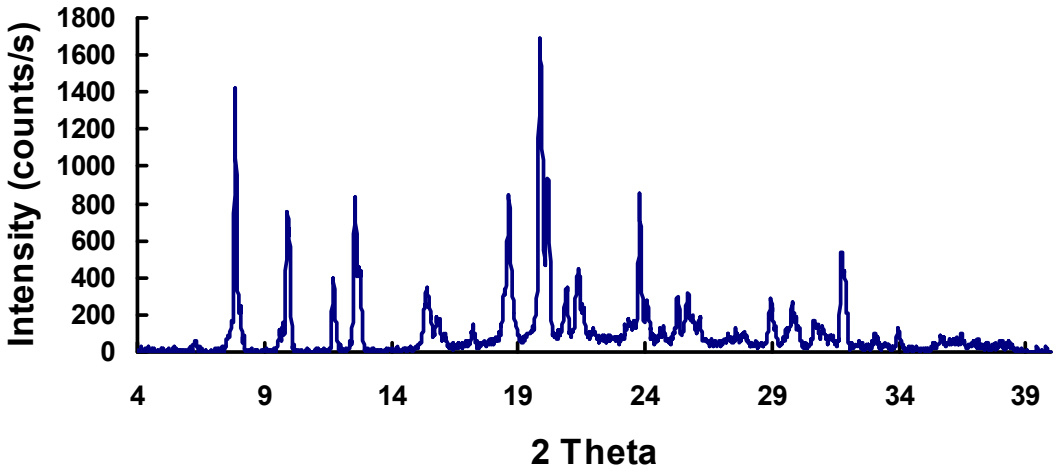

Angle (2θ°)	d-spacing (Å)	Intensity (%)	h,k,l
6.27781	14.06728	3.12	1,0,1
7.86871	11.22636	83.82	0.0.3
9.91398	8.91446	44.68	2,-1,0
11.72797	7.53940	23.68	2,0,-1
12.58202	7.02949	49.21	2,0,2
12.74479	6.94008	25.42	2,-1,-3
15.41841	5.74213	18.86	3,-2,-1
15.83742	5.59114	9.80	0,0,6
17.21652	5.14625	7.51	2,0,5
18.63945	4.75647	49.00	2,-1,6
19.87423	4.46365	100.00	4,-2,0
20.18876	4.39482	54.47	3,-2,5
20.89932	4.24697	19.86	4,-1,-1
21.38430	4.15174	26.32	4,-2,3
31.74929	2.81630	31.65	0,0,12

$Zn(Ad)(Py)(O_2CN(CH_{3)2}) \cdot 1.75DMF$ (2), Simulated

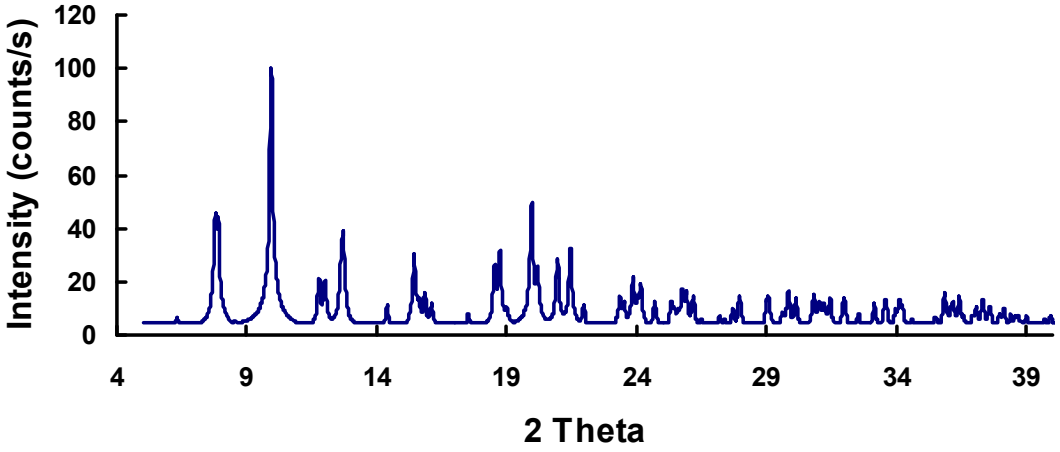

Angle (2θ°)	h,k,l
6.321	1,0,1
7.894	0,0,3
9.944	2,-1,0
11.788	2,0,-1
12.639	2,0,2
12.716	2,-1,-3
14.393	1,0,-5
15.450	3,-2,-1
15.837	0,0,6
17.511	2,0,5
18.544	3,-2,-4
18.751	2,-1,6
19.963	4,-2,0
20.195	3,-2,5
20.943	4,-1,-1
21.484	4,-2,3
32.006	0,0,12

$Zn_2(Ad)(BPDC)_{1.5}O_{0.25} \cdot 0.5(NH_2(CH_3)_2)^+$, 2DMF, 2.75$H_2O$ (4), As-synthesized

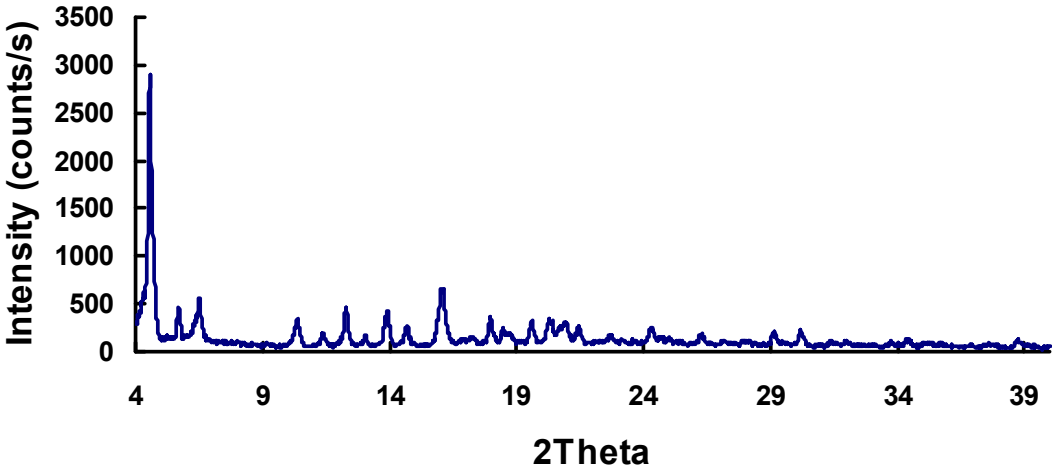

Angle (2θ°)	d-spacing (Å)	Intensity (%)	h, k, l
4.55925	19.36523	100.00	2,0,0
5.69606	15.50262	14.71	
6.51161	13.56272	17.89	2,2,0
9.22689	9.57668	1.23	4,0,0
10.38387	8.51210	9.67	3,0,1
11.38788	7.76378	5.24	3,2,1
12.29343	7.19385	14.62	4,1,1
13.05253	6.77713	4.71	4,4,0
13.81852	6.40314	9.97	6,0,0
13.92470	6.35455	13.19	5,0,1
14.69138	6.02461	7.92	5,2,1
16.07009	5.51071	21.48	1,1,2
17.24766	5.13703	3.77	6,3,1
17.97972	4.92949	11.21	7,0,1
18.48134	4.79681	6.91	7,2,1
19.62525	4.51972	9.04	5,1,2
20.29189	4.37271	10.28	7,4,1
20.96708	4.23340	9.10	6,0,2
21.45366	4.13847	6.70	6,2,2
22.72341	3.91001	4.21	7,6,1
23.17838	3.83428	2.77	8,6,0
24.30972	3.65834	6.94	8,0,2
24.70042	3.60135	3.62	8,2,2
26.28142	3.38818	4.53	9,1,2
29.15324	3.06062	4.94	9,8,1
30.21907	2.95506	5.40	11,1,2
31.99027	2.79537	2.11	7,6,3

34.41264	2.60394	2.47	11,7,2
35.19189	2.54804	1.52	11,0,3
37.66051	2.38650	1.12	14,4,2
38.74428	2.32220	2.90	12,5,3

$Zn_2(Ad)(BPDC)_{1.5}O_{0.25} \cdot 0.5(NH_2(CH_3)_2)^+$, 2DMF, 2.75$H_2O$ (4), Simulated

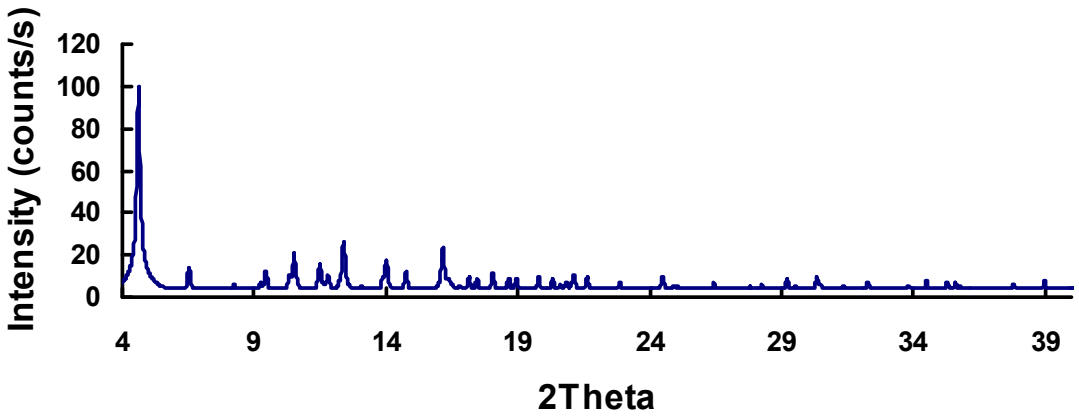

Angle (2θ°)	h,k,l
4.633	2,0,0
6.553	2,2,0
7.307	3,1,0
8.261	1,0,1
10.521	3,0,1
11.475	3,2,1
11.776	5,1,0
12.379	4,1,1
13.136	4,4,0
13.886	6,0,0
14.036	5,0,1
14.790	5,2,1
16.196	1,1,2
17.112	2,2,2
17.460	6,3,1
18.069	7,0,1
18.641	7,2,1
18.955	4,2,2
19.803	5,1,2
20.328	7,4,1
21.137	6,0,2
21.626	6,2,2
22.826	7,6,1
23.274	8,6,0
23.945	9,5,0
24.494	8,0,2
24.914	8,2,2

25.585	7,5,2
26.439	9,1,2
29.206	9,8,1
30.357	11,1,2
32.295	7,6,3
34.545	11,7,2
35.272	11,0,3
37.811	14,4,2
39.004	12,5,3

$Zn_3(Ad)(BTC)_2 \cdot (NH_2(CH_3)_2)^+$, 5.75DMF, 0.25$H_2O$ (5), As -synthesized

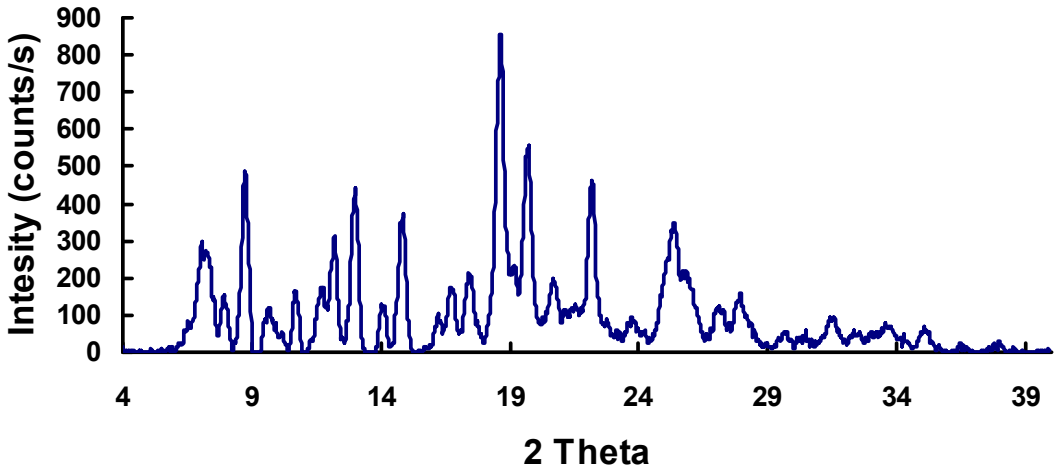

Angle (2θ°)	d-spacing (Å)	Intensity (%)	h,k,l
7.08621	12.46418	30.95	0,2,0
7.24497	12.19142	29.45	1,1,0
7.91919	11.15492	17.53	1,1,-1
8.68098	10.17766	53.63	0,2,1
9.64255	9.16478	12.35	1,1,1
10.69305	8.26666	17.79	0,0,2
11.7211	7.54380	18.97	0,3,1
12.21293	7.24109	36.02	1,3,0
12.89172	6.86131	36.51	2,1,-1
14.07952	6.28502	13.79	1,3,1
14.87247	5.95166	43.43	0,4,1
16.81319	5.26878	20.03	1,4,1
18.64463	4.75516	100	3,1,-1
19.74843	4.49180	60.15	3,1,-2
22.17819	4.00488	49.43	1,5,2
25.35310	3.51010	38.51	1,6,2

$Zn_3(Ad)(BTC)_2 \cdot (NH_2(CH_3)_2)^+$, 5.75DMF, 0.25$H_2O$ (5), Simulated

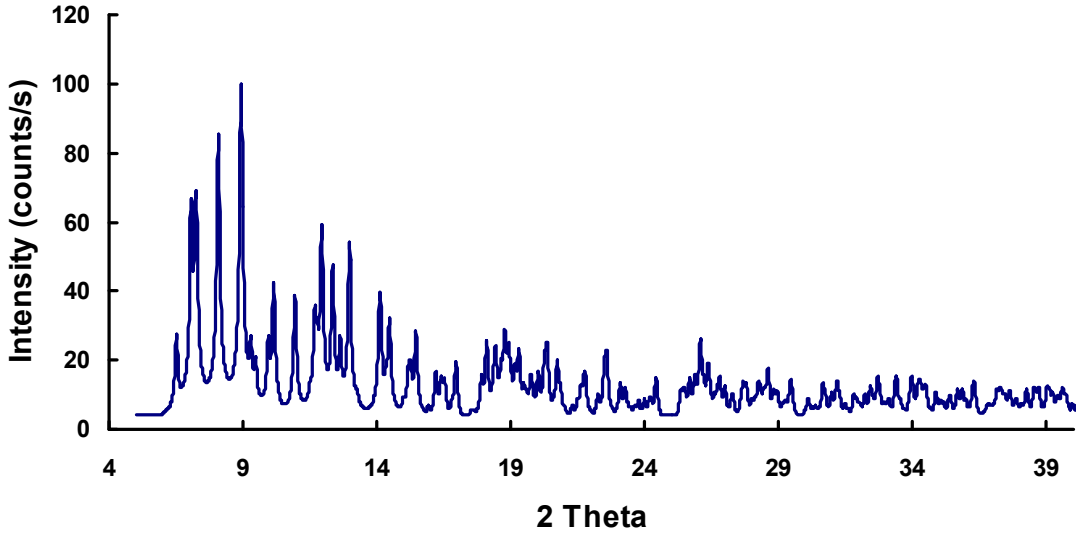

Angle (2θ°)	h,k,l
6.501	0,1,1
7.043	0,2,0
7.213	1,1,0
8.070	1,1,-1
8.920	0,2,1
9.930	1,1,1
10.128	1,2,-1
10.922	0,0,2
11.92	0,3,1
12.323	1,3,0
12.955	2,1,-1
14.090	1,3,1
14.452	2,2,0
15.167	0,4,1
16.926	1,4,1
18.739	3,1,-1
19.780	3,1,-2
22.500	1,5,2
25.485	1,6,2

$Co(Ad)(CH_3CO_2) \cdot DMF, 0.25H_2O$ (6) , As-synthesized

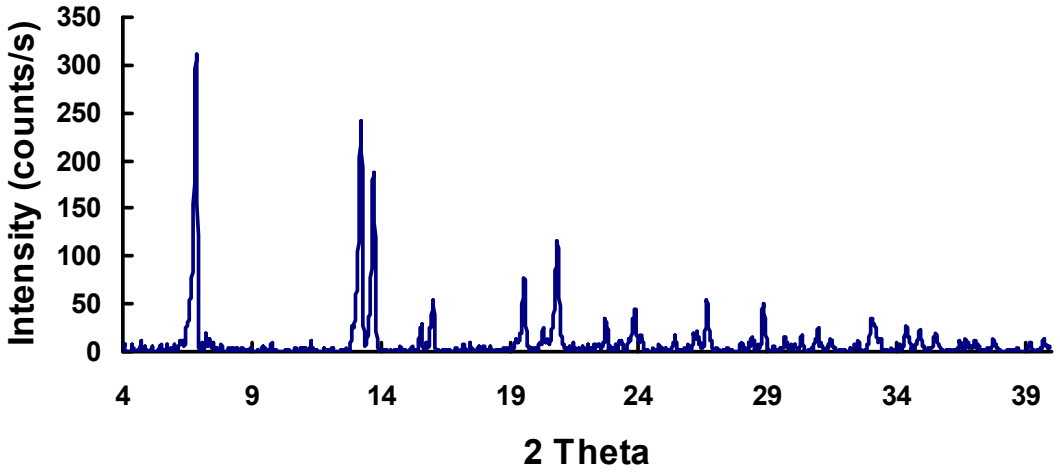

Angle (2θ°)	d-spacing (Å)	Intensity (%)	h,k,l
6.83580	12.92021	100	1,0,1
13.23343	6.68489	68.04	2,-1,1
13.71606	6.45074	57.89	2,0,2
15.55743	5.69113	7.43	0,0,4
16.03610	5.52231	19.36	2,2,0
19.5549	4.53582	24.40	3,-1,2
20.84656	4.25760	36.37	3,2,1
22.73292	3.90839	9.49	4,0,0
23.83461	3.73017	13.53	4,-1,1
25.39599	3.50427	3.98	3,3,2
26.65555	3.34147	16.97	4,2,2
28.82982	3.09422	15.21	4,-3,1
33.06447	2.70697	10.22	5,2,3
34.38786	2.60576	7.65	5,3,2
34.88726	2.56959	6.84	4,-2,6

$Co(Ad)(CH_3CO_2) \cdot DMF, 0.25H_2O$ (6), Simulated

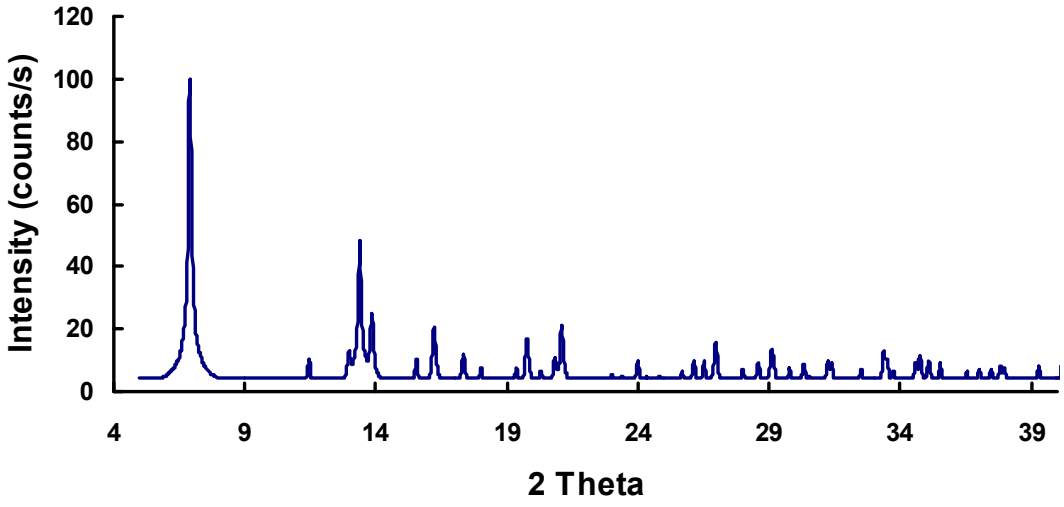

Angle (2θ°)	h,k,l
6.907	1,0,1
13.408	2,-1,1
13.837	2,0,2
15.549	0,0,4
16.211	2,2,0
19.753	3,-1,2
21.116	3,2,1
23.033	4,0,0
24.084	4,-1,1
25.687	3,3,2
26.959	4,2,2
29.171	4,-3,1
33.401	5,2,3
34.755	5,3,2
35.142	4,-2,6

$Zn_2(Ad)(CH_3CO_2)_2 \cdot 0.75DMA, 0.5H_2O$ (7), As synthesized

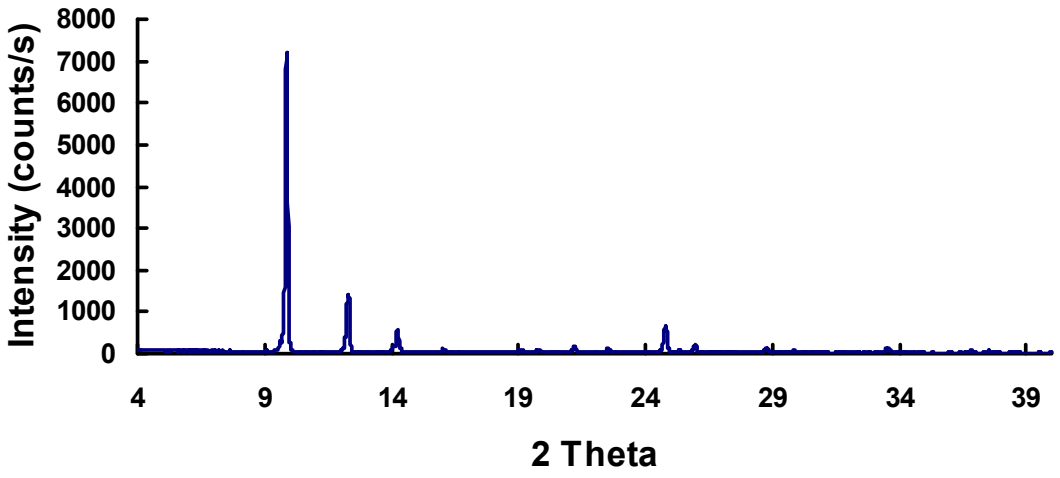

Angle (2θ°)	d-spacing (Å)	Intensity (%)	h,k,l
9.87262	8.95171	100	0,1,1
12.30106	7.18941	19.12	1,1,0
14.24853	6.21085	7.69	1,1,1
16.04743	5.51844	1.10	0,2,1
19.12489	4.63682	1.09	1,2,1
19.84328	4.47055	0.96	2,0,0
21.20411	4.18661	2.34	0,1,3
22.53145	3.94288	1.15	2,1,1
24.80184	3.58685	8.78	0,2,3
25.96514	3.42873	2.53	2,2,1
28.83098	3.09409	1.43	1,1,-4

$Zn_2(Ad)(CH_3CO_2)_2 \cdot 0.75DMA, 0.5H_2O$ (7), Simulated

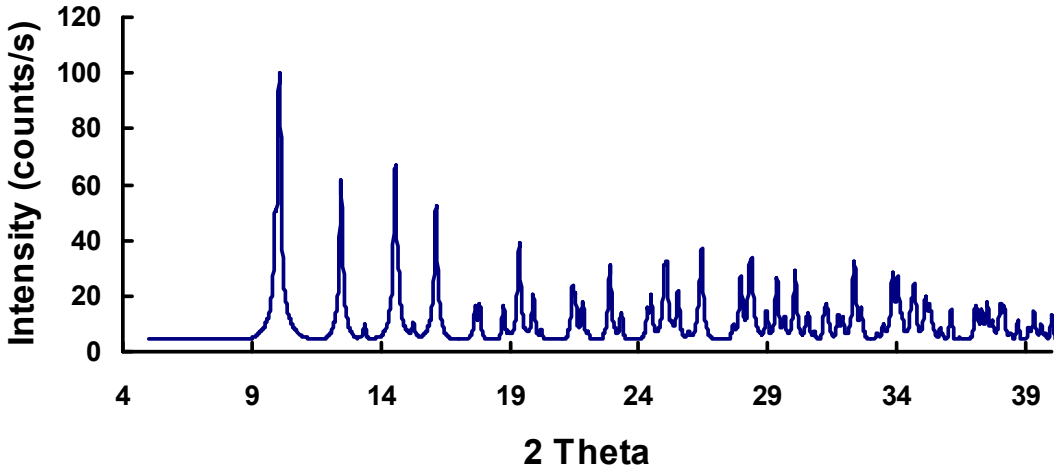

Angle (2θ°)	h,k,l
9.905	0,1,1
12.355	1,1,0
13.722	1,1,-1
14.341	1,1,1
16.172	0,2,1
17.693	1,1,-2
19.241	1,2,1
19.911	2,0,0
21.330	0,1,3
22.696	2,1,1
24.914	0,2,3
26.100	2,2,1
28.937	1,1,-4
30.020	0,3,3
32.160	3,1,1
34.481	1,4,2

FT-IR Spectrum for **Zn(Ad)(Py)(CH_3CO_2) · 1.5DMF (1), As-synthesized**

(KBr4000-400cm^{-1})

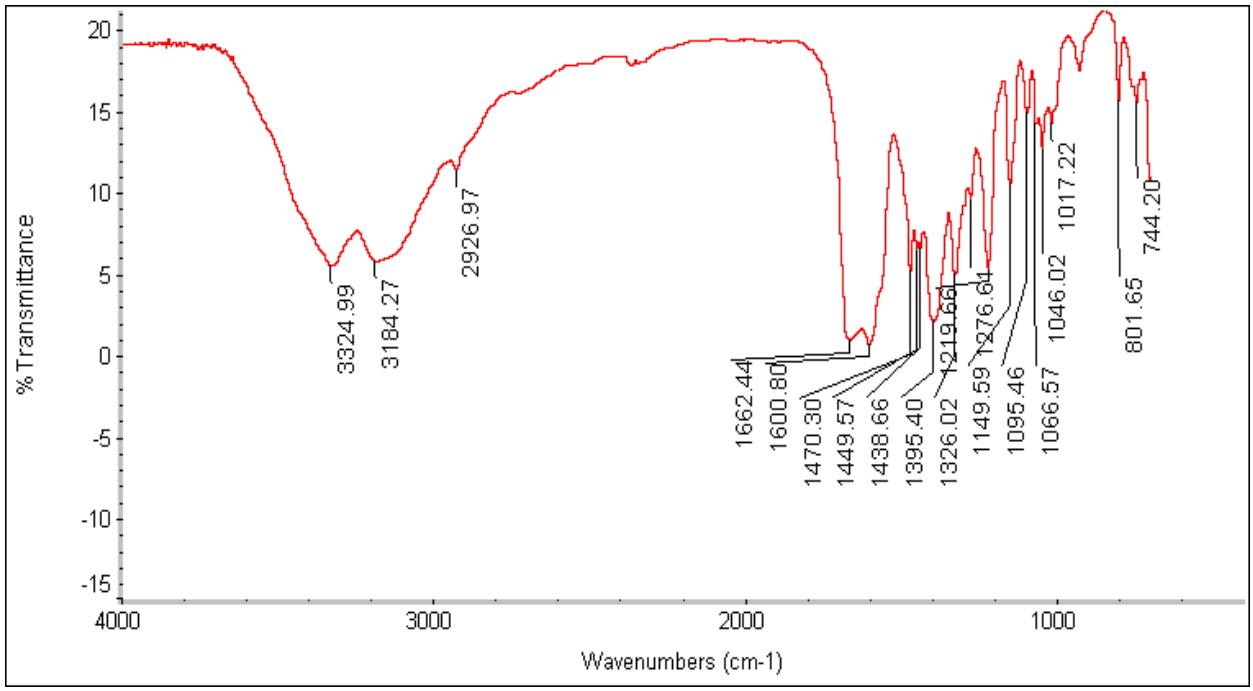

FT-IR Spectrum for **Zn(Ad)(Py)($O_2CN(CH_3)_2$) · 1.75DMF(2), As-synthesized**

(KBr4000-400cm^{-1})

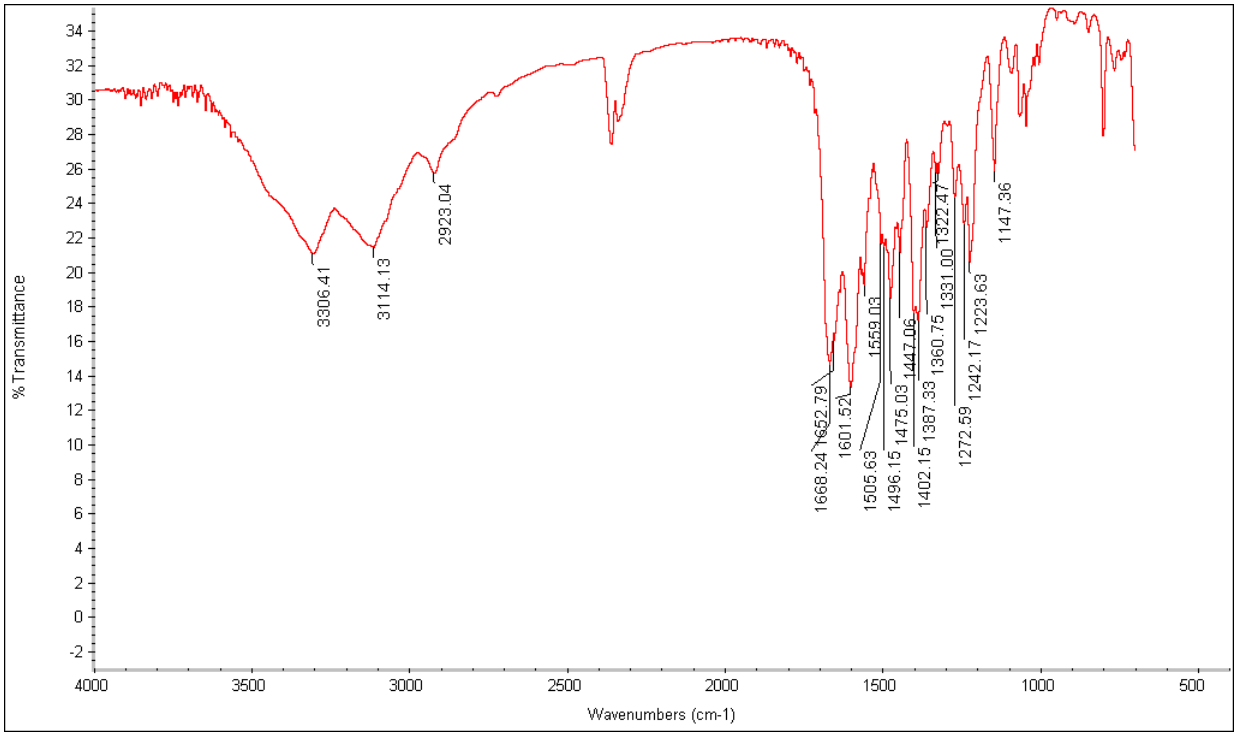

FT-IR Spectrum for **Zn(Ad)(Py)(NO_3)·(xDMF) (3), As-synthesized**

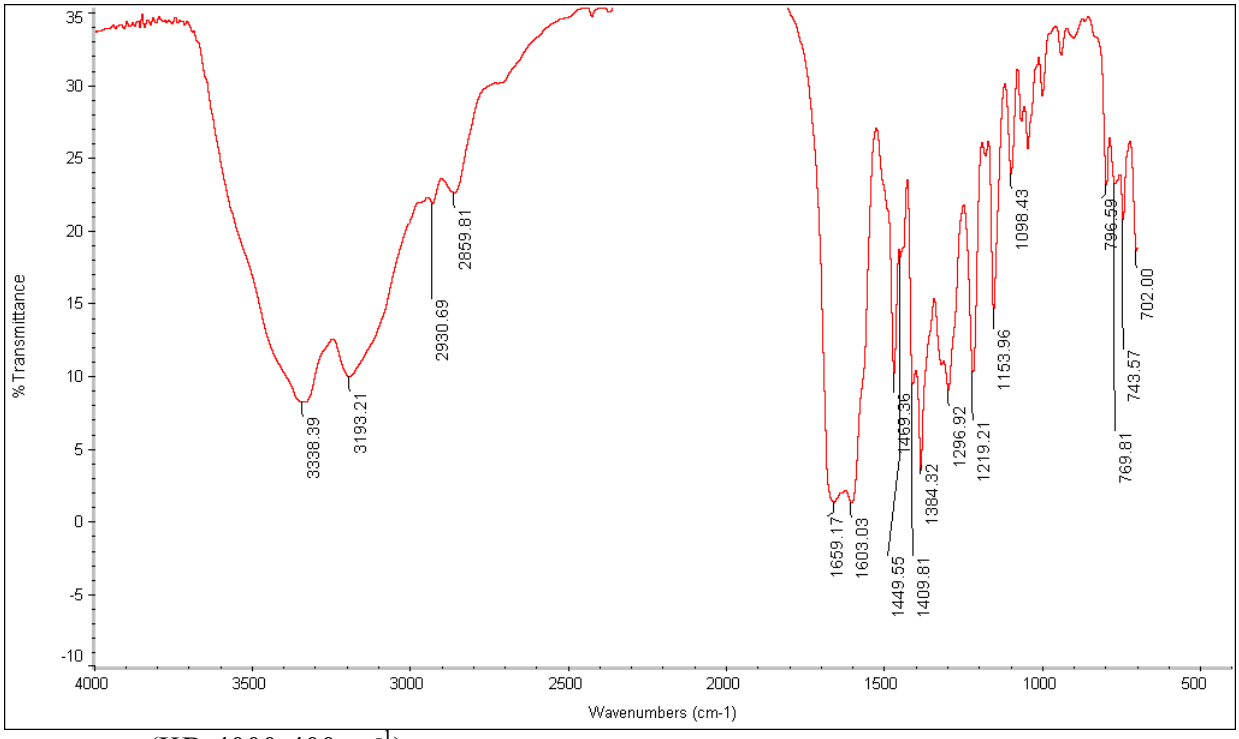

(KBr4000-400cm^{-1})

FT-IR Spectrum for **$Zn_2(Ad)(BPDC)_{1.5}O_{0.25} \cdot 0.5(NH_2(CH_3)_2)^+$, 2DMF, 2.75$H_2O$ (4), As-synthesized** (KBr4000-400cm^{-1})

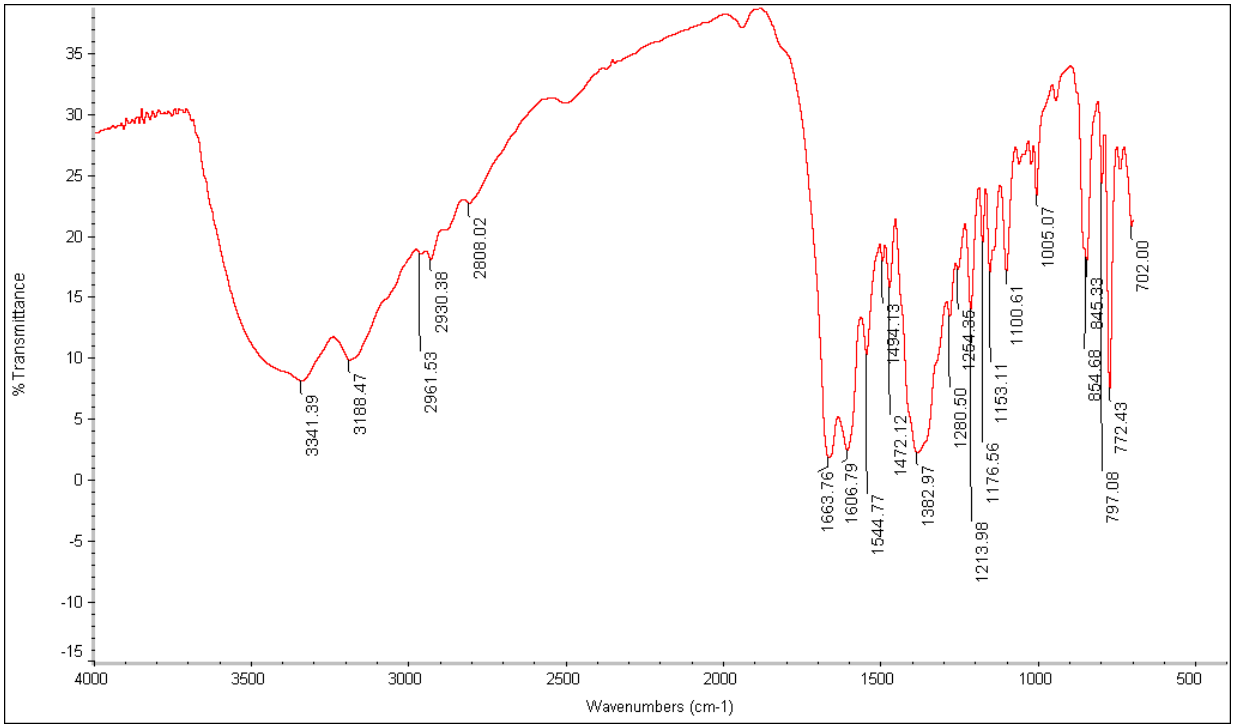

FT-IR Spectrum for **$Zn_3(Ad)(BTC)_2 \cdot (NH_2(CH_3)_2)^+$, 5.75DMF, 0.25$H_2O$ (5), As-synthesized** (KBr4000-400cm^{-1})

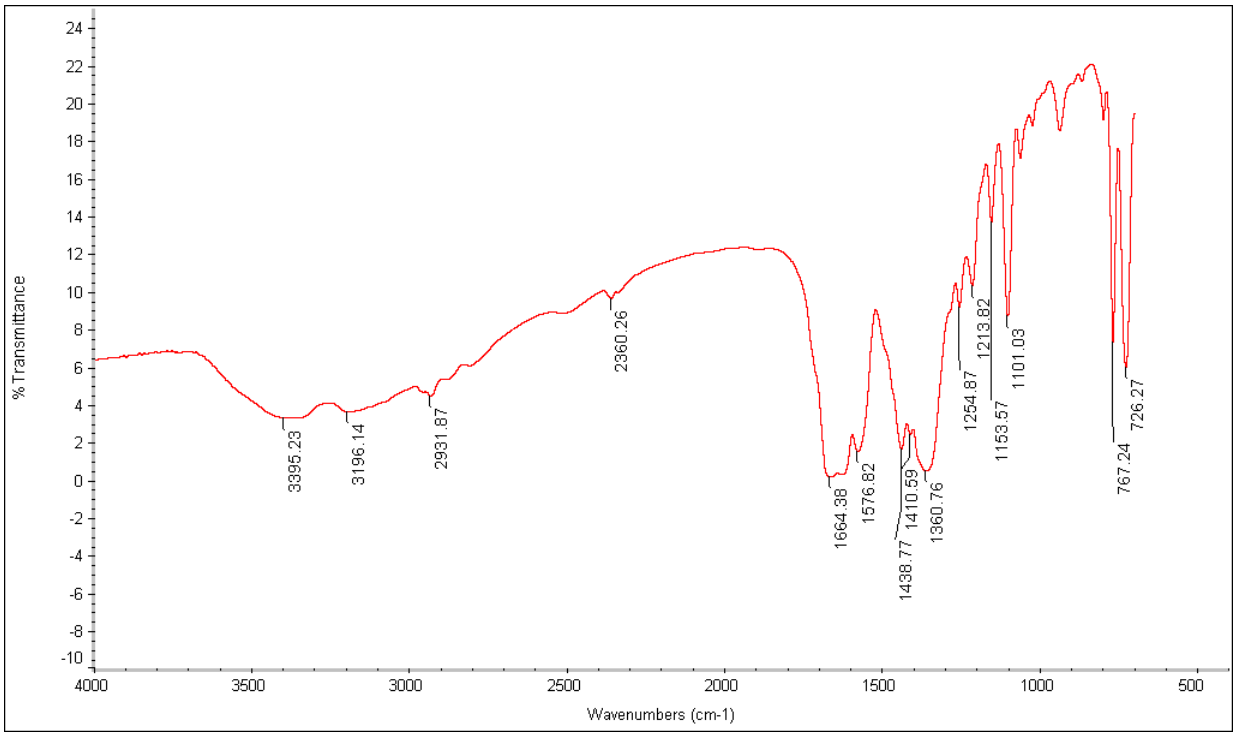

FT-IR Spectrum for **Co(Ad)(CH_3CO_2) · DMF, 0.25H_2O (6), As-synthesized** (KBr4000-400cm^{-1})

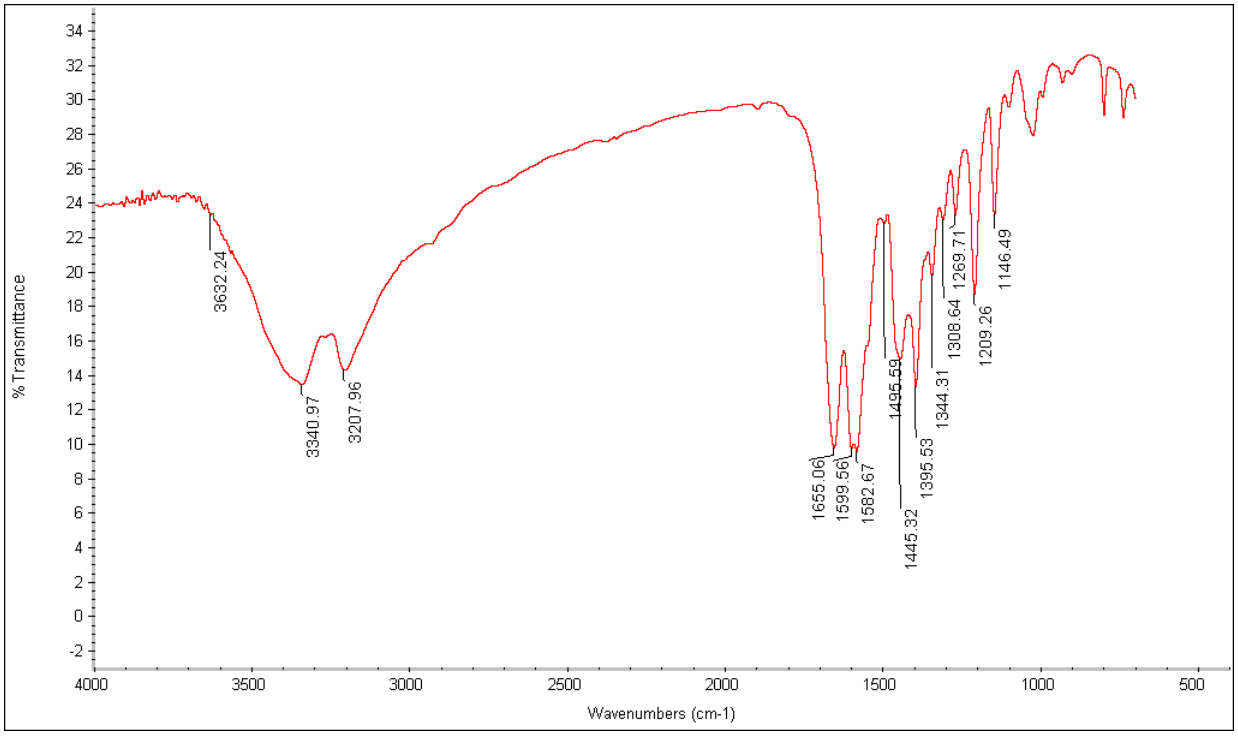

FT-IR Spectrum for **$Zn_2(Ad)(CH_3CO_2)_2 \cdot 0.75DMA, 0.5H_2O$ (7), As-synthesized**

(KBr4000-400cm^{-1})

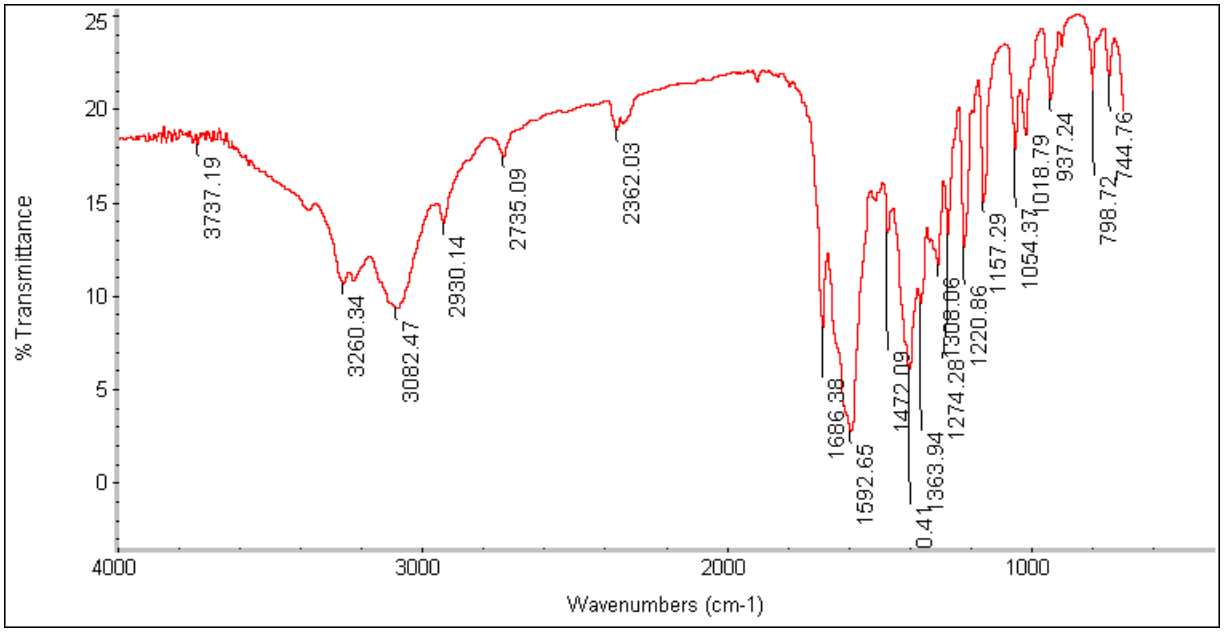

Crystal data and structure refinement for $Zn(Ad)(Py)(CH_3CO_2) \cdot 1.5DMF$ (1).

Identification code	$Zn(Ad)(Py)(CH_3CO_2) \cdot 1.5DMF$	
Empirical formula	C12 H12 N6 O2 Zn	
Formula weight	337.65	
Temperature	295(2) K	
Wavelength	0.71073 Å	
Crystal system	Rhombohedral	
Space group	R-3	
Unit cell dimensions	a = 17.7407(18) Å	α= 90°.
	b = 17.7407(18) Å	β= 90°.
	c = 33.450(3) Å	γ = 120°.
Volume	9117.3(16) $Å^3$	
Z	18	
Density (calculated)	1.107 Mg/m^3	
Absorption coefficient	1.222 mm^{-1}	
F(000)	3096	
Crystal size	0.18 x 0.22 x 0.26 mm^3	
Theta range for data collection	1.46 to 24.98°.	
Index ranges	-21<=h<=21, -21<=k<=21, -39<=l<=39	
Reflections collected	24288	
Independent reflections	3544 [R(int) = 0.0703]	
Completeness to theta = 24.98°	99.7 %	
Absorption correction	multi-scan (SADABS)	
Refinement method	Full-matrix least-squares on F^2	
Data / restraints / parameters	3544 / 0 / 190	
Goodness-of-fit on F^2	0.959	
Final R indices [I>2sigma(I)]	R1 = 0.0444, wR2 = 0.1111	
R indices (all data)	R1 = 0.0622, wR2 = 0.1187	
Largest diff. peak and hole	0.351 and -0.227 $e.Å^{-3}$	

Atomic coordinates (x 10^4) and equivalent isotropic displacement parameters ($Å^2$ x 10^3)
for Zn(Ad)(Py)(CH_3CO_2) · 1.5DMF (1). U(eq) is defined as one third of the trace of the orthogonalized U^{ij} tensor.

	x	y	z	U(eq)
Zn	6498(1)	7439(1)	1203(1)	57(1)
N(1)	5635(2)	6168(2)	1294(1)	54(1)
C(1)	5345(2)	5837(2)	1657(1)	54(1)
O(1)	6239(2)	7658(2)	671(1)	103(1)
C(2)	5190(2)	5452(2)	1048(1)	53(1)
O(2)	7193(3)	8990(2)	753(1)	153(2)
N(2)	4773(2)	4991(2)	1670(1)	52(1)
C(3)	5172(2)	5335(2)	631(1)	70(1)
N(3)	4149(2)	3923(2)	1145(1)	74(1)
N(4)	4654(2)	4523(2)	492(1)	87(1)
C(4)	4184(3)	3893(2)	755(1)	92(1)
N(5)	5627(2)	5956(2)	366(1)	101(1)
C(5)	4673(2)	4738(2)	1276(1)	53(1)
C(6)	6684(4)	8423(3)	543(1)	98(1)
N(6)	7666(2)	7500(2)	1180(1)	83(1)
C(7)	6543(5)	8606(4)	125(2)	188(3)
C(8)	7734(5)	6813(5)	1151(3)	183(4)
C(9)	8486(7)	6797(8)	1149(3)	222(4)
C(10)	9195(5)	7525(8)	1125(3)	179(3)
C(11)	9168(6)	8206(7)	1169(6)	349(11)
C(12)	8336(4)	8157(5)	1198(4)	298(8)

Bond lengths [Å] and angles [°] for Zn(Ad)(Py)(CH_3CO_2) · 1.5DMF (1)..

Zn-O(1)	1.925(3)
Zn-N(2)#1	1.973(2)
Zn-N(1)	2.017(2)
Zn-N(6)	2.022(3)
N(1)-C(1)	1.336(3)
N(1)-C(2)	1.382(3)
C(1)-N(2)	1.328(4)
C(1)-H(1A)	0.9300
O(1)-C(6)	1.256(5)
C(2)-C(5)	1.367(4)
C(2)-C(3)	1.408(4)
O(2)-C(6)	1.190(5)
N(2)-C(5)	1.372(3)
N(2)-Zn#2	1.973(2)
C(3)-N(5)	1.327(4)
C(3)-N(4)	1.346(4)
N(3)-C(4)	1.308(4)
N(3)-C(5)	1.343(4)
N(4)-C(4)	1.338(4)
C(4)-H(4A)	0.9300
N(5)-H(5A)	0.8600
N(5)-H(5B)	0.8600
C(6)-C(7)	1.485(6)
N(6)-C(12)	1.179(7)
N(6)-C(8)	1.286(6)
C(7)-H(7A)	0.9600
C(7)-H(7B)	0.9600
C(7)-H(7C)	0.9600
C(8)-C(9)	1.348(10)
C(8)-H(8A)	0.9300
C(9)-C(10)	1.278(10)
C(9)-H(9A)	0.9300
C(10)-C(11)	1.242(10)
C(10)-H(10A)	0.9300

C(11)-C(12)	1.437(11)
C(11)-H(11A)	0.9300
C(12)-H(12A)	0.9300

O(1)-Zn-N(2)#1	121.00(12)
O(1)-Zn-N(1)	103.95(11)
N(2)#1-Zn-N(1)	108.39(10)
O(1)-Zn-N(6)	107.19(15)
N(2)#1-Zn-N(6)	110.46(13)
N(1)-Zn-N(6)	104.49(13)
C(1)-N(1)-C(2)	102.8(2)
C(1)-N(1)-Zn	122.64(19)
C(2)-N(1)-Zn	134.60(19)
N(2)-C(1)-N(1)	115.7(2)
N(2)-C(1)-H(1A)	122.1
N(1)-C(1)-H(1A)	122.1
C(6)-O(1)-Zn	116.6(3)
C(5)-C(2)-N(1)	109.2(2)
C(5)-C(2)-C(3)	117.5(3)
N(1)-C(2)-C(3)	133.3(3)
C(1)-N(2)-C(5)	103.9(2)
C(1)-N(2)-Zn#2	128.79(19)
C(5)-N(2)-Zn#2	127.0(2)
N(5)-C(3)-N(4)	117.7(3)
N(5)-C(3)-C(2)	125.3(3)
N(4)-C(3)-C(2)	117.0(3)
C(4)-N(3)-C(5)	110.4(3)
C(4)-N(4)-C(3)	118.2(3)
N(3)-C(4)-N(4)	130.2(3)
N(3)-C(4)-H(4A)	114.9
N(4)-C(4)-H(4A)	114.9
C(3)-N(5)-H(5A)	120.0
C(3)-N(5)-H(5B)	120.0
H(5A)-N(5)-H(5B)	120.0
N(3)-C(5)-C(2)	126.7(3)
N(3)-C(5)-N(2)	124.8(3)

C(2)-C(5)-N(2)	108.5(3)
O(2)-C(6)-O(1)	120.9(4)
O(2)-C(6)-C(7)	120.8(5)
O(1)-C(6)-C(7)	118.3(5)
C(12)-N(6)-C(8)	114.6(6)
C(12)-N(6)-Zn	123.3(4)
C(8)-N(6)-Zn	122.0(4)
C(6)-C(7)-H(7A)	109.5
C(6)-C(7)-H(7B)	109.5
H(7A)-C(7)-H(7B)	109.5
C(6)-C(7)-H(7C)	109.5
H(7A)-C(7)-H(7C)	109.5
H(7B)-C(7)-H(7C)	109.5
N(6)-C(8)-C(9)	125.6(8)
N(6)-C(8)-H(8A)	117.2
C(9)-C(8)-H(8A)	117.2
C(10)-C(9)-C(8)	117.6(9)
C(10)-C(9)-H(9A)	121.2
C(8)-C(9)-H(9A)	121.2
C(11)-C(10)-C(9)	118.6(8)
C(11)-C(10)-H(10A)	120.7
C(9)-C(10)-H(10A)	120.7
C(10)-C(11)-C(12)	119.1(9)
C(10)-C(11)-H(11A)	120.4
C(12)-C(11)-H(11A)	120.4
N(6)-C(12)-C(11)	123.6(8)
N(6)-C(12)-H(12A)	118.2
C(11)-C(12)-H(12A)	118.2

Symmetry transformations used to generate equivalent atoms:

#1 x-y+2/3,x+1/3,-z+1/3 #2 y-1/3,-x+y+1/3,-z+1/3

Anisotropic displacement parameters ($Å^2$ x 10^3) for Zn(Ad)(Py)(CH_3CO_2) · 1.5DMF (1).

The anisotropic displacement factor exponent takes the form: $-2\pi^2[h^2 a^{*2}U^{11} + ... + 2 h k a^* b^* U^{12}]$

	U^{11}	U^{22}	U^{33}	U^{23}	U^{13}	U^{12}
Zn	71(1)	51(1)	38(1)	-6(1)	7(1)	24(1)
N(1)	66(2)	52(2)	33(1)	-4(1)	8(1)	21(1)
C(1)	62(2)	58(2)	34(2)	-5(1)	2(1)	24(2)
O(1)	155(3)	62(2)	60(2)	-1(1)	-11(2)	30(2)
C(2)	66(2)	48(2)	33(2)	-2(1)	10(1)	20(2)
O(2)	203(4)	73(2)	117(3)	-7(2)	-14(3)	20(2)
N(2)	55(2)	55(2)	35(1)	4(1)	7(1)	19(1)
C(3)	92(3)	50(2)	40(2)	-6(1)	18(2)	15(2)
N(3)	92(2)	54(2)	44(2)	-1(1)	18(1)	12(2)
N(4)	120(3)	53(2)	43(2)	-8(1)	25(2)	10(2)
C(4)	123(3)	50(2)	58(2)	-9(2)	24(2)	11(2)
N(5)	151(3)	55(2)	36(2)	-4(1)	24(2)	7(2)
C(5)	66(2)	51(2)	37(2)	-2(1)	8(1)	24(2)
C(6)	145(4)	63(3)	67(3)	-2(2)	-2(3)	37(3)
N(6)	73(2)	78(2)	96(2)	4(2)	21(2)	35(2)
C(7)	308(10)	141(5)	76(4)	35(3)	-23(5)	84(6)
C(8)	145(6)	151(6)	299(11)	-24(6)	35(6)	108(5)
C(9)	189(9)	230(10)	316(13)	22(9)	82(9)	157(9)
C(10)	93(5)	197(9)	250(9)	22(7)	60(5)	73(6)
C(11)	102(6)	134(8)	790(40)	89(12)	74(10)	45(6)
C(12)	58(4)	116(5)	710(20)	48(9)	2(7)	33(4)

Hydrogen coordinates (x 10^4) and isotropic displacement parameters ($Å^2$ x 10^3)

$Zn(Ad)(Py)(CH_3CO_2) \cdot 1.5DMF$ (1).

	x	y	z	U(eq)
H(1A)	5532	6178	1887	65
H(4A)	3824	3348	644	110
H(5A)	5585	5833	116	121
H(5B)	5964	6482	445	121
H(7A)	6923	9211	67	282
H(7B)	5949	8466	92	282
H(7C)	6664	8258	-55	282
H(8A)	7220	6281	1129	220
H(9A)	8488	6275	1165	267
H(10A)	9720	7544	1075	215
H(11A)	9679	8741	1182	419
H(12A)	8326	8672	1233	358

Crystal data and structure refinement for Zn(Ad)(Py)($O_2CN(CH_3)_2$) · 1.75DMF (2).

Identification code	Zn(Ad)(Py)($O_2CN(CH_3)_2$) · 1.75DMF	
Empirical formula	C60 H25 N30 O18 Zn6	
Formula weight	1846.32	
Temperature	173(2) K	
Wavelength	0.71073 Å	
Crystal system	Rhombohedral	
Space group	R-3	
Unit cell dimensions	a = 17.780(3) Å	α= 90°.
	b = 17.780(3) Å	β= 90°.
	c = 33.531(7) Å	γ = 120°.
Volume	9180(3) $Å^3$	
Z	4	
Density (calculated)	1.336 Mg/m^3	
Absorption coefficient	1.614 mm^{-1}	
F(000)	3676	
Crystal size	? x ? x ? mm^3	
Theta range for data collection	1.80 to 26.41°.	
Index ranges	-22<=h<=22, -22<=k<=22, -41<=l<=41	
Reflections collected	25940	
Independent reflections	4016 [R(int) = 0.1071]	
Completeness to theta = 26.41°	95.8 %	
Absorption correction	mult-scan	
Refinement method	Full-matrix least-squares on F^2	
Data / restraints / parameters	4016 / 0 / 213	
Goodness-of-fit on F^2	1.066	
Final R indices [I>2sigma(I)]	R1 = 0.0658, wR2 = 0.1831	
R indices (all data)	R1 = 0.1041, wR2 = 0.2083	
Largest diff. peak and hole	1.308 and -0.677 $e.Å^{-3}$	

Atomic coordinates (x 10^4) and equivalent isotropic displacement parameters ($Å^2$x 10^3) for Zn(Ad)(Py)($O_2CN(CH_3)_2$) · 1.75DMF (2). U(eq) is defined as one third of the trace of the orthogonalized U^{ij} tensor.

	x	y	z	U(eq)
Zn	2385(1)	9212(1)	471(1)	27(1)
N(1)	2738(3)	10477(3)	378(1)	27(1)
C(1)	3031(3)	11190(3)	621(1)	26(1)
O(1)	1799(3)	8961(2)	986(1)	43(1)
C(2)	3106(4)	11308(3)	1039(2)	37(1)
N(2)	3446(4)	12131(3)	1175(1)	50(1)
O(2)	1794(3)	7723(3)	877(1)	56(1)
C(3)	3645(5)	12773(4)	916(2)	59(2)
N(3)	3585(4)	12745(3)	519(1)	42(1)
N(4)	3110(3)	11672(3)	-8(1)	27(1)
C(4)	3263(4)	11926(3)	386(1)	30(1)
N(5)	2884(4)	10685(3)	1300(1)	54(2)
C(5)	2806(3)	10819(3)	7(1)	30(1)
C(6)	1625(4)	8166(4)	1094(2)	39(1)
N(6)	1261(4)	7901(4)	1457(2)	64(2)
N(7)	3560(3)	9271(3)	498(1)	35(1)
C(7)	1040(7)	8415(6)	1710(2)	112(4)
C(8)	1095(6)	7052(6)	1602(3)	97(3)
C(9)	4303(4)	10028(4)	489(2)	46(2)
C(10)	5101(4)	10085(5)	503(2)	59(2)
C(11)	5151(5)	9361(5)	525(2)	58(2)
C(12)	4411(5)	8583(5)	540(3)	83(3)
C(13)	3622(5)	8553(5)	533(3)	72(2)
O(3)	0	10000	695(19)	120
O(4)	3333	6667	1024(6)	120
O(5)	3333	6667	1667	120

Bond lengths [Å] and angles [°] for Zn(Ad)(Py)($O_2CN(CH_{3)2}$) · 1.75DMF (2).

Zn-O(1)	1.949(4)
Zn-N(4)#1	1.971(4)
Zn-N(1)	2.033(4)
Zn-N(7)	2.041(5)
N(1)-C(5)	1.364(6)
N(1)-C(1)	1.373(6)
C(1)-C(4)	1.401(7)
C(1)-C(2)	1.416(7)
O(1)-C(6)	1.337(7)
C(2)-N(5)	1.307(7)
C(2)-N(2)	1.353(7)
N(2)-C(3)	1.334(7)
O(2)-C(6)	1.216(7)
C(3)-N(3)	1.332(7)
C(3)-H(5A)	0.9500
N(3)-C(4)	1.347(7)
N(4)-C(5)	1.333(6)
N(4)-C(4)	1.380(6)
N(4)-Zn#2	1.971(4)
N(5)-H(5B)	0.8800
N(5)-H(3C)	0.8800
C(5)-H(5)	0.9500
C(6)-N(6)	1.350(7)
N(6)-C(7)	1.438(10)
N(6)-C(8)	1.468(10)
N(7)-C(9)	1.333(7)
N(7)-C(13)	1.340(8)
C(7)-H(7A)	0.9800
C(7)-H(7B)	0.9800
C(7)-H(7C)	0.9800
C(8)-H(8A)	0.9800
C(8)-H(8B)	0.9800
C(8)-H(8C)	0.9800
C(9)-C(10)	1.371(9)

C(9)-H(9A)	0.9500
C(10)-C(11)	1.336(10)
C(10)-H(10A)	0.9500
C(11)-C(12)	1.351(10)
C(11)-H(11A)	0.9500
C(12)-C(13)	1.378(10)
C(12)-H(12A)	0.9500
C(13)-H(13A)	0.9500

O(1)-Zn-N(4)#1	116.72(17)
O(1)-Zn-N(1)	102.97(16)
N(4)#1-Zn-N(1)	106.18(17)
O(1)-Zn-N(7)	112.87(19)
N(4)#1-Zn-N(7)	114.01(18)
N(1)-Zn-N(7)	101.99(18)
C(5)-N(1)-C(1)	102.8(4)
C(5)-N(1)-Zn	122.9(3)
C(1)-N(1)-Zn	134.0(3)
N(1)-C(1)-C(4)	109.2(4)
N(1)-C(1)-C(2)	133.6(4)
C(4)-C(1)-C(2)	117.2(4)
C(6)-O(1)-Zn	107.2(3)
N(5)-C(2)-N(2)	118.2(5)
N(5)-C(2)-C(1)	124.9(5)
N(2)-C(2)-C(1)	116.8(5)
C(3)-N(2)-C(2)	119.3(5)
N(3)-C(3)-N(2)	129.6(5)
N(3)-C(3)-H(5A)	115.2
N(2)-C(3)-H(5A)	115.2
C(3)-N(3)-C(4)	110.7(5)
C(5)-N(4)-C(4)	103.8(4)
C(5)-N(4)-Zn#2	128.4(3)
C(4)-N(4)-Zn#2	127.3(3)
N(3)-C(4)-N(4)	125.4(4)
N(3)-C(4)-C(1)	126.2(4)
N(4)-C(4)-C(1)	108.3(4)

C(2)-N(5)-H(5B)	120.0
C(2)-N(5)-H(3C)	120.0
H(5B)-N(5)-H(3C)	120.0
N(4)-C(5)-N(1)	115.9(4)
N(4)-C(5)-H(5)	122.0
N(1)-C(5)-H(5)	122.0
O(2)-C(6)-O(1)	121.5(5)
O(2)-C(6)-N(6)	123.0(6)
O(1)-C(6)-N(6)	115.4(6)
C(6)-N(6)-C(7)	123.1(6)
C(6)-N(6)-C(8)	118.1(7)
C(7)-N(6)-C(8)	118.8(6)
C(9)-N(7)-C(13)	116.9(5)
C(9)-N(7)-Zn	121.5(4)
C(13)-N(7)-Zn	121.6(4)
N(6)-C(7)-H(7A)	109.5
N(6)-C(7)-H(7B)	109.5
H(7A)-C(7)-H(7B)	109.5
N(6)-C(7)-H(7C)	109.5
H(7A)-C(7)-H(7C)	109.5
H(7B)-C(7)-H(7C)	109.5
N(6)-C(8)-H(8A)	109.5
N(6)-C(8)-H(8B)	109.5
H(8A)-C(8)-H(8B)	109.5
N(6)-C(8)-H(8C)	109.5
H(8A)-C(8)-H(8C)	109.5
H(8B)-C(8)-H(8C)	109.5
N(7)-C(9)-C(10)	122.6(7)
N(7)-C(9)-H(9A)	118.7
C(10)-C(9)-H(9A)	118.7
C(11)-C(10)-C(9)	119.7(7)
C(11)-C(10)-H(10A)	120.1
C(9)-C(10)-H(10A)	120.1
C(10)-C(11)-C(12)	119.3(7)
C(10)-C(11)-H(11A)	120.4
C(12)-C(11)-H(11A)	120.4

C(11)-C(12)-C(13)	119.3(7)
C(11)-C(12)-H(12A)	120.3
C(13)-C(12)-H(12A)	120.3
N(7)-C(13)-C(12)	122.1(7)
N(7)-C(13)-H(13A)	118.9
C(12)-C(13)-H(13A)	118.9

Symmetry transformations used to generate equivalent atoms:

#1 y-1,-x+y,-z #2 x-y+1,x+1,-z

Anisotropic displacement parameters ($Å^2 x\ 10^3$) for $Zn(Ad)(Py)(O_2CN(CH_{3)2})$ · 1.75DMF (2). The anisotropic displacement factor exponent takes the form: $-2\pi^2[\ h^2\ a^{*2}U^{11} + ...\ + 2\ h\ k\ a^*\ b^*\ U^{12}\ ]$

	U^{11}	U^{22}	U^{33}	U^{23}	U^{13}	U^{12}
Zn	33(1)	25(1)	19(1)	-2(1)	-4(1)	11(1)
N(1)	36(2)	28(2)	18(2)	-2(2)	-4(2)	16(2)
C(1)	37(3)	21(2)	18(2)	-2(2)	-8(2)	13(2)
O(1)	58(3)	34(2)	25(2)	-2(2)	5(2)	13(2)
C(2)	61(4)	33(3)	19(3)	-2(2)	-8(2)	23(3)
N(2)	96(4)	31(3)	18(2)	-4(2)	-13(3)	28(3)
O(2)	72(3)	33(2)	55(3)	4(2)	18(2)	20(2)
C(3)	108(6)	27(3)	30(3)	-8(3)	-16(3)	25(4)
N(3)	71(4)	25(2)	23(2)	1(2)	-10(2)	19(2)
N(4)	38(2)	30(2)	15(2)	2(2)	-2(2)	18(2)
C(4)	41(3)	33(3)	18(2)	0(2)	-5(2)	21(3)
N(5)	109(5)	32(3)	17(2)	-3(2)	-13(3)	32(3)
C(5)	39(3)	30(3)	20(3)	-1(2)	-2(2)	17(2)
C(6)	37(3)	35(3)	25(3)	4(2)	1(2)	2(3)
N(6)	81(4)	54(4)	36(3)	14(3)	17(3)	18(3)
N(7)	38(3)	32(2)	34(3)	2(2)	-4(2)	17(2)
C(7)	149(10)	86(7)	48(5)	-6(4)	46(6)	18(6)
C(8)	105(7)	87(6)	70(6)	54(5)	17(5)	27(5)
C(9)	37(3)	47(4)	48(4)	-1(3)	-7(3)	16(3)
C(10)	39(4)	60(5)	72(5)	-2(4)	-9(3)	20(3)
C(11)	47(4)	76(5)	54(4)	8(4)	-8(3)	33(4)
C(12)	58(5)	47(4)	153(9)	13(5)	1(5)	33(4)
C(13)	50(4)	37(4)	127(7)	8(4)	-1(4)	22(3)

Hydrogen coordinates (x 10^4) and isotropic displacement parameters ($Å^2$x 10^3) for Zn(Ad)(Py)($O_2CN(CH_{3)2}$) · 1.75DMF (2).

	x	y	z	U(eq)
H(5A)	3861	13332	1031	70
H(5B)	2958	10808	1556	65
H(3C)	2661	10144	1220	65
H(5)	2646	10470	-227	35
H(7A)	1170	8952	1572	169
H(7B)	1381	8559	1957	169
H(7C)	420	8085	1775	169
H(8A)	1275	6778	1398	145
H(8B)	474	6681	1656	145
H(8C)	1427	7130	1847	145
H(9A)	4278	10549	471	55
H(10A)	5615	10637	496	71
H(11A)	5700	9393	530	70
H(12A)	4436	8062	556	99
H(13A)	3104	8006	552	86

Crystal data and structure refinement for $Zn_2(Ad)(BPDC)_{1.5}O_{0.25} \cdot 0.5(NH_2(CH_3)_2)^+$, 2DMF, 2.75$H_2O$ (4).

Identification code	$Zn_2(Ad)(BPDC)_{1.5}O_{0.25} \cdot 0.5(NH_2(CH_3)_2)^+$, 2DMF, 2.75$H_2O$	
Empirical formula	C26 H16 N5 O6.25 Zn2	
Formula weight	629.18	
Temperature	173(2) K	
Wavelength	0.71073 Å	
Crystal system	Tetragonal	
Space group	I4(1)22	
Unit cell dimensions	a = 38.237(2) Å	α= 90°.
	b = 38.237(2) Å	β= 90°.
	c = 11.1753(12) Å	γ = 90°.
Volume	16339(2) $Å^3$	
Z	16	
Density (calculated)	1.023 Mg/m^3	
Absorption coefficient	1.207 mm^{-1}	
F(000)	5072	
Crystal size	0.20 x 0.16 x 0.16 mm^3	
Theta range for data collection	1.90 to 25.00°.	
Index ranges	-45<=h<=45, -45<=k<=45, -13<=l<=13	
Reflections collected	66011	
Independent reflections	7226 [R(int) = 0.1261]	
Completeness to theta = 25.00°	99.8 %	
Absorption correction	Semi-empirical from equivalents	
Max. and min. transmission	0.8303 and 0.7942	
Refinement method	Full-matrix least-squares on F^2	
Data / restraints / parameters	7226 / 0 / 319	
Goodness-of-fit on F^2	1.054	
Final R indices [I>2sigma(I)]	R1 = 0.0824, wR2 = 0.2133	
R indices (all data)	R1 = 0.1040, wR2 = 0.2272	
Absolute structure parameter	0.56(4)	
Largest diff. peak and hole	0.785 and -0.614 e.$Å^{-3}$	

Atomic coordinates (x 10^4) and equivalent isotropic displacement parameters ($Å^2$x 10^3) for $Zn_2(Ad)(BPDC)_{1.5}O_{0.25} \cdot 0.5(NH_2(CH_3)_2)^+$, 2DMF, $2.75H_2O$ (4). U(eq) is defined as one third of the trace of the orthogonalized U^{ij} tensor.

	x	y	z	U(eq)
Zn(1)	4592(1)	5008(1)	3965(1)	44(1)
Zn(2)	5883(1)	5883(1)	0	42(1)
Zn(3)	4132(1)	5868(1)	0	40(1)
O(1)	5000	5000	5000	25(2)
O(2)	3923(2)	5005(3)	3265(7)	101(3)
O(3)	4181(2)	4891(3)	4962(8)	112(4)
O(4)	1303(2)	4292(2)	6769(7)	77(3)
O(5)	1517(2)	4014(2)	8263(7)	72(2)
O(6)	3706(2)	5692(2)	885(8)	84(3)
O(7)	3842(5)	6235(4)	-1434(12)	175(5)
N(1)	5345(1)	5374(1)	2856(4)	50(2)
N(2)	4712(1)	5408(1)	2704(4)	72(3)
N(3)	4545(1)	5778(1)	1097(4)	49(2)
N(4)	5500(1)	5726(1)	1340(5)	69(3)
N(5)	4925(2)	6072(1)	-193(4)	77(3)
C(1)	5041(1)	5490(1)	2362(3)	67(3)
C(2)	4475(1)	5560(1)	2040(5)	60(3)
C(3)	4874(1)	5864(1)	733(3)	73(3)
C(4)	5141(1)	5709(1)	1423(3)	75(3)
C(5)	5611(1)	5520(2)	2214(5)	78(4)
C(6)	3924(3)	4921(3)	4307(10)	70(3)
C(7)	3575(2)	4846(3)	4855(14)	94(4)
C(8)	3262(3)	4913(5)	4287(13)	129(7)
C(9)	3572(3)	4684(5)	6025(12)	138(8)
C(10)	2957(3)	4802(6)	4735(15)	173(10)
C(11)	3228(4)	4578(5)	6438(12)	132(7)
C(12)	2922(3)	4646(4)	5834(13)	106(5)
C(13)	2589(3)	4539(4)	6288(12)	92(4)
C(14)	2292(3)	4685(7)	5850(20)	269(18)
C(15)	2544(2)	4290(5)	7003(13)	125(7)

C(16)	1961(3)	4582(7)	6280(20)	223(15)
C(17)	2204(3)	4140(4)	7403(13)	97(5)
C(18)	1922(3)	4324(3)	7033(11)	75(3)
C(19)	1544(2)	4199(3)	7407(12)	67(3)
C(20)	3500(9)	5804(9)	1010(70)	610(60)
C(21)	3169(5)	6200(4)	2660(20)	1020(120)
C(22)	2865(5)	6193(4)	3341(19)	290(20)
C(23)	2680(4)	5883(6)	3475(15)	175(10)
C(24)	2799(5)	5579(4)	2927(19)	380(40)
C(25)	3103(5)	5586(4)	2244(16)	194(12)
C(26)	3288(3)	5896(5)	2110(14)	169(10)

Bond lengths [Å] and angles [°] for $Zn_2(Ad)(BPDC)_{1.5}O_{0.25} \cdot 0.5(NH_2(CH_3)_2)^+$, 2DMF, $2.75H_2O$ (4).

Zn(1)-N(1)#1	1.929(4)
Zn(1)-O(1)	1.9433(7)
Zn(1)-O(3)	1.976(7)
Zn(1)-N(2)	2.130(3)
Zn(1)-Zn(1)#1	3.1232(15)
Zn(2)-O(4)#2	1.922(6)
Zn(2)-O(4)#3	1.922(6)
Zn(2)-N(4)	2.178(4)
Zn(2)-N(4)#4	2.178(5)
Zn(2)-C(19)#2	2.547(9)
Zn(2)-C(19)#3	2.548(9)
Zn(3)-O(6)	2.020(7)
Zn(3)-O(6)#5	2.020(7)
Zn(3)-N(3)	2.027(4)
Zn(3)-N(3)#5	2.027(4)
Zn(3)-O(7)#5	2.402(13)
Zn(3)-O(7)	2.402(13)
O(1)-Zn(1)#6	1.9433(7)
O(1)-Zn(1)#1	1.9434(7)
O(1)-Zn(1)#7	1.9435(7)
O(2)-C(6)	1.209(12)
O(3)-C(6)	1.233(13)
O(4)-C(19)	1.217(13)
O(4)-Zn(2)#8	1.922(6)
O(5)-C(19)	1.193(13)
O(6)-C(20)	0.91(2)
O(7)-C(20)#5	1.76(5)
N(1)-C(1)	1.3616
N(1)-C(5)	1.3651
N(1)-Zn(1)#1	1.929(4)
N(2)-C(2)	1.3080
N(2)-C(1)	1.3532
N(3)-C(3)	1.3640
N(3)-C(2)	1.3712

N(4)-C(5)	1.3232
N(4)-C(4)	1.3803
N(5)-C(3)	1.3202
C(1)-C(4)	1.3939
C(3)-C(4)	1.4083
C(6)-C(7)	1.496(14)
C(7)-C(8)	1.377(14)
C(7)-C(9)	1.446(18)
C(8)-C(10)	1.340(16)
C(9)-C(11)	1.453(16)
C(10)-C(12)	1.371(18)
C(11)-C(12)	1.373(17)
C(12)-C(13)	1.433(15)
C(13)-C(15)	1.254(17)
C(13)-C(14)	1.356(17)
C(14)-C(16)	1.411(16)
C(15)-C(17)	1.490(14)
C(16)-C(18)	1.301(17)
C(17)-C(18)	1.353(16)
C(18)-C(19)	1.579(14)
C(19)-Zn(2)#8	2.548(9)
C(20)-C(26)	1.52(5)
C(20)-O(7)#5	1.76(5)
C(21)-C(22)	1.3900
C(21)-C(26)	1.3900
C(22)-C(23)	1.3900
C(23)-C(24)	1.3900
C(23)-C(23)#9	1.508(19)
C(24)-C(25)	1.3900
C(25)-C(26)	1.3900

N(1)#1-Zn(1)-O(1)	105.64(15)
N(1)#1-Zn(1)-O(3)	107.0(4)
O(1)-Zn(1)-O(3)	107.4(2)
N(1)#1-Zn(1)-N(2)	95.2(2)
O(1)-Zn(1)-N(2)	103.39(14)

O(3)-Zn(1)-N(2)	134.9(3)
N(1)#1-Zn(1)-Zn(1)#1	81.93(15)
O(1)-Zn(1)-Zn(1)#1	36.53(2)
O(3)-Zn(1)-Zn(1)#1	142.2(3)
N(2)-Zn(1)-Zn(1)#1	78.37(12)
O(4)#2-Zn(2)-O(4)#3	139.7(5)
O(4)#2-Zn(2)-N(4)	106.8(3)
O(4)#3-Zn(2)-N(4)	100.0(2)
O(4)#2-Zn(2)-N(4)#4	100.0(3)
O(4)#3-Zn(2)-N(4)#4	106.8(4)
N(4)-Zn(2)-N(4)#4	95.9(4)
O(4)#2-Zn(2)-C(19)#2	27.3(4)
O(4)#3-Zn(2)-C(19)#2	117.7(4)
N(4)-Zn(2)-C(19)#2	102.6(3)
N(4)#4-Zn(2)-C(19)#2	127.2(4)
O(4)#2-Zn(2)-C(19)#3	117.7(4)
O(4)#3-Zn(2)-C(19)#3	27.3(4)
N(4)-Zn(2)-C(19)#3	127.2(3)
N(4)#4-Zn(2)-C(19)#3	102.6(4)
C(19)#2-Zn(2)-C(19)#3	104.2(5)
O(6)-Zn(3)-O(6)#5	141.0(4)
O(6)-Zn(3)-N(3)	105.9(3)
O(6)#5-Zn(3)-N(3)	100.0(3)
O(6)-Zn(3)-N(3)#5	100.0(4)
O(6)#5-Zn(3)-N(3)#5	105.9(4)
N(3)-Zn(3)-N(3)#5	95.9(4)
O(6)-Zn(3)-O(7)#5	49.9(5)
O(6)#5-Zn(3)-O(7)#5	98.6(5)
N(3)-Zn(3)-O(7)#5	97.5(4)
N(3)#5-Zn(3)-O(7)#5	149.5(5)
O(6)-Zn(3)-O(7)	98.6(5)
O(6)#5-Zn(3)-O(7)	49.9(5)
N(3)-Zn(3)-O(7)	149.5(5)
N(3)#5-Zn(3)-O(7)	97.5(4)
O(7)#5-Zn(3)-O(7)	84.5(7)
Zn(1)#6-O(1)-Zn(1)	109.24(8)

Zn(1)#6-O(1)-Zn(1)#1	112.28(7)
Zn(1)-O(1)-Zn(1)#1	106.94(5)
Zn(1)#6-O(1)-Zn(1)#7	106.94(5)
Zn(1)-O(1)-Zn(1)#7	112.29(7)
Zn(1)#1-O(1)-Zn(1)#7	109.23(7)
C(6)-O(3)-Zn(1)	106.2(7)
C(19)-O(4)-Zn(2)#8	106.3(7)
C(20)-O(6)-Zn(3)	128(3)
C(20)#5-O(7)-Zn(3)	78.4(11)
C(1)-N(1)-C(5)	106.7
C(1)-N(1)-Zn(1)#1	128.0(2)
C(5)-N(1)-Zn(1)#1	123.7(2)
C(2)-N(2)-C(1)	112.4
C(2)-N(2)-Zn(1)	123.0(2)
C(1)-N(2)-Zn(1)	123.7(2)
C(3)-N(3)-C(2)	123.8
C(3)-N(3)-Zn(3)	119.9(2)
C(2)-N(3)-Zn(3)	114.6(2)
C(5)-N(4)-C(4)	103.9
C(5)-N(4)-Zn(2)	117.2(2)
C(4)-N(4)-Zn(2)	136.8(2)
N(2)-C(1)-N(1)	127.1
N(2)-C(1)-C(4)	127.3
N(1)-C(1)-C(4)	105.6
N(2)-C(2)-N(3)	124.8
N(5)-C(3)-N(3)	120.9
N(5)-C(3)-C(4)	125.3
N(3)-C(3)-C(4)	113.8
N(4)-C(4)-C(1)	110.6
N(4)-C(4)-C(3)	131.6
C(1)-C(4)-C(3)	117.8
N(4)-C(5)-N(1)	113.2
O(2)-C(6)-O(3)	126.8(9)
O(2)-C(6)-C(7)	116.3(11)
O(3)-C(6)-C(7)	116.9(10)
C(8)-C(7)-C(9)	119.3(11)

C(8)-C(7)-C(6)	123.4(12)
C(9)-C(7)-C(6)	117.3(10)
C(10)-C(8)-C(7)	121.6(12)
C(7)-C(9)-C(11)	114.4(12)
C(8)-C(10)-C(12)	123.8(10)
C(12)-C(11)-C(9)	124.0(13)
C(10)-C(12)-C(11)	116.2(11)
C(10)-C(12)-C(13)	121.8(10)
C(11)-C(12)-C(13)	121.8(13)
C(15)-C(13)-C(14)	115.2(11)
C(15)-C(13)-C(12)	124.5(13)
C(14)-C(13)-C(12)	119.9(12)
C(13)-C(14)-C(16)	120.8(13)
C(13)-C(15)-C(17)	127.1(12)
C(18)-C(16)-C(14)	122.4(13)
C(18)-C(17)-C(15)	113.8(11)
C(16)-C(18)-C(17)	119.9(10)
C(16)-C(18)-C(19)	120.4(10)
C(17)-C(18)-C(19)	119.4(10)
O(5)-C(19)-O(4)	125.3(10)
O(5)-C(19)-C(18)	118.0(9)
O(4)-C(19)-C(18)	116.6(11)
O(5)-C(19)-Zn(2)#8	79.0(6)
O(4)-C(19)-Zn(2)#8	46.4(5)
C(18)-C(19)-Zn(2)#8	162.9(9)
O(6)-C(20)-C(26)	134(7)
O(6)-C(20)-O(7)#5	84(3)
C(26)-C(20)-O(7)#5	85(3)
C(22)-C(21)-C(26)	120.0
C(21)-C(22)-C(23)	120.0
C(24)-C(23)-C(22)	120.0
C(24)-C(23)-C(23)#9	118.6(8)
C(22)-C(23)-C(23)#9	120.6(3)
C(23)-C(24)-C(25)	120.0
C(26)-C(25)-C(24)	120.0
C(25)-C(26)-C(21)	120.0

C(25)-C(26)-C(20)	99.3(19)
C(21)-C(26)-C(20)	136.6(19)

Symmetry transformations used to generate equivalent atoms:

#1 -x+1,-y+1,z+0 #2 -y+1,x+1/2,z-3/4 #3 x+1/2,-y+1,-z+3/4

#4 y+0,x+0,-z+0 #5 -y+1,-x+1,-z #6 -y+1,-x+1,-z+1

#7 y+0,x+0,-z+1 #8 y-1/2,-x+1,z+3/4 #9 -x+1/2,y,-z+3/4

Anisotropic displacement parameters ($Å^2 x\ 10^3$) for $Zn_2(Ad)(BPDC)_{1.5}O_{0.25} \cdot 0.5(NH_2(CH_3)_2)^+$, 2DMF, $2.75H_2O$ (4). The anisotropic displacement factor exponent takes the form: $-2\pi^2[h^2 a^{*2}U^{11} + ... + 2 h k a^* b^* U^{12}]$

	U^{11}	U^{22}	U^{33}	U^{23}	U^{13}	U^{12}
Zn(1)	28(1)	64(1)	40(1)	16(1)	-5(1)	6(1)
Zn(2)	36(1)	36(1)	54(1)	-1(1)	1(1)	10(1)
Zn(3)	38(1)	38(1)	43(1)	18(1)	18(1)	23(1)
O(2)	54(4)	165(8)	85(5)	53(7)	17(3)	-39(6)
O(3)	30(4)	209(12)	98(6)	18(7)	8(4)	-19(5)
O(4)	18(3)	125(7)	88(6)	52(5)	-26(4)	-26(3)
O(5)	41(4)	116(6)	60(5)	16(5)	5(3)	-15(4)
O(6)	72(5)	89(6)	90(6)	56(5)	61(5)	48(4)
O(7)	235(17)	171(13)	118(9)	11(9)	-22(11)	39(11)
N(1)	43(5)	61(5)	45(5)	4(4)	12(4)	-9(3)
N(2)	84(7)	51(5)	81(7)	28(5)	-21(5)	20(4)
N(3)	22(4)	55(4)	70(5)	37(4)	-23(3)	10(3)
N(4)	41(5)	78(6)	90(7)	-51(6)	3(5)	-2(4)
N(5)	128(9)	48(4)	56(4)	32(4)	23(5)	4(5)
C(1)	110(9)	59(5)	34(4)	-1(4)	33(7)	-40(6)
C(2)	78(7)	53(6)	50(6)	33(5)	-32(5)	-7(5)
C(3)	30(5)	79(8)	110(10)	-24(7)	-7(5)	20(4)
C(4)	69(7)	81(8)	76(7)	-29(6)	10(6)	-12(6)
C(5)	75(8)	65(7)	93(10)	14(7)	32(7)	25(6)
C(6)	55(6)	83(10)	73(7)	-7(6)	17(5)	-35(5)
C(7)	20(5)	123(10)	138(12)	31(9)	-22(6)	-12(5)
C(8)	65(7)	206(19)	115(11)	115(13)	-22(7)	-14(9)
C(9)	67(8)	290(20)	61(8)	21(11)	-5(7)	-86(11)
C(10)	18(5)	350(30)	150(13)	165(16)	-33(6)	-44(9)
C(11)	78(9)	260(20)	56(7)	32(11)	9(7)	-53(11)
C(12)	38(6)	177(15)	102(10)	34(10)	-30(6)	-3(7)
C(13)	55(7)	137(11)	85(9)	49(9)	24(6)	-15(7)
C(14)	15(6)	490(40)	300(30)	330(30)	-17(10)	-14(11)
C(15)	11(5)	249(19)	115(11)	77(13)	-7(6)	-15(7)
C(16)	22(6)	380(30)	270(20)	270(20)	3(9)	-6(11)
C(17)	46(6)	127(11)	118(11)	57(9)	26(7)	8(6)

C(18)	38(5)	106(9)	81(8)	26(7)	2(5)	-12(5)
C(19)	34(5)	68(7)	98(9)	0(7)	-5(6)	-13(5)
C(20)	280(40)	230(30)	1310(170)	-50(60)	560(70)	50(30)
C(21)	170(30)	1330(180)	1600(200)	1220(190)	370(80)	280(70)
C(22)	230(30)	200(20)	440(50)	-160(30)	250(30)	-70(20)
C(23)	133(17)	230(30)	161(19)	-9(19)	82(15)	-29(16)
C(24)	700(100)	190(30)	270(40)	40(30)	300(50)	-80(40)
C(25)	210(20)	133(17)	240(30)	-3(18)	150(20)	34(16)
C(26)	64(10)	220(20)	220(20)	90(20)	65(12)	67(12)

Hydrogen coordinates (x 10^4) and isotropic displacement parameters ($Å^2$x 10^3)
for $Zn_2(Ad)(BPDC)_{1.5}O_{0.25} \cdot 0.5(NH_2(CH_3)_2)^+$, 2DMF, $2.75H_2O$ (4).

	x	y	z	U(eq)
H(5A)	4744	6158	-584	92
H(5B)	5139	6125	-419	92
H(2A)	4236	5516	2225	72
H(5C)	5851	5479	2379	93
H(8A)	3263	5042	3559	154
H(9A)	3778	4650	6485	166
H(10A)	2752	4832	4264	207
H(11A)	3213	4453	7171	158
H(14A)	2307	4858	5245	323
H(15A)	2749	4186	7325	150
H(16A)	1760	4705	6018	267
H(17A)	2186	3934	7873	116
H(21A)	3295	6412	2566	1220
H(22A)	2784	6401	3715	351
H(24A)	2673	5367	3019	461
H(25A)	3184	5378	1870	233

Crystal data and structure refinement for $Zn_3(Ad)(BTC)_2 \cdot (NH_2(CH_3)_2)^+$, 5.75DMF, $0.25H_2O$ (5).

Identification code	$Zn_3(Ad)(BTC)_2 \cdot (NH_2(CH_3)_2)^+$, 5.75DMF, $0.25H_2O$	
Empirical formula	C16 H13.14 N4 O7.43 Zn1.71	
Formula weight	492.37	
Temperature	173(2) K	
Wavelength	0.71073 Å	
Crystal system	Monoclinic	
Space group	P2(1)/n	
Unit cell dimensions	a = 14.468(5) Å	α= 90°.
	b = 25.046(9) Å	β= 104.039(7)°.
	c = 16.684(6) Å	γ = 90°.
Volume	5865(4) $Å^3$	
Z	7	
Density (calculated)	0.976 Mg/m^3	
Absorption coefficient	1.260 mm^{-1}	
F(000)	1736	
Crystal size	? x ? x ? mm^3	
Theta range for data collection	1.63 to 25.00°.	
Index ranges	-17<=h<=17, -29<=k<=29, -19<=l<=19	
Reflections collected	45777	
Independent reflections	10337 [R(int) = 0.0634]	
Completeness to theta = 25.00°	100.0 %	
Absorption correction	None	
Refinement method	Full-matrix least-squares on F^2	
Data / restraints / parameters	10337 / 0 / 487	
Goodness-of-fit on F^2	1.240	
Final R indices [I>2sigma(I)]	R1 = 0.0663, wR2 = 0.1714	
R indices (all data)	R1 = 0.0909, wR2 = 0.1781	
Largest diff. peak and hole	1.278 and -0.508 $e.Å^{-3}$	

Atomic coordinates (x 10^4) and equivalent isotropic displacement parameters ($Å^2$x 10^3) for $Zn_3(Ad)(BTC)_2 \cdot (NH_2(CH_3)_2)^+$, 5.75DMF, 0.25$H_2O$ (5). U(eq) is defined as one third of the trace of the orthogonalized U^{ij} tensor.

	x	y	z	U(eq)
C(1)	3056(3)	8724(2)	7128(3)	41(1)
N(1)	2561(3)	9086(2)	7463(2)	42(1)
O(1)	130(3)	9147(2)	7146(2)	72(1)
Zn(1)	1788(1)	9947(1)	8779(1)	44(1)
C(2)	3156(4)	9215(2)	8200(3)	42(1)
N(2)	3017(3)	9579(2)	8768(2)	46(1)
O(2)	820(3)	9366(2)	8436(2)	57(1)
Zn(2)	1303(1)	9339(1)	6832(1)	46(1)
C(3)	3776(4)	9637(2)	9405(3)	56(2)
N(3)	4578(3)	9377(2)	9553(3)	59(1)
Zn(3)	4859(1)	8234(1)	7057(1)	47(1)
O(3)	-1401(3)	9896(2)	10193(2)	61(1)
C(4)	4707(4)	9002(2)	9021(3)	48(1)
N(4)	3917(3)	8618(2)	7584(2)	40(1)
O(4)	-2669(3)	9373(2)	10087(2)	64(1)
C(5)	3997(3)	8929(2)	8287(3)	39(1)
N(5)	5506(3)	8730(2)	9203(3)	52(1)
O(5)	-4095(3)	8717(2)	7289(3)	81(1)
C(6)	-820(4)	9168(2)	8097(3)	50(1)
N(6)	4027(6)	8635(4)	4595(5)	132(3)
O(6)	-3136(4)	8295(4)	6618(4)	175(4)
C(7)	-945(4)	9370(2)	8850(3)	50(1)
O(7)	1325(3)	10133(2)	6896(2)	73(1)
N(7)	-2463(12)	9554(7)	5484(11)	132(6)
C(8)	-1822(4)	9333(2)	9033(3)	53(1)
O(8)	1268(3)	10542(2)	8059(2)	57(1)
N(8)	1501(11)	8943(9)	11532(13)	190(11)
C(9)	-2565(4)	9095(3)	8476(4)	67(2)
O(9)	291(3)	12456(1)	7802(2)	62(1)
C(10)	-2440(5)	8883(3)	7735(4)	77(2)

O(10)	-612(3)	12744(2)	6643(3)	88(2)
C(11)	-1571(4)	8932(3)	7546(4)	73(2)
O(11)	-921(3)	10711(2)	4363(2)	67(1)
C(12)	104(4)	9229(2)	7885(3)	51(1)
O(12)	-1176(3)	11575(2)	4149(3)	82(1)
C(13)	-1981(5)	9545(3)	9823(3)	56(2)
O(13)	4161(3)	8322(2)	5885(2)	61(1)
C(14)	-3276(6)	8602(4)	7152(5)	110(3)
C(15)	561(4)	10955(2)	6799(3)	44(1)
C(16)	451(4)	11443(2)	7154(3)	46(1)
C(17)	-51(4)	11850(2)	6686(3)	51(1)
C(18)	-479(4)	11766(2)	5856(3)	50(1)
C(19)	-414(4)	11277(2)	5485(3)	49(1)
C(20)	108(4)	10875(2)	5961(3)	47(1)
C(21)	1087(4)	10508(2)	7285(3)	46(1)
C(22)	-140(4)	12390(2)	7062(4)	59(2)
C(23)	-878(4)	11196(3)	4600(3)	60(2)
C(24)	4460(10)	8838(7)	3925(7)	229(8)
C(25)	2957(7)	8657(6)	4492(7)	179(6)
C(26)	4491(7)	8476(4)	5364(6)	117(3)
C(27)	-3246(14)	9663(11)	5806(13)	194(14)
C(28)	-1795(17)	9619(16)	5383(17)	280(20)
C(29)	1813(17)	8360(7)	11880(14)	164(11)
C(30)	840(14)	9107(6)	11145(12)	115(7)

Bond lengths [Å] and angles [°] for $Zn_3(Ad)(BTC)_2 \cdot (NH_2(CH_3)_2)^+$, 5.75DMF, $0.25H_2O$ (5).

C(1)-N(4)	1.318(6)
C(1)-N(1)	1.358(6)
C(1)-H(1A)	0.9500
N(1)-C(2)	1.359(6)
N(1)-Zn(2)	1.972(4)
O(1)-C(12)	1.259(6)
O(1)-Zn(2)	1.954(4)
Zn(1)-O(8)	1.947(4)
Zn(1)-O(3)#1	1.969(4)
Zn(1)-N(2)	2.007(4)
Zn(1)-O(2)	2.004(4)
C(2)-N(2)	1.364(6)
C(2)-C(5)	1.389(7)
N(2)-C(3)	1.338(6)
O(2)-C(12)	1.254(6)
Zn(2)-O(11)#2	1.939(4)
Zn(2)-O(7)	1.990(4)
C(3)-N(3)	1.302(7)
C(3)-H(3A)	0.9500
N(3)-C(4)	1.336(7)
Zn(3)-O(5)#3	1.902(4)
Zn(3)-O(9)#4	1.981(4)
Zn(3)-O(13)	1.983(4)
Zn(3)-N(4)	2.033(4)
Zn(3)-C(22)#4	2.550(6)
O(3)-C(13)	1.267(7)
O(3)-Zn(1)#1	1.969(4)
C(4)-N(5)	1.312(6)
C(4)-C(5)	1.407(7)
N(4)-C(5)	1.389(6)
O(4)-C(13)	1.259(7)
N(5)-H(5A)	0.8800
N(5)-H(5B)	0.8800
O(5)-C(14)	1.293(9)

O(5)-Zn(3)#5	1.902(4)
C(6)-C(11)	1.375(7)
C(6)-C(7)	1.407(7)
C(6)-C(12)	1.472(8)
N(6)-C(26)	1.355(11)
N(6)-C(24)	1.496(12)
N(6)-C(25)	1.517(11)
O(6)-C(14)	1.229(9)
C(7)-C(8)	1.379(8)
C(7)-H(7A)	0.9500
O(7)-C(21)	1.237(6)
N(7)-C(28)	1.03(2)
N(7)-C(27)	1.39(3)
C(8)-C(9)	1.375(8)
C(8)-C(13)	1.489(8)
O(8)-C(21)	1.257(6)
N(8)-C(30)	1.10(2)
N(8)-C(29)	1.60(2)
C(9)-C(10)	1.397(8)
C(9)-H(9A)	0.9500
O(9)-C(22)	1.252(7)
O(9)-Zn(3)#6	1.981(4)
C(10)-C(11)	1.373(8)
C(10)-C(14)	1.528(9)
O(10)-C(22)	1.228(7)
C(11)-H(11A)	0.9500
O(11)-C(23)	1.277(7)
O(11)-Zn(2)#2	1.939(4)
O(12)-C(23)	1.222(7)
O(13)-C(26)	1.155(11)
C(15)-C(16)	1.384(7)
C(15)-C(20)	1.407(7)
C(15)-C(21)	1.480(7)
C(16)-C(17)	1.379(7)
C(16)-H(16A)	0.9500
C(17)-C(18)	1.390(7)

C(17)-C(22)	1.509(8)
C(18)-C(19)	1.384(8)
C(18)-H(18A)	0.9500
C(19)-C(20)	1.387(7)
C(19)-C(23)	1.480(7)
C(20)-H(20A)	0.9500
C(22)-Zn(3)#6	2.550(6)
C(24)-H(24A)	0.9800
C(24)-H(24B)	0.9800
C(24)-H(24C)	0.9800
C(25)-H(25A)	0.9800
C(25)-H(25B)	0.9800
C(25)-H(25C)	0.9800
C(26)-H(26A)	0.9500
C(27)-H(27A)	0.9800
C(27)-H(27B)	0.9800
C(27)-H(27C)	0.9800
C(28)-H(28A)	0.9800
C(28)-H(28B)	0.9800
C(28)-H(28C)	0.9800
C(29)-H(29A)	0.9800
C(29)-H(29B)	0.9800
C(29)-H(29C)	0.9800
C(30)-H(30A)	0.9800
C(30)-H(30B)	0.9800
C(30)-H(30C)	0.9800

N(4)-C(1)-N(1)	114.6(4)
N(4)-C(1)-H(1A)	122.7
N(1)-C(1)-H(1A)	122.7
C(1)-N(1)-C(2)	104.4(4)
C(1)-N(1)-Zn(2)	120.4(3)
C(2)-N(1)-Zn(2)	135.0(4)
C(12)-O(1)-Zn(2)	117.2(4)
O(8)-Zn(1)-O(3)#1	103.61(17)
O(8)-Zn(1)-N(2)	123.78(18)

O(3)#1-Zn(1)-N(2)	122.67(17)
O(8)-Zn(1)-O(2)	103.93(16)
O(3)#1-Zn(1)-O(2)	93.88(17)
N(2)-Zn(1)-O(2)	102.93(17)
N(2)-C(2)-N(1)	128.3(5)
N(2)-C(2)-C(5)	123.1(4)
N(1)-C(2)-C(5)	108.6(4)
C(3)-N(2)-C(2)	113.2(4)
C(3)-N(2)-Zn(1)	120.1(4)
C(2)-N(2)-Zn(1)	126.4(3)
C(12)-O(2)-Zn(1)	143.5(4)
O(1)-Zn(2)-O(11)#2	102.15(17)
O(1)-Zn(2)-N(1)	121.76(18)
O(11)#2-Zn(2)-N(1)	121.60(18)
O(1)-Zn(2)-O(7)	103.6(2)
O(11)#2-Zn(2)-O(7)	96.68(18)
N(1)-Zn(2)-O(7)	106.96(18)
N(3)-C(3)-N(2)	128.2(5)
N(3)-C(3)-H(3A)	115.9
N(2)-C(3)-H(3A)	115.9
C(4)-N(3)-C(3)	119.2(4)
O(5)#3-Zn(3)-O(9)#4	134.9(2)
O(5)#3-Zn(3)-O(13)	108.64(19)
O(9)#4-Zn(3)-O(13)	100.47(17)
O(5)#3-Zn(3)-N(4)	101.28(19)
O(9)#4-Zn(3)-N(4)	108.05(17)
O(13)-Zn(3)-N(4)	98.03(17)
O(5)#3-Zn(3)-C(22)#4	113.7(2)
O(9)#4-Zn(3)-C(22)#4	28.73(17)
O(13)-Zn(3)-C(22)#4	129.20(19)
N(4)-Zn(3)-C(22)#4	99.94(17)
C(13)-O(3)-Zn(1)#1	105.6(4)
N(3)-C(4)-N(5)	117.9(5)
N(3)-C(4)-C(5)	118.7(5)
N(5)-C(4)-C(5)	123.4(5)
C(1)-N(4)-C(5)	104.4(4)

C(1)-N(4)-Zn(3)	118.9(3)
C(5)-N(4)-Zn(3)	134.6(3)
N(4)-C(5)-C(4)	134.6(5)
N(4)-C(5)-C(2)	108.0(4)
C(4)-C(5)-C(2)	117.4(5)
C(4)-N(5)-H(5A)	120.0
C(4)-N(5)-H(5B)	120.0
H(5A)-N(5)-H(5B)	120.0
C(14)-O(5)-Zn(3)#5	122.7(5)
C(11)-C(6)-C(7)	120.0(5)
C(11)-C(6)-C(12)	120.1(5)
C(7)-C(6)-C(12)	119.9(5)
C(26)-N(6)-C(24)	127.3(10)
C(26)-N(6)-C(25)	112.1(8)
C(24)-N(6)-C(25)	120.3(10)
C(8)-C(7)-C(6)	119.9(5)
C(8)-C(7)-H(7A)	120.1
C(6)-C(7)-H(7A)	120.1
C(21)-O(7)-Zn(2)	141.6(4)
C(28)-N(7)-C(27)	156(3)
C(9)-C(8)-C(7)	119.4(5)
C(9)-C(8)-C(13)	119.3(6)
C(7)-C(8)-C(13)	121.3(5)
C(21)-O(8)-Zn(1)	122.3(3)
C(30)-N(8)-C(29)	133(2)
C(8)-C(9)-C(10)	120.9(6)
C(8)-C(9)-H(9A)	119.5
C(10)-C(9)-H(9A)	119.5
C(22)-O(9)-Zn(3)#6	101.7(4)
C(11)-C(10)-C(9)	119.5(5)
C(11)-C(10)-C(14)	121.5(6)
C(9)-C(10)-C(14)	119.0(6)
C(10)-C(11)-C(6)	120.2(5)
C(10)-C(11)-H(11A)	119.9
C(6)-C(11)-H(11A)	119.9
C(23)-O(11)-Zn(2)#2	111.1(4)

O(2)-C(12)-O(1)	123.1(5)
O(2)-C(12)-C(6)	119.3(5)
O(1)-C(12)-C(6)	117.6(5)
O(4)-C(13)-O(3)	123.6(5)
O(4)-C(13)-C(8)	119.5(6)
O(3)-C(13)-C(8)	116.9(6)
C(26)-O(13)-Zn(3)	125.1(6)
O(6)-C(14)-O(5)	125.9(7)
O(6)-C(14)-C(10)	120.3(8)
O(5)-C(14)-C(10)	113.7(7)
C(16)-C(15)-C(20)	118.4(5)
C(16)-C(15)-C(21)	122.1(4)
C(20)-C(15)-C(21)	119.4(5)
C(15)-C(16)-C(17)	120.7(5)
C(15)-C(16)-H(16A)	119.6
C(17)-C(16)-H(16A)	119.6
C(16)-C(17)-C(18)	119.8(5)
C(16)-C(17)-C(22)	121.0(5)
C(18)-C(17)-C(22)	119.2(5)
C(19)-C(18)-C(17)	121.2(5)
C(19)-C(18)-H(18A)	119.4
C(17)-C(18)-H(18A)	119.4
C(20)-C(19)-C(18)	118.2(5)
C(20)-C(19)-C(23)	121.6(5)
C(18)-C(19)-C(23)	120.2(5)
C(19)-C(20)-C(15)	121.6(5)
C(19)-C(20)-H(20A)	119.2
C(15)-C(20)-H(20A)	119.2
O(8)-C(21)-O(7)	125.2(5)
O(8)-C(21)-C(15)	117.5(5)
O(7)-C(21)-C(15)	117.3(5)
O(10)-C(22)-O(9)	122.8(6)
O(10)-C(22)-C(17)	120.1(6)
O(9)-C(22)-C(17)	117.1(5)
O(10)-C(22)-Zn(3)#6	73.7(4)
O(9)-C(22)-Zn(3)#6	49.5(3)

C(17)-C(22)-Zn(3)#6	164.7(4)
O(12)-C(23)-O(11)	124.4(5)
O(12)-C(23)-C(19)	121.0(6)
O(11)-C(23)-C(19)	114.6(6)
N(6)-C(24)-H(24A)	109.5
N(6)-C(24)-H(24B)	109.5
H(24A)-C(24)-H(24B)	109.5
N(6)-C(24)-H(24C)	109.5
H(24A)-C(24)-H(24C)	109.5
H(24B)-C(24)-H(24C)	109.5
N(6)-C(25)-H(25A)	109.5
N(6)-C(25)-H(25B)	109.5
H(25A)-C(25)-H(25B)	109.5
N(6)-C(25)-H(25C)	109.5
H(25A)-C(25)-H(25C)	109.5
H(25B)-C(25)-H(25C)	109.5
O(13)-C(26)-N(6)	127.6(9)
O(13)-C(26)-H(26A)	116.2
N(6)-C(26)-H(26A)	116.2
N(7)-C(27)-H(27A)	109.5
N(7)-C(27)-H(27B)	109.5
H(27A)-C(27)-H(27B)	109.5
N(7)-C(27)-H(27C)	109.5
H(27A)-C(27)-H(27C)	109.5
H(27B)-C(27)-H(27C)	109.5
N(7)-C(28)-H(28A)	109.4
N(7)-C(28)-H(28B)	109.5
H(28A)-C(28)-H(28B)	109.5
N(7)-C(28)-H(28C)	109.5
H(28A)-C(28)-H(28C)	109.5
H(28B)-C(28)-H(28C)	109.5
N(8)-C(29)-H(29A)	109.5
N(8)-C(29)-H(29B)	109.5
H(29A)-C(29)-H(29B)	109.5
N(8)-C(29)-H(29C)	109.5
H(29A)-C(29)-H(29C)	109.5

H(29B)-C(29)-H(29C)	109.5
N(8)-C(30)-H(30A)	109.5
N(8)-C(30)-H(30B)	109.5
H(30A)-C(30)-H(30B)	109.5
N(8)-C(30)-H(30C)	109.5
H(30A)-C(30)-H(30C)	109.5
H(30B)-C(30)-H(30C)	109.5

Symmetry transformations used to generate equivalent atoms:

#1 -x,-y+2,-z+2 #2 -x,-y+2,-z+1 #3 x+1,y,z

#4 -x+1/2,y-1/2,-z+3/2 #5 x-1,y,z #6 -x+1/2,y+1/2,-z+3/2

Anisotropic displacement parameters ($Å^2$x 10^3) for $Zn_3(Ad)(BTC)_2 \cdot (NH_2(CH_3)_2)^+$, 5.75DMF, 0.25$H_2O$ (5). The anisotropic displacement factor exponent takes the form: $-2\pi^2[h^2 a^{*2}U^{11} + ... + 2 h k a^* b^* U^{12}]$

	U^{11}	U^{22}	U^{33}	U^{23}	U^{13}	U^{12}
C(1)	41(3)	43(3)	36(3)	-5(2)	6(2)	4(2)
N(1)	36(2)	52(3)	31(2)	0(2)	-6(2)	0(2)
O(1)	51(2)	121(4)	43(2)	-22(2)	10(2)	-11(2)
Zn(1)	45(1)	51(1)	32(1)	-6(1)	4(1)	4(1)
C(2)	49(3)	40(3)	34(3)	0(2)	6(2)	-4(2)
N(2)	44(3)	53(3)	40(2)	-9(2)	7(2)	4(2)
O(2)	55(2)	64(3)	46(2)	-10(2)	-2(2)	-9(2)
Zn(2)	45(1)	58(1)	30(1)	-5(1)	2(1)	10(1)
C(3)	50(3)	64(4)	46(3)	-12(3)	-4(3)	5(3)
N(3)	49(3)	62(3)	54(3)	-22(2)	-9(2)	12(2)
Zn(3)	49(1)	32(1)	53(1)	-5(1)	-2(1)	0(1)
O(3)	78(3)	70(3)	35(2)	-14(2)	14(2)	-1(2)
C(4)	44(3)	38(3)	54(3)	-1(3)	-3(3)	3(2)
N(4)	44(3)	33(2)	39(2)	-2(2)	5(2)	1(2)
O(4)	66(3)	84(3)	44(2)	-2(2)	20(2)	9(2)
C(5)	38(3)	35(3)	38(3)	0(2)	0(2)	-2(2)
N(5)	42(3)	55(3)	51(3)	-19(2)	-5(2)	1(2)
O(5)	54(3)	111(4)	81(3)	-30(3)	22(2)	-39(3)
C(6)	53(3)	61(4)	37(3)	-7(3)	9(3)	-8(3)
N(6)	124(7)	180(9)	101(6)	17(6)	42(5)	-15(6)
O(6)	84(4)	305(11)	141(6)	-156(7)	32(4)	-33(5)
C(7)	59(4)	52(3)	34(3)	-9(2)	0(3)	-3(3)
O(7)	112(4)	52(3)	57(2)	-3(2)	26(3)	26(2)
N(7)	101(11)	160(15)	155(15)	-30(12)	73(11)	-62(11)
C(8)	59(4)	58(4)	39(3)	-8(3)	9(3)	-1(3)
O(8)	76(3)	50(2)	39(2)	-3(2)	-1(2)	11(2)
N(8)	77(10)	240(20)	230(20)	176(19)	-9(11)	61(12)
C(9)	60(4)	93(5)	52(3)	-18(3)	21(3)	-18(3)
O(9)	92(3)	35(2)	56(2)	-6(2)	13(2)	-3(2)
C(10)	62(4)	108(6)	57(4)	-32(4)	5(3)	-23(4)
O(10)	101(4)	34(2)	110(4)	12(2)	-9(3)	-7(2)

C(11)	60(4)	116(6)	46(3)	-38(4)	16(3)	-26(4)
O(11)	75(3)	91(3)	30(2)	-12(2)	5(2)	-7(2)
C(12)	55(4)	54(4)	42(3)	-12(3)	7(3)	-5(3)
O(12)	90(3)	90(3)	49(2)	18(2)	-18(2)	-17(3)
C(13)	69(4)	61(4)	36(3)	-1(3)	10(3)	17(3)
O(13)	73(3)	72(3)	43(2)	4(2)	21(2)	-6(2)
C(14)	78(6)	172(9)	78(5)	-53(6)	15(5)	-52(6)
C(15)	55(3)	43(3)	36(3)	-9(2)	11(2)	-2(2)
C(16)	63(4)	40(3)	31(3)	-3(2)	2(2)	-6(3)
C(17)	65(4)	39(3)	47(3)	1(3)	12(3)	-13(3)
C(18)	52(3)	51(3)	43(3)	11(3)	3(3)	-5(3)
C(19)	51(3)	57(4)	40(3)	-9(3)	10(3)	-8(3)
C(20)	56(3)	46(3)	40(3)	-8(2)	14(3)	-3(3)
C(21)	51(3)	40(3)	44(3)	-6(3)	3(3)	5(2)
C(22)	70(4)	41(3)	64(4)	1(3)	13(3)	-10(3)
C(23)	49(4)	86(5)	41(3)	-2(4)	6(3)	-5(3)
C(24)	203(14)	370(20)	144(11)	58(13)	108(10)	-6(14)
C(25)	96(8)	242(15)	184(12)	69(11)	6(8)	5(8)
C(26)	91(7)	144(9)	98(7)	-25(7)	-12(6)	5(6)
C(27)	121(16)	310(30)	146(18)	170(20)	25(14)	-50(19)
C(28)	118(18)	500(60)	240(30)	300(40)	100(20)	130(30)
C(29)	250(30)	82(13)	230(30)	-21(15)	200(20)	-11(15)
C(30)	158(18)	69(11)	151(17)	23(11)	104(16)	6(11)

Hydrogen coordinates (x 10^4) and isotropic displacement parameters ($Å^2$x 10^3)
for $Zn_3(Ad)(BTC)_2 \cdot (NH_2(CH_3)_2)^+$, 5.75DMF, $0.25H_2O$ (5).

	x	y	z	U(eq)
H(1A)	2804	8559	6608	49
H(3A)	3722	9902	9799	67
H(5A)	5936	8796	9664	62
H(5B)	5611	8480	8864	62
H(7A)	-426	9533	9231	60
H(9A)	-3173	9074	8597	80
H(11A)	-1489	8802	7033	88
H(16A)	724	11498	7726	55
H(18A)	-822	12049	5536	60
H(20A)	160	10538	5716	56
H(24A)	5152	8790	4090	343
H(24B)	4310	9218	3831	343
H(24C)	4200	8638	3415	343
H(25A)	2799	8520	4993	268
H(25B)	2642	8437	4018	268
H(25C)	2738	9027	4398	268
H(26A)	5167	8494	5488	141
H(27A)	-3794	9453	5509	290
H(27B)	-3400	10045	5742	290
H(27C)	-3095	9569	6394	290
H(28A)	-1691	9373	4957	417
H(28B)	-1309	9558	5898	417
H(28C)	-1750	9988	5200	417
H(29A)	2468	8371	12221	246
H(29B)	1778	8113	11418	246
H(29C)	1384	8237	12216	246
H(30A)	908	9494	11090	172
H(30B)	312	9034	11402	172
H(30C)	709	8941	10597	172

Crystal data and structure refinement for $Co(Ad)(CH_3CO_2) \cdot DMF, 0.25H_2O$ (6).

Identification code	$Co(Ad)(CH_3CO_2) \cdot DMF, 0.25H_2O$	
Empirical formula	C7 H7 Co N5 O2	
Formula weight	252.11	
Temperature	173(2) K	
Wavelength	0.71073 Å	
Crystal system	Tetragonal	
Space group	I4(1)/a	
Unit cell dimensions	a = 15.4355(18) Å	α= 90°.
	b = 15.4355(18) Å	β= 90°.
	c = 22.775(5) Å	γ = 90°.
Volume	5426.3(16) $Å^3$	
Z	16	
Density (calculated)	1.234 Mg/m^3	
Absorption coefficient	1.255 mm^{-1}	
F(000)	2032	
Crystal size	0.30 x 0.20 x 0.20 mm^3	
Theta range for data collection	5.28 to 23.26°.	
Index ranges	-17<=h<=17, -17<=k<=17, -25<=l<=25	
Reflections collected	14256	
Independent reflections	1935 [R(int) = 0.0936]	
Completeness to theta = 23.26°	98.9 %	
Absorption correction	multi-scan	
Max. and min. transmission	0.7873 and 0.7045	
Refinement method	Full-matrix least-squares on F^2	
Data / restraints / parameters	1935 / 0 / 136	
Goodness-of-fit on F^2	2.477	
Final R indices [I>2sigma(I)]	R1 = 0.1059, wR2 = 0.2938	
R indices (all data)	R1 = 0.1381, wR2 = 0.3075	
Largest diff. peak and hole	1.762 and -0.578 $e.Å^{-3}$	

Atomic coordinates (x 10^4) and equivalent isotropic displacement parameters ($Å^2$x 10^3)
for Co(Ad)(CH_3CO_2) · DMF, 0.25H_2O (6). U(eq) is defined as one third of the trace of the orthogonalized U^{ij} tensor.

	x	y	z	U(eq)
Co(1)	10435(1)	4821(1)	560(1)	35(1)
C(1)	8971(9)	3835(8)	1206(5)	48(3)
N(1)	9263(6)	4206(6)	705(4)	35(2)
O(1)	9879(5)	5953(5)	817(3)	45(2)
C(2)	8567(7)	4150(7)	349(5)	29(3)
O(2)	9187(6)	6155(6)	-23(4)	54(2)
N(2)	8529(6)	4447(7)	-210(4)	45(3)
C(3)	7797(10)	4236(12)	-480(7)	84(6)
N(3)	7120(8)	3780(10)	-274(6)	85(5)
N(4)	8174(6)	3522(6)	1193(4)	33(2)
C(4)	7129(9)	3548(12)	317(7)	76(5)
C(5)	7917(7)	3727(8)	629(5)	41(3)
N(5)	6477(8)	3137(12)	543(6)	126(8)
C(6)	9362(8)	6356(8)	497(6)	41(3)
C(7)	8912(11)	7151(8)	748(8)	81(5)

Bond lengths [Å] and angles [°] for $Co(Ad)(CH_3CO_2) \cdot DMF, 0.25H_2O$ (6).

Co(1)-O(2)#1	2.027(9)
Co(1)-O(1)	2.032(8)
Co(1)-N(1)	2.070(9)
Co(1)-N(4)#2	2.072(8)
Co(1)-N(2)#1	2.115(9)
Co(1)-Co(1)#1	2.937(3)
C(1)-N(4)	1.323(15)
C(1)-N(1)	1.354(14)
C(1)-H(1A)	0.9500
N(1)-C(2)	1.348(14)
O(1)-C(6)	1.246(14)
C(2)-N(2)	1.354(14)
C(2)-C(5)	1.356(15)
O(2)-C(6)	1.254(14)
O(2)-Co(1)#1	2.028(9)
N(2)-C(3)	1.326(16)
N(2)-Co(1)#1	2.115(9)
C(3)-N(3)	1.345(18)
C(3)-H(3A)	0.9500
N(3)-C(4)	1.391(18)
N(4)-C(5)	1.382(14)
N(4)-Co(1)#3	2.072(8)
C(4)-N(5)	1.296(18)
C(4)-C(5)	1.436(18)
N(5)-H(5A)	0.8800
N(5)-H(5B)	0.8800
C(6)-C(7)	1.522(17)
C(7)-H(7A)	0.9800
C(7)-H(7B)	0.9800
C(7)-H(7C)	0.9800

O(2)#1-Co(1)-O(1)	159.0(3)
O(2)#1-Co(1)-N(1)	90.4(4)
O(1)-Co(1)-N(1)	88.8(3)

O(2)#1-Co(1)-N(4)#2	95.5(4)
O(1)-Co(1)-N(4)#2	105.4(3)
N(1)-Co(1)-N(4)#2	94.7(4)
O(2)#1-Co(1)-N(2)#1	87.2(4)
O(1)-Co(1)-N(2)#1	88.2(4)
N(1)-Co(1)-N(2)#1	165.1(4)
N(4)#2-Co(1)-N(2)#1	100.2(4)
O(2)#1-Co(1)-Co(1)#1	75.3(3)
O(1)-Co(1)-Co(1)#1	84.0(2)
N(1)-Co(1)-Co(1)#1	79.9(2)
N(4)#2-Co(1)-Co(1)#1	169.2(3)
N(2)#1-Co(1)-Co(1)#1	85.2(3)
N(4)-C(1)-N(1)	116.4(11)
N(4)-C(1)-H(1A)	121.8
N(1)-C(1)-H(1A)	121.8
C(2)-N(1)-C(1)	102.5(9)
C(2)-N(1)-Co(1)	129.1(7)
C(1)-N(1)-Co(1)	128.2(8)
C(6)-O(1)-Co(1)	122.1(8)
N(1)-C(2)-N(2)	125.3(9)
N(1)-C(2)-C(5)	109.8(10)
N(2)-C(2)-C(5)	124.9(11)
C(6)-O(2)-Co(1)#1	133.8(8)
C(3)-N(2)-C(2)	112.9(10)
C(3)-N(2)-Co(1)#1	126.9(9)
C(2)-N(2)-Co(1)#1	120.2(7)
N(2)-C(3)-N(3)	129.0(13)
N(2)-C(3)-H(3A)	115.5
N(3)-C(3)-H(3A)	115.5
C(3)-N(3)-C(4)	117.7(13)
C(1)-N(4)-C(5)	101.8(9)
C(1)-N(4)-Co(1)#3	119.0(8)
C(5)-N(4)-Co(1)#3	139.2(8)
N(5)-C(4)-N(3)	120.2(14)
N(5)-C(4)-C(5)	123.7(13)
N(3)-C(4)-C(5)	115.9(12)

C(2)-C(5)-N(4)	109.5(10)
C(2)-C(5)-C(4)	119.2(12)
N(4)-C(5)-C(4)	131.3(11)
C(4)-N(5)-H(5A)	120.0
C(4)-N(5)-H(5B)	120.0
H(5A)-N(5)-H(5B)	120.0
O(1)-C(6)-O(2)	124.5(11)
O(1)-C(6)-C(7)	118.4(13)
O(2)-C(6)-C(7)	117.1(13)
C(6)-C(7)-H(7A)	109.5
C(6)-C(7)-H(7B)	109.5
H(7A)-C(7)-H(7B)	109.5
C(6)-C(7)-H(7C)	109.5
H(7A)-C(7)-H(7C)	109.5
H(7B)-C(7)-H(7C)	109.5

Symmetry transformations used to generate equivalent atoms:

#1 -x+2,-y+1,-z #2 y+3/4,-x+5/4,-z+1/4 #3 -y+5/4,x-3/4,-z+1/4

Anisotropic displacement parameters ($Å^2 x\ 10^3$) for $Co(Ad)(CH_3CO_2) \cdot DMF, 0.25H_2O$ (6).. The anisotropic displacement factor exponent takes the form: $-2\pi^2[h^2 a^{*2} U^{11} + ... + 2 h k a^* b^* U^{12}]$

	U^{11}	U^{22}	U^{33}	U^{23}	U^{13}	U^{12}
Co(1)	31(1)	41(1)	33(1)	13(1)	-4(1)	-4(1)
C(1)	58(9)	41(8)	46(8)	16(6)	-1(6)	-10(7)
N(1)	33(6)	36(6)	34(5)	12(4)	5(4)	0(5)
O(1)	46(5)	35(5)	54(5)	3(4)	-15(4)	8(4)
C(2)	26(6)	26(6)	35(6)	1(5)	12(5)	3(5)
O(2)	66(6)	57(6)	38(5)	1(4)	0(4)	-2(5)
N(2)	24(6)	67(7)	44(6)	20(5)	-1(4)	-5(5)
C(3)	48(10)	135(15)	69(11)	52(10)	-18(8)	-31(10)
N(3)	50(8)	135(13)	72(9)	47(9)	-14(7)	-28(8)
N(4)	34(6)	37(6)	30(5)	9(4)	5(4)	2(5)
C(4)	45(9)	114(14)	70(10)	42(10)	-10(8)	-12(9)
C(5)	29(7)	49(8)	46(8)	8(6)	7(6)	9(6)
N(5)	33(7)	260(20)	88(10)	99(12)	-22(7)	-70(10)
C(6)	31(7)	35(7)	57(9)	0(6)	24(6)	-11(6)
C(7)	84(12)	26(7)	132(15)	-25(8)	9(10)	22(8)

Hydrogen coordinates (x 10^4) and isotropic displacement parameters ($Å^2$x 10^3) for Co(Ad)(CH_3CO_2) · DMF, 0.25H_2O (6)..

	x	y	z	U(eq)
H(1A)	9321	3803	1549	58
H(3A)	7745	4434	-873	101
H(5A)	6028	3004	323	151
H(5B)	6485	2992	917	151
H(7A)	9098	7240	1155	121
H(7B)	8283	7065	737	121
H(7C)	9065	7661	514	121

Crystal data and structure refinement for $Zn_{1.5}(Ad)(CH_3CO_2)_2 \cdot 0.75DMA, 0.5H_2O$ (7).

Identification code	$Zn_{1.5}(Ad)(CH_3CO_2)_2 \cdot 0.75DMA, 0.5H_2O$	
Empirical formula	C14 H10 N5 O4 Zn1.50	
Formula weight	410.33	
Temperature	173(2) K	
Wavelength	0.71073 Å	
Crystal system	Monoclinic	
Space group	P2(1)/c	
Unit cell dimensions	a = 8.9292(5) Å	α= 90°.
	b = 12.0207(7) Å	β= 93.8590(10)°.
	c = 13.3461(8) Å	γ = 90°.
Volume	1429.26(14) $Å^3$	
Z	4	
Density (calculated)	1.907 Mg/m^3	
Absorption coefficient	2.571 mm^{-1}	
F(000)	824	
Crystal size	0.34 x 0.20 x 0.14 mm^3	
Theta range for data collection	2.28 to 28.30°.	
Index ranges	-11<=h<=11, -16<=k<=16, -17<=l<=17	
Reflections collected	14389	
Independent reflections	3534 [R(int) = 0.0456]	
Completeness to theta = 28.30°	99.9 %	
Absorption correction	Multi-scan (Sadabs)	
Max. and min. transmission	0.7148 and 0.4752	
Refinement method	Full-matrix least-squares on F^2	
Data / restraints / parameters	3534 / 0 / 210	
Goodness-of-fit on F^2	2.848	
Final R indices [I>2sigma(I)]	R1 = 0.0839, wR2 = 0.2206	
R indices (all data)	R1 = 0.0915, wR2 = 0.2222	
Largest diff. peak and hole	1.393 and -1.258 $e.Å^{-3}$	

Atomic coordinates (x 10^4) and equivalent isotropic displacement parameters ($Å^2$x 10^3) for $Zn_{1.5}(Ad)(CH_3CO_2)_2 \cdot 0.75DMA, 0.5H_2O$ (7). U(eq) is defined as one third of the trace of the orthogonalized U^{ij} tensor.

	x	y	z	U(eq)
Zn(1)	3615(1)	1349(1)	2013(1)	26(1)
Zn(2)	5000	5000	5000	18(1)
O(1)	2231(6)	71(4)	1968(4)	30(1)
O(2)	2992(5)	-628(4)	551(3)	28(1)
O(3)	5456(5)	808(4)	1434(3)	25(1)
N(1)	3214(6)	2261(4)	3246(4)	20(1)
N(2)	3916(6)	3538(4)	4434(4)	19(1)
N(3)	2636(6)	2755(5)	5831(4)	26(1)
C(1)	4011(8)	3184(5)	3480(5)	21(1)
C(2)	3038(7)	2786(5)	4858(4)	19(1)
C(3)	1675(8)	1940(6)	6002(5)	32(2)
O(4)	6347(8)	2242(6)	2269(6)	75(2)
N(4)	1076(7)	1209(5)	5350(4)	31(1)
C(4)	1528(8)	1204(6)	4393(5)	25(1)
N(5)	877(7)	436(5)	3769(5)	29(1)
C(5)	2566(7)	1995(5)	4138(5)	22(1)
C(6)	2144(7)	-623(5)	1252(5)	23(1)
C(7)	913(9)	-1471(6)	1252(6)	36(2)
C(8)	6582(9)	1392(7)	1804(6)	36(2)
C(9)	8145(9)	983(10)	1670(7)	63(3)
C(10)	5034(14)	35(11)	3355(10)	74(3)
C(11)	5064(17)	-175(12)	4021(12)	89(4)
C(12)	4575(15)	-317(11)	5020(11)	79(4)
C(13)	3600(20)	-1190(18)	4594(17)	139(7)
C(14)	3530(20)	-1315(15)	5422(15)	117(6)

Bond lengths [Å] and angles [°] for $Zn_{1.5}(Ad)(CH_3CO_2)_2 \cdot 0.75DMA, 0.5H_2O$ (7).

Zn(1)-O(1)	1.970(5)
Zn(1)-O(3)	1.973(5)
Zn(1)-N(1)	2.029(5)
Zn(1)-N(3)#1	2.056(5)
Zn(2)-N(2)	2.120(5)
Zn(2)-N(2)#2	2.120(5)
Zn(2)-O(2)#3	2.123(5)
Zn(2)-O(2)#4	2.123(5)
Zn(2)-O(3)#3	2.161(4)
Zn(2)-O(3)#4	2.161(4)
O(1)-C(6)	1.266(8)
O(2)-C(6)	1.242(8)
O(2)-Zn(2)#5	2.123(5)
O(3)-C(8)	1.296(9)
O(3)-Zn(2)#5	2.161(4)
N(1)-C(1)	1.343(8)
N(1)-C(5)	1.395(8)
N(2)-C(2)	1.346(8)
N(2)-C(1)	1.351(7)
N(3)-C(3)	1.333(9)
N(3)-C(2)	1.371(8)
N(3)-Zn(1)#3	2.056(5)
C(1)-H(1)	1.14(8)
C(2)-C(5)	1.397(9)
C(3)-N(4)	1.324(10)
C(3)-H(3A)	0.9500
O(4)-C(8)	1.221(9)
N(4)-C(4)	1.365(8)
C(4)-N(5)	1.349(9)
C(4)-C(5)	1.387(9)
N(5)-H(5NA)	1.06(8)
N(5)-H(5NB)	0.71(6)
C(6)-C(7)	1.499(9)
C(7)-H(7A)	0.9800

C(7)-H(7B)	0.9800
C(7)-H(7C)	0.9800
C(8)-C(9)	1.502(11)
C(9)-H(9A)	0.9800
C(9)-H(9B)	0.9800
C(9)-H(9C)	0.9800
C(10)-C(11)	0.922(16)
C(11)-C(12)#6	1.43(2)
C(11)-C(12)	1.44(2)
C(11)-C(13)	1.98(3)
C(12)-C(12)#6	1.08(2)
C(12)-C(11)#6	1.43(2)
C(12)-C(13)	1.46(2)
C(12)-C(14)	1.63(2)
C(13)-C(14)	1.12(2)

O(1)-Zn(1)-O(3)	105.6(2)
O(1)-Zn(1)-N(1)	107.5(2)
O(3)-Zn(1)-N(1)	133.9(2)
O(1)-Zn(1)-N(3)#1	98.7(2)
O(3)-Zn(1)-N(3)#1	101.2(2)
N(1)-Zn(1)-N(3)#1	104.5(2)
N(2)-Zn(2)-N(2)#2	179.999(1)
N(2)-Zn(2)-O(2)#3	92.43(19)
N(2)#2-Zn(2)-O(2)#3	87.57(19)
N(2)-Zn(2)-O(2)#4	87.57(19)
N(2)#2-Zn(2)-O(2)#4	92.43(19)
O(2)#3-Zn(2)-O(2)#4	179.998(1)
N(2)-Zn(2)-O(3)#3	89.84(18)
N(2)#2-Zn(2)-O(3)#3	90.16(18)
O(2)#3-Zn(2)-O(3)#3	88.06(18)
O(2)#4-Zn(2)-O(3)#3	91.93(18)
N(2)-Zn(2)-O(3)#4	90.16(18)
N(2)#2-Zn(2)-O(3)#4	89.84(18)
O(2)#3-Zn(2)-O(3)#4	91.94(18)
O(2)#4-Zn(2)-O(3)#4	88.06(18)

O(3)#3-Zn(2)-O(3)#4	179.998(1)
C(6)-O(1)-Zn(1)	122.9(4)
C(6)-O(2)-Zn(2)#5	146.2(5)
C(8)-O(3)-Zn(1)	108.5(4)
C(8)-O(3)-Zn(2)#5	132.5(5)
Zn(1)-O(3)-Zn(2)#5	112.5(2)
C(1)-N(1)-C(5)	103.5(5)
C(1)-N(1)-Zn(1)	121.0(4)
C(5)-N(1)-Zn(1)	132.4(4)
C(2)-N(2)-C(1)	105.0(5)
C(2)-N(2)-Zn(2)	132.2(4)
C(1)-N(2)-Zn(2)	122.8(4)
C(3)-N(3)-C(2)	113.3(6)
C(3)-N(3)-Zn(1)#3	119.9(5)
C(2)-N(3)-Zn(1)#3	126.0(4)
N(1)-C(1)-N(2)	114.5(6)
N(1)-C(1)-H(1)	117(4)
N(2)-C(1)-H(1)	126(4)
N(2)-C(2)-N(3)	127.8(6)
N(2)-C(2)-C(5)	109.0(5)
N(3)-C(2)-C(5)	123.2(6)
N(4)-C(3)-N(3)	127.7(6)
N(4)-C(3)-H(3A)	116.2
N(3)-C(3)-H(3A)	116.2
C(3)-N(4)-C(4)	119.1(6)
N(5)-C(4)-N(4)	116.1(6)
N(5)-C(4)-C(5)	125.8(6)
N(4)-C(4)-C(5)	118.1(6)
C(4)-N(5)-H(5NA)	118(4)
C(4)-N(5)-H(5NB)	119(5)
H(5NA)-N(5)-H(5NB)	123(7)
C(4)-C(5)-N(1)	133.6(6)
C(4)-C(5)-C(2)	118.3(6)
N(1)-C(5)-C(2)	107.9(5)
O(2)-C(6)-O(1)	124.2(6)
O(2)-C(6)-C(7)	118.7(6)

O(1)-C(6)-C(7)	117.1(6)
C(6)-C(7)-H(7A)	109.5
C(6)-C(7)-H(7B)	109.5
H(7A)-C(7)-H(7B)	109.5
C(6)-C(7)-H(7C)	109.5
H(7A)-C(7)-H(7C)	109.5
H(7B)-C(7)-H(7C)	109.5
O(4)-C(8)-O(3)	119.4(7)
O(4)-C(8)-C(9)	121.8(8)
O(3)-C(8)-C(9)	118.7(7)
C(8)-C(9)-H(9A)	109.5
C(8)-C(9)-H(9B)	109.5
H(9A)-C(9)-H(9B)	109.5
C(8)-C(9)-H(9C)	109.5
H(9A)-C(9)-H(9C)	109.5
H(9B)-C(9)-H(9C)	109.5
C(10)-C(11)-C(12)#6	137.8(19)
C(10)-C(11)-C(12)	158.9(19)
C(12)#6-C(11)-C(12)	44.2(10)
C(10)-C(11)-C(13)	124.3(17)
C(12)#6-C(11)-C(13)	91.4(13)
C(12)-C(11)-C(13)	47.2(9)
C(12)#6-C(12)-C(11)#6	68.6(15)
C(12)#6-C(12)-C(11)	67.2(14)
C(11)#6-C(12)-C(11)	135.8(10)
C(12)#6-C(12)-C(13)	153(2)
C(11)#6-C(12)-C(13)	137.9(15)
C(11)-C(12)-C(13)	86.3(14)
C(12)#6-C(12)-C(14)	163(2)
C(11)#6-C(12)-C(14)	96.3(13)
C(11)-C(12)-C(14)	127.3(13)
C(13)-C(12)-C(14)	42.0(10)
C(14)-C(13)-C(12)	77.4(17)
C(14)-C(13)-C(11)	123(2)
C(12)-C(13)-C(11)	46.5(10)
C(13)-C(14)-C(12)	60.6(15)

Symmetry transformations used to generate equivalent atoms:

#1 x,-y+1/2,z-1/2 #2 -x+1,-y+1,-z+1 #3 x,-y+1/2,z+1/2

#4 -x+1,y+1/2,-z+1/2 #5 -x+1,y-1/2,-z+1/2 #6 -x+1,-y,-z+1

Anisotropic displacement parameters ($Å^2 x\ 10^3$) for $Zn_{1.5}(Ad)(CH_3CO_2)_2 \cdot 0.75DMA, 0.5H_2O$ (7). The anisotropic displacement factor exponent takes the form: $-2\pi^2[h^2 a^{*2}U^{11} + ... + 2 h k a^* b^* U^{12}]$

	U^{11}	U^{22}	U^{33}	U^{23}	U^{13}	U^{12}
Zn(1)	31(1)	29(1)	19(1)	-9(1)	10(1)	-5(1)
Zn(2)	25(1)	14(1)	15(1)	0(1)	3(1)	-1(1)
O(1)	39(3)	27(3)	25(2)	-8(2)	10(2)	-9(2)
O(2)	30(3)	28(3)	26(2)	-2(2)	7(2)	-5(2)
O(3)	30(3)	23(2)	21(2)	-2(2)	0(2)	3(2)
N(1)	28(3)	19(3)	14(2)	1(2)	2(2)	-6(2)
N(2)	28(3)	16(3)	14(2)	0(2)	2(2)	3(2)
N(3)	30(3)	30(3)	17(3)	1(2)	4(2)	-11(2)
C(1)	31(4)	16(3)	17(3)	-3(2)	3(3)	1(3)
C(2)	23(3)	17(3)	17(3)	0(2)	2(2)	2(2)
C(3)	35(4)	38(4)	23(3)	3(3)	13(3)	-10(3)
O(4)	54(4)	58(4)	113(7)	-59(5)	17(4)	-10(3)
N(4)	33(3)	41(4)	22(3)	2(3)	9(3)	-13(3)
C(4)	26(3)	27(4)	23(3)	8(3)	1(3)	2(3)
N(5)	35(3)	36(3)	16(3)	-3(3)	7(3)	-16(3)
C(5)	25(3)	23(3)	17(3)	0(2)	4(3)	2(3)
C(6)	27(3)	17(3)	25(3)	0(2)	1(3)	4(3)
C(7)	32(4)	27(4)	49(5)	1(3)	5(3)	-9(3)
C(8)	26(4)	40(4)	41(4)	-15(4)	5(3)	1(3)
C(9)	28(5)	106(9)	53(6)	-41(6)	-9(4)	6(5)

Hydrogen coordinates (x 10^4) and isotropic displacement parameters ($Å^2$x 10^3) for $Zn_{1.5}(Ad)(CH_3CO_2)_2 \cdot 0.75DMA, 0.5H_2O$ (7).

	x	y	z	U(eq)
H(1)	4920(90)	3410(60)	2960(60)	30(20)
H(3A)	1385	1875	6672	38
H(5NA)	160(90)	-160(70)	4080(60)	40(20)
H(5NB)	1130(70)	380(50)	3280(50)	0(15)
H(7A)	959	-1954	664	53
H(7B)	-61	-1093	1228	53
H(7C)	1037	-1920	1865	53
H(9A)	8873	1503	1992	95
H(9B)	8303	931	952	95
H(9C)	8279	247	1980	95

BIBLIOGRAPHY

[1] (a) Wikoff, W. R.; Liljas, L.; Duda, R. L.; Tsuruta, H.; Hendrix, R. W.; Johnson, J. E. ; *Science*, **2000**, *289*, 2129. (b) Teschke, C. M..; McGough, A.; Thuman-Commike, *P. A. Biophysical Journal***, 2003**, *84*, 2585.

[2] (a) Beauvais, L. G.; Shores, M.. P.; Long, J. R. *J. Am. Chem. Soc*. **2000**, *122*, 2763. (b) Jianghua, H.; Jihong, Y.; Yuetao, Z.; Qinhe, P.; Ruren, X. *Inorg. Chem.* **2005**, *44*, 9279.

[3] (a) Eddaudi, M.; Kim, J.; Rosi, N.; Vodak, D.; O'Keeffe, M.; Yaghi, O. M. *Science* **2002**, *295*, 469 (b) Rowell, J. L. C.; Spencer, E. C.; Eckert, J.; Howard, J.A.K.; Yaghi, O. M. *Science* **2005**, *309*, 1350. (c) Ma, S.; Zhou, H.-C. *J. Am. Chem. Soc*. **2006**, *128*, 11734. (d) Peterson, V. K.; Liu, Y.; Brown, C. M.; Kepert, C. J. *J. Am. Chem. Soc*. **2006**, *128*, 15578

[4] (a) Snurr, R. Q.; Hupp, J. T.; Nguyen, S. T. *AIChE J.* **2004**, *50*, 1090 (b) Matsuda, R.; Kitaura, R.; Kitagawa, S.; Kubota, Y.; Belosludov, R. V.; Kobayashi, T. C.; Sakamoto, H.; Chiba, T.; Takata, M.; Kawazoe Y.; Mita, Y. *Nature*, **2005**, *436*, 238

[5] (a) Seo J. S.; Whang, D.; Lee, H.; Jun, S. I.; Oh, J.; Young, J.; Kim, K. *Nature* **2000**, *404*, 982. (b) Corma, A. *Catal.* **2003**, *216*, 298. (c) Zou, R.; Sakura, H.; Xu, Q. *Angew. Chem. Int. Ed.* **2006**, *45*, 2542

[6] Shvareva, T. Y.; Skanthakumar, S.; Soderholm, L.; Clearfield, A.; Albrecht-Schmitt, T. E. *Chem. Mater*. **2007**, *19*, 132

[7] (a) Tashiro, S.; Tominaga, M.; Yamaguchi, Y.; Kato, K.; Fujita, M. *Chem. Eur. J*., **2006**, *12*, 3211. (b) Suzuki, K.; Kawano, M.; Sato, S.; Fujita, M. *J. Am. Chem. Soc*. **2007**, *129*, 10652.

[8] (a) Garcia-Teran, J. P.; Castillo, O.; Luque, A.; Garcia-Couceiro, U.; Roman, P.; Lezama, L. *Inorg. Chem.,* **2004**, *43*, 4549. (b) Shekhar, C. S.; Verma, S. *J. Am. Chem. Soc.* **2006**, *128*, 400. (c) Yang E.C.; Zhao, H. K.; Ding B.; Wang X. G.; Zhao. X. *J. New J. Chem*. **2007**, *31*, 1887. (d) Kru1ger, T.; Ru1ffer, T.; Lang, H.; Wagner, C.; Steinborn, D. *Inorg. Chem.* **2008**,

[9] Mantion, A.; Massüger, L.; Rabu, P.; Palivan, C.; McCusker, L.B.; Taubert, A. *J. Am. Chem. Soc*. **2008**, *130*, 2517.

[10] (a) Horcajada, P.; Serre, C.; Vallet-Regí, M.; Sebban, M.; Taulelle, F.;and Férey G.*Angew. Chem. Int. Ed*. **2006**, *45*, 5974. (b) Vallet-Regí, M.; Balas, F.; Arcos, D. *Angew. Chem. Int. Ed.* **2007**, *46*, 7548.

[11] (a) Lippert, B. *Prog. Inorg. Chem.* **2005**, *54*, 385. (b) Sivakova, S.; Rowan, S. J. *Chem. Soc. Re*V. **2005**, *34*, 9. (c) Terro´n, A.; Fiol, J. J.; Garcı´a-Raso, A.; Barcelo´-Oliver, M.; Moreno V. *Coord. Chem. Re*V. **2007**, *251*, 1973. (d) Freisinger, E.; Sigel, R. K.O. *Coord. Chem. Re*V. **2007**, *251*, 1834.

[12] Hayashi, H.; Côté, A.P.; Furukawa, H.; O'Keeffe, M.; Yaghi, O.M. *Nat. Mater.*, **2007**, *6*, 501.

[13] Banerjee, R.; Phan,A.; Wang, B.; Knobler, C.; Furukawa, H.; O'Keeffe, M..; Yaghi, O.M. *SCIENCE*, **2008,** *319*, 939.

[14] Adsorption, surface area and porosity, S.J. Gregg, and K.S.W. Sing, Academic Press, 1967

[15] Dell'Amico, D.; Calderazzo, F.; Labella, C.; Marchetti F. Inorg. Chim. Acta, **2003**, *350*, 661.

[16] (a) Calzaferri, G.l Huber, S.; Maas, H.; Minkowski, C. *Agew. Chem. Int. Ed.* **2003**, *42*,3 732. (b)Dinca, M.; Long, J.R. *J. Am. Chem. Soc*. **2007**, *129*, 11172. (c) Fang, Q.R.; Zhu, G.S.; Jin, Z.; Ji, Y.Y.; Ye, J.W.; Xue, M.; Yang, H.; Wang, Y.; Qiu, S.L. *Agew. Chem. Int. Ed.* **2007**, *46*,3 6638.

[17] (a) Zheng, N.; Bu. X.; Feng, P. *Nature*, **2003**, *426*, 428. (b) Wang, X.; Liu, R.; Waje, M. M.; Chen, Z.; Yan, Y.; Bozhilov, K.N.; Feng, P. *Chem. Mater.* **2007**, *19*, 2397. (c) Holmberg, B.; Yan, Y. *J. Electrochem. Soc.,* **2006**, *153*, A146.

[18] Kaye S. S.; Dailly, A.; Yaghi, O.M.; Long, J.R. *J. Am. Chem. Soc* **2007**, *129*, 14176.

[19] (a) Rivera, A.; Farias, T.; Ruiz-Salvador, A.R.; Ménorval, L.C. *Micropor. Mesopor. Mater*. **2003**, *61*, 249. (b) Revera, A.; Farias,T. . *Micropor. Mesopor. Mater*. **2005**, *80*, 337. (c) Lai, C.Y.; Trewyn, B.G.; Jeftinija, D.M.; Jeftinija, K.; Xu, S.; Jeftinija, S.; Lin, V. S.-Y. *J. Am. Chem. Soc*. **2003**, *125*, 4451. (d) Vallet-Regi, M.; Rámila, A.; der Real, P.; Pérez-Pariente *Chem. Mater.* **2001,** *13*, 308. (e) Vallet-Regi, M.; Balas, F.; Arcos, D. *Agew. Chem. Int. Ed.* **2007**, *46*, 7548.

.